

P1299
5325



C10038
43982

BIBLIOTHEEK TU Delft
P 1299 5325



C

384398

**CALCULATION OF THE EDGE EFFECT
OF SOUND-ABSORBING
STRUCTURES**

CALCULATION OF THE EDGE EFFECT OF SOUND-ABSORBING STRUCTURES

PROEFSCHRIFT

TER VERKRIJGING VAN DE GRAAD VAN DOCTOR
IN DE TECHNISCHE WETENSCHAPPEN AAN DE
TECHNISCHE HOGESCHOOL DELFT OP GEZAG
VAN DE RECTOR MAGNIFICUS IR. H. J. DE WIJS,
HOGLERAAR IN DE AFDELING DER MIJN-
BOUWKUNDE, VOOR EEN COMMISSIE UIT DE
SENAAT TE VERDEDIGEN OP
WOENSDAG 7 JUNI 1967 TE 14 UUR

DOOR

ALEX DE BRUIJN

NATUURKUNDIG INGENIEUR
GEBOREN TE 'S-GRAVENHAGE



DIT PROEFSCHRIFT IS GOEDGEKEURD DOOR DE PROMOTOREN

Prof. Dr. Ir. A.T. DE HOOP

EN

Prof. Dr. Ir. C.W. KOSTEN

Aan mijn ouders.

Contents		page
Chapter I	General Introduction	9
Chapter II	Diffraction and absorption by an absorbing half-plane	21
2.1	Introduction	21
2.2	Mathematical formulation of the problem	22
2.3	The solution of the dual integral equations	25
2.4	The factorization of $K(\alpha)$	27
2.5	Asymptotic evaluation of the scattered field	30
2.6	The quantities P_{edge} , b and b_{stat}	31
2.7	Numerical results and discussion	35
Chapter III	Diffraction and absorption by an absorbing strip	39
3.1	Introduction	39
3.2	Mathematical formulation of the problem	40
3.3	The absorption coefficient and the cross-sections	44
3.4	Numerical computations	48
3.5	Discussion of the results	50
Chapter IV	Diffraction and absorption by an absorbing periodically uneven surface of rectangular profile	62
4.1	Introduction	62
4.2	Diffraction by a periodically uneven surface of rectangular profile	63
4.3	The infinite systems of linear equations	65
4.4	Considerations concerning the scattered and the absorbed power by the uneven surface	69
4.5	Considerations concerning the Wood anomaly, the surface resonance and the waveguide resonance	71
4.6	Numerical computations	73
4.7	Discussion of the results	75
	References	104
	Additional References	108
	Summary	111
	Samenvatting	113

Errata

- p. 12 Line 20 from bottom should read
..... is not known a priori and has to be determined
- p. 35 Line 3 in Section 2.7 should read
..... in the integrals, Eq. (2.46) yields
- p. 47 for $\underline{n} \cdot \underline{u}^{t*} = u^{t*}$
read $\underline{n} \cdot \underline{u}^{s*} = \underline{n} \cdot \underline{u}^{t*}$.
- p. 62 Line 9 from bottom should read
... to an investigation of a periodically uneven structure
- p. 66 Eq. (4.12) should read
$$\partial \phi_I^t / \partial z - jk\eta \phi_I^t = \partial \phi_{II}^t / \partial z - jk\eta \phi_{II}^t.$$
- p. 72 Line 3 from bottom should read
..... of the column. There is an end correction
- p. 104 and p. 105 have been interchanged.

CHAPTER I

General Introduction

In 1895 SABINE initiated his famous investigation of quantitative measurements in room acoustics, which gave the impulse to a firm foundation of scientific knowledge on this subject. Through extensive experimental studies of the acoustical properties of a room SABINE arrived at an empirical relation between the reverberation characteristics of an enclosure, its size and the amount of absorption present.

He defined the reverberation time of an enclosure to be the time required for the sound energy density to reduce to 10^{-6} times its initial value when suddenly silencing the sound source, or in decibel-language the time required for a drop of 60 dB in sound pressure level. Since SABINE's investigations the reverberation time has remained the most important objective quantity to characterize a hall acoustically.

If a sound source is radiating sound power at a constant rate in a large hall one can observe that the sound field is gradually being built up. It takes a few seconds before the hall has been "filled" with sound. Obviously the energy density reaches a finite level, since the intensity, heard subjectively, remains finite. In this steady state the radiated power must be equal to the rate of absorption of sound energy in the hall. For low and medium frequencies the sound energy is absorbed by the boundary surfaces of the enclosure and the objects therein. At high frequencies, say 4000 Hz and up, sound energy is appreciable dissipated in the air.

When the steady state has been reached and the sound source is suddenly stopped the balance between the radiating power and the absorbed power is disturbed; the sound dies away. Since the rate of energy absorption will be proportional to the energy present, an exponential decay is to be expected. SABINE succeeded, first along empirical lines and afterwards theoretically, to derive the following equation

$$(1.1) \quad T = 0.163 V/A, \quad (\text{in SI-units}),$$

where T is the reverberation time of an enclosure, V its volume and A the total absorption of the enclosure, defined as

$$A = \sum a_g S,$$

where a_g is the absorption coefficient of the boundary, S its area, the summation being taken over all surfaces of the enclosure. Eq. (1.1) is dimensionally correct, the reason being that the factor 0.163 contains the reciprocal of the sound velocity. The theoretical derivation of Eq. (1.1) is based upon the inaccurate assumption that the energy is distributed uniform throughout the entire volume of the enclosure. The fact that the totally absorbed power equals the

diminution of the energy per unit time leads to a differential equation of the first order. Its solution yields Sabine's law (KINSLER & FREY [1950]).

The absorption coefficient of a surface is usually defined as the non-reflected fraction of the incident energy. If a_S is defined in this way, Sabine's law turns out to be an approximation. A different approach is to assume the validity of Eq. (1.1) and to use it for calculating A from the measurable quantities V and T . When this is done twice in the same enclosure with different amounts of absorbing materials one can compute the difference $\Delta A = A_1 - A_2$ between the two situations. If the two situations only differ in this respect that the first situation, as compared with the second one, contains a known extra surface S having an unknown absorption coefficient one is able to compute a_S from the quantity $\Delta A (=a_S S)$. The absorption coefficient thus computed from measurements is approximately equal to the true absorption coefficient as defined above. This is the reason for the subscript S (from "SABINE") to a .

The standard method of measuring the absorption coefficient of a material is through an investigation of its effect on the reverberation time in an enclosure. Specially constructed enclosures known as reverberation chambers are generally used for this purpose. The primary requirements of such a chamber are that its wall surfaces should be highly reflecting, so as to produce a large reverberation time when the test sample is not present, that its volume should be large enough to contain a large number of normal vibrational modes in any given frequency interval, and that it should have irregular wall surfaces and be equipped with a number of diffusers, e.g., curved plates of plywood of a few square meters each, so as to increase the rate of diffusion of sound waves. According to a recommendation of the International Organization for Standardization, its volume ought to be larger than 180 m^3 .

EYRING [1930] derived an improved fashion for the relation between the absorption coefficient and the reverberation time. In order to calculate the absorption coefficient a_E (the subscript E from "EYRING") two reverberation times T_0 and T_1 (without and with the sample under test in the reverberation chamber) are measured. The absorption coefficient a_E is then given by

$$(1.2) \quad a_E = \frac{F}{S} \left\{ \exp \left[-0.163 V / F T_0 \right] - \exp \left[-0.163 V / F T_1 \right] \right\},$$

in which S = the area of the sample;

F = the total wall area in the chamber;

V = volume of the chamber.

The derivation of this equation is based upon the concept of geometrical or ray acoustics in which sound is assumed to travel along straight paths or rays. Sabine's law can be derived as an approximation from this equation if T_0 and T_1 are taken to be large.

The absorption coefficient a_S or a_E of a sample turns out to depend not only upon the properties of the material, but also on the size and shape of the sample. From a theoretical point of view this is not so surprising, if we bear in mind that additional sound energy flows inwards to a sample from all around by diffraction of the waves at the edges of the sample. In other words more energy strikes the sample than would reach it if the sample affected the wave front through its own area only. The effective absorbing area appears to be larger than the geometrical area of the sample. It may be remarked that similar

phenomena occur in any type of scattering problem, such as scattering of electromagnetic waves and scattering by atomic systems. Until recently the development of theoretical considerations of this so-called edge effect was hardly possible, because of the fact that the results of a mathematical analysis were not feasible for numerical treatment due to the lack of computational facilities. In this thesis the results of a mathematical investigation of three sound absorbing structures, incorporating edges, are finally presented in a numerical form. Some new aspects, which may well be of practical value, are drawn from the numerical results.

For a long time the edge effect has been felt to be a curious phenomenon in the practical application of sound absorbing materials. As early as 1900 SABINE already noticed this effect. Concerning his investigation of the influence of sound absorbing materials, such as cushions, upon the acoustics of the lecture room of the Fogg Art Museum of Harvard University, he wrote in *The American Architect* and *The Engineering Record*:

"Some early experiments in which the cushions were placed with one edge pushed against the backs of the settees gave results whose anomalous character suggested that, perhaps, their absorbing power depended not merely on the amount present but also on the area of the surface exposed. It was then recalled that about two years before, at the beginning of an evening's work, the first lot of cushions brought into the room were placed on the floor, side by side, with edges touching, but that after a few observations had been taken the cushions were scattered about the room, and the work was repeated. This was done not at all to uncover the edges, but in the primitive uncertainty as to whether near cushions would draw from each other's supply of sound, as it were, and thus diminish each other's efficiency. No further thought was then given to these discarded observations until recalled by the above-mentioned discrepancy. They were sought out from the notes of that period, and it was found that, as suspected, the absorbing power of the cushions when touching edges was less than when separated."

The sound field encountered in the reverberation chamber is very complicated, indeed. Sound is incident from all directions upon the sample and the absorption coefficient thus obtained applies to random incidence of sound.

In contrast to such complicated situations one might consider the simple case where a plane wave is incident upon an absorbing area of infinite dimensions, the incidence being normal or oblique. There will be a reflected plane wave which has a smaller amplitude than the incident one. The absorption coefficient is now defined as

$$(1.3) \quad a = 1 - |r|^2,$$

where r is the pressure reflection coefficient.

The case of normal incidence of a plane wave can be simply realized in the laboratory by isolating a part of the infinite plane wave in a rigid cylindrical tube terminated by the absorbing material and, subsequently, forgetting for the sound field outside the tube, which does not longer interest us. An instrument which is based on this concept is called an interferometer. It can be described

as a tube in which a sound source and the sample under test are inserted in opposition at either end thus closing the tube from both sides. The sound source is operated at such a low frequency that only plane waves can travel in the tube. We may describe the sound field in the tube as the superposition of two plane waves: an incident one and a reflected one. Owing to absorption, the reflected wave will have a smaller amplitude than the incident one. From the location and the values of the maxima and the minima of the pressure in the standing wave the reflection coefficient of the sample can be evaluated. The case of oblique incidence can be realized in a similar way. In addition to the plane wave component in the tube higher-order modes are possible. It can be shown that if the waveguide has a rectangular cross-section and is excited in a higher-order mode the situation is similar to oblique incidence of a plane wave. We shall not proceed further along these lines since it would take us too far.

It will be the general practise in this thesis to analyse problems by the complex exponential method. We represent a sinusoidal function of time with an angular frequency ω by the real part of a complex function. For example, at a fixed point in space \mathbf{R} we have the sound pressure

$$\psi(\mathbf{R}, t) = \text{Re} \left[p(\mathbf{R}) \exp(j\omega t) \right].$$

The function $p(\mathbf{R})$ denotes the complex representation of the sound pressure.

Since the major problem attacked in this thesis is to calculate the absorption of some sound absorbing structures, it is worthwhile to deal with the simplest problem of this kind, i.e., the absorption of a plane wave by an infinite sound-absorbing surface at normal and oblique incidence.

It now becomes desirable to discuss the behaviour of sound in the neighbourhood of a boundary surface and express it in terms of a boundary condition to be imposed on the sound pressure. The ratio of the sound pressure and the normal component of the velocity is referred to as the normal acoustic impedance. Often this quantity is not known a priori has to be determined experimentally. If the surface is porous so that air can penetrate into the surface material then there can be an average air velocity into the surface without motion of the boundary itself. The particle velocity perpendicular to the boundary at a particular point needs not be governed exclusively by the sound pressure at the same point, but may also be influenced by pressures at neighbouring points on the boundary. If the pores do not interconnect then it would be true that the mean normal velocity of penetration of the air into the pores has a constant ratio to the local pressure independent of the pressure and velocities of the sound field at the other points of the surface. For such a "locally reacting" boundary the normal impedance will be independent of the configuration of the incident wave and can be specified in advance as a characteristic property of the boundary. Many materials may be assumed to be approximately locally reacting, e.g., materials with a rather large air resistance and perforated porous tiles. Since the assumption that the boundary is locally reacting simplifies the problems considerably and since the assumption is frequently approximately fulfilled we shall accept its validity as a basis for our considerations.

We now define a complex parameter \hat{Z}_S , the normal specific acoustic impedance of the boundary

$$(1.4) \quad Z_s = p/u_n,$$

where p = the pressure at the boundary;
 u_n = the particle velocity normal to the boundary into the wall.

From the equation of motion we know that u_n is proportional to $\partial p/\partial n$, since

$$(1.5) \quad \partial p/\partial n = -j\omega\rho_0 u_n,$$

where ρ_0 = the density of the medium above the acoustic surface.

Then the boundary condition can be written in terms of p only, as follows

$$(1.6) \quad jk p = -\frac{Z_s}{\rho_0 c} \frac{\partial p}{\partial n},$$

where $k = \omega/c$ (the wave number);
 c = the sound velocity in the medium above the acoustic surface.

For plane waves the quantity $\rho_0 c$ is the ratio of the pressure to the associated particle velocity. It may be observed that the product of these quantities has greater significance as a characteristic property of the medium than does either ρ_0 or c , individually. For this reason $\rho_0 c$ is called the characteristic impedance of the medium above the sound absorbing surface.

For convenience' sake we introduce the reduced specific acoustic admittance

$$(1.7) \quad \eta = \rho_0 c/Z_s$$

With this notation the boundary condition Eq. (1.6), to be imposed on the sound pressure p , becomes:

$$(1.8) \quad \partial p/\partial n + jk\eta p = 0.$$

This type of boundary condition will be assumed valid for all sound absorbing surfaces discussed in this thesis.

A material which has recently been the subject of a profound experimental study concerning the edge effect, is the porous sound-absorbing material Sillan, consisting of rockwool and obtainable in different densities and thicknesses. This material may approximately be considered as locally reacting. In our computations we employ the data of Sillan SP 100, 5 cm thick; its impedance diagram is shown in Fig. 1.1.

Returning to our problem we suppose a plane sound wave to impinge upon a surface consisting of uniform acoustic material with admittance η , in a direction making an angle θ with the normal to the surface. The boundary coincides with the x,y -plane (Fig. 1.2). The representation of the incident wave, which satisfies the Helmholtz equation in rectangular co-ordinates

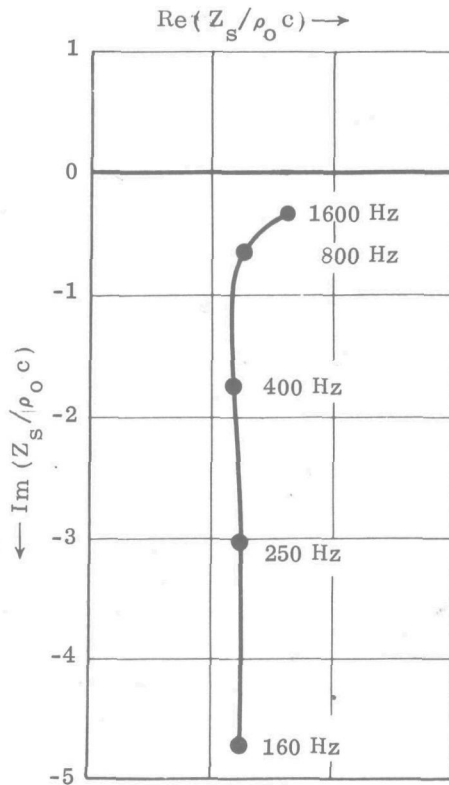


Fig. 1.1 The impedance diagram of Sillan SP 100, 5 cm thick.

$$(1.9) \quad \partial^2 p / \partial x^2 + \partial^2 p / \partial y^2 + \partial^2 p / \partial z^2 + k^2 p = 0$$

is

$$(1.10) \quad p^i = A_i \exp \left[j k x \sin(\theta) \cos(\varphi) + j k y \sin(\theta) \sin(\varphi) + j k z \cos(\theta) \right].$$

where A_i = the amplitude of the incident wave.

The reflected wave is then given by:

$$(1.11) \quad p^r = A_r \exp \left[j k x \sin(\theta) \cos(\varphi) + j k y \sin(\theta) \sin(\varphi) - j k z \cos(\theta) \right].$$

where A_r = the amplitude of the reflected wave, and the total pressure p^t by

$$(1.12) \quad p^t = p^i + p^r.$$

In order to express A_r in terms of A_i we insert the total pressure into the boundary condition Eq. (1.8). We then obtain

$$(1.13) \quad \frac{A_r}{A_i} = r = \frac{\cos(\theta) - \eta}{\cos(\theta) + \eta},$$

where r is the reflection coefficient.

The absorption coefficient a_{θ} of this infinitely large absorbing surface is now defined as

$$(1.14) \quad a_{\theta} = 1 - |r|^2.$$

Introducing the notation that $\eta = \text{Re}(\eta) + j \text{Im}(\eta)$, we obtain an expression for a_{θ} , being

$$(1.15) \quad a_{\theta} = \frac{4 \text{Re}(\eta) \cos(\theta)}{[\cos(\theta) + \text{Re}(\eta)]^2 + \text{Im}(\eta)^2}$$

For three values of η , borrowed from the impedance diagram of Sillan SP 100, 5 cm thick, a_{θ} has been plotted as a function of θ (Fig. 1.3). It is worth remarking that the amount of absorbed power has a maximum value at about $\theta = 60^{\circ}$. The curves also show that the fraction of power absorbed approaches zero as the angle of incidence approaches 90° . In fact Eq. (1.15) indicates that the surface would not absorb any power from a wave travelling parallel to the surface, no matter what the value of η is. This seems to be a contradiction of terms, for the pressure fluctuations in a wave parallel to the surface would cause motion of the medium above the surface in the direction perpendicular to the assumed direction of the wave. The fact of the matter is that a plane wave can not travel parallel to an infinite plane surface of non-zero admittance.

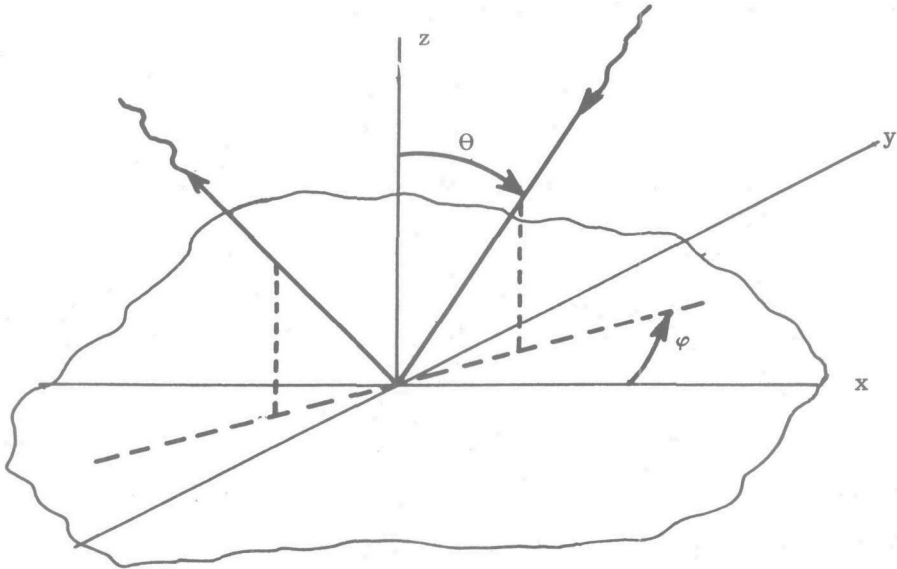


Fig. 1.2. A plane wave is incident upon the x, y - plane.

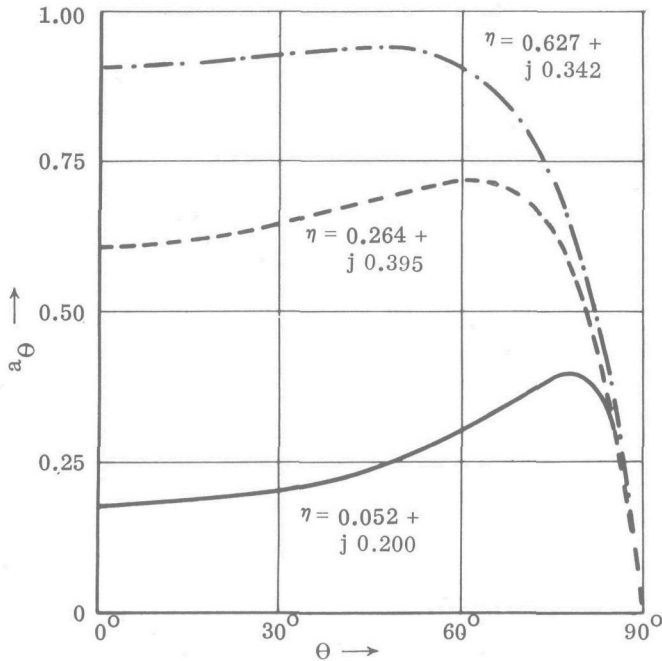


Fig. 1.3. The absorption coefficient a_θ as a function of the angle of incidence θ for three values of the reduced specific acoustic admittance η .

A different approach for the derivation of the absorption coefficient is to calculate directly the ratio of the absorbed power to the incident power. In order to find these quantities we start with the general formula for the time-averaged power flow density vector \underline{i}

$$(1.16) \quad \underline{i} = \frac{1}{2} \operatorname{Re} \left[p \underline{u}^* \right],$$

where \underline{u} is the particle velocity.

The power flow passing through a surface S is then given by

$$(1.17) \quad P = \frac{1}{2} \operatorname{Re} \left[\iint_S (p \underline{u}^* \cdot \underline{n}) dS \right]$$

where the quantity $\underline{u} \cdot \underline{n}$ represents the component of the particle velocity in the direction of the normal \underline{n} to the surface.

The power absorbed by a surface of area S , consisting of acoustical material with admittance η is now given by

$$(1.18) \quad P_a = \frac{1}{2} \frac{\operatorname{Re}(\eta)}{\rho_0 c} \iint_S |p|^2 dS$$

This result has been obtained with the aid of Eq. (1.4) for the particle velocity.

For a plane wave, represented by Eq. (1.10), the power incident upon an area S of the x,y -plane follows from Eq. (1.17) and the fact that $p = \rho_0 c u$:

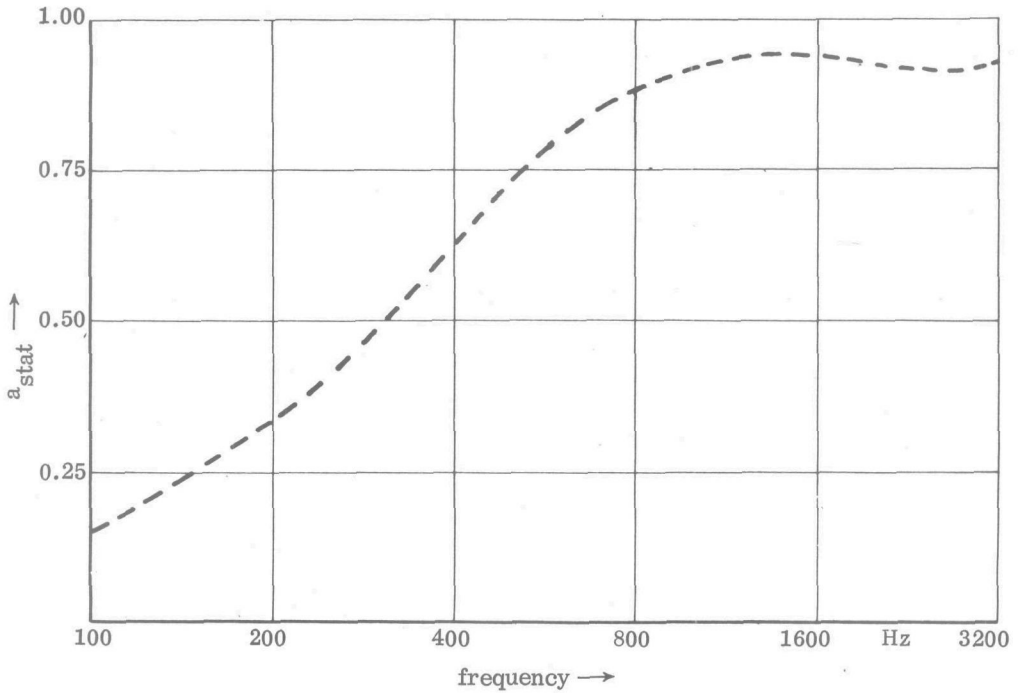


Fig. 1.4. The absorption coefficient a_{stat} as a function of frequency. The absorbing material is Sillan SP 100, 5 cm thick.

$$(1.19) \quad P_i = \frac{1}{2} |A_i|^2 \cos(\theta) S / \rho_0 c.$$

The absorption coefficient is determined as the ratio of P_a and P_i . Hence

$$(1.20) \quad a = \frac{\text{Re}(\eta)}{|A_i|^2 \cos(\theta) S} \iint_S |p|^2 dS$$

This definition is quite general and is often used for the computation of absorption coefficient in the problems, encountered in the thesis. If we insert the expression for the total pressure Eq. (1.12) at $z = 0$ into Eq. (1.20) we obtain again Eq. (1.15) for a_θ .

An adequate mean value of the absorption for locally reacting materials is found if the energy absorbed by a surface element that is exposed to a complete diffuse sound field is considered. The incident energy per unit area comprised in a small solid angle $d\Omega$ in a direction with an angle θ to the normal is proportional to $\cos(\theta)$, since the apparent surface of the surface element under consideration is proportional to $\cos(\theta)$. The mean value for statistical sound incidence is defined as

$$(1.21) \quad a_{\text{stat}} = \frac{\int a_\theta \cos(\theta) d\Omega}{\int \cos(\theta) d\Omega}$$

Now a_θ is only dependent upon θ ; therefore, take as an elementary solid angle $d\Omega$ the small angle between a circular cone around the normal with vertical

angle 2θ and a similar cone with vertical angle $2(\theta + d\theta)$, then $d\Omega = 2\pi \sin(\theta) d\theta$ and

$$(1.22) \quad a_{\text{stat}} = 2 \int_0^{\pi/2} a(\theta) \sin(\theta) \cos(\theta) d\theta.$$

This coefficient is usually referred to as the statistical average absorption coefficient. For locally reacting surfaces a_{θ} is known as a function of θ , so the integral can be evaluated (ZWIKKER & KOSTEN [1949]). For the acoustic material Sillan SP 100, 5 cm thick, a_{stat} has been plotted as function of frequency in Fig. 1.4.

Experiments show that a_E differs substantially from the coefficient a_{stat} by computing from interferometer data, even in the case of locally reacting materials. Moreover, it appears that a_E for a small area is substantially greater than that for a very large area. These differences in absorption coefficients are a consequence of the edge effect.

Many investigators have measured the dependence of the absorption coefficient on the dimensions of the sample. All these results are doubtful, however, because up till 1960 it was not known that the reverberant field in most reverberation chambers was far from diffuse and the results for the absorption coefficient were, therefore, considerably too low, so that comparison of these old values of the absorption coefficient with a_{stat} is meaningless.

In many of the older papers, the authors appear to be unaware of the fact that the important quantity is the edge length of the sample rather than the area. Only PARKINSON [1930] appreciated this essential point. His publication was, however, overlooked. An excellent review of these older papers concerning the edge effect has been represented in detail by KUHLE [1960].

KOSTEN [1960] suggested that the increased absorption is directly proportional to the relative edge length E (in m^{-1}) of the sample. The implication is that

$$(1.23) \quad a_E = a_{\text{stat}} + b_{\text{stat}} E.$$

where b_{stat} (in m) is the edge effect constant.

Results of a round robin, reported by KOSTEN [1960] illustrate the existence of such a proportionality factor b_{stat} . Starting from this idea KUHLE [1960] has plotted different experimental results of former investigators in a new way. He also found agreement between these results and KOSTEN's statement. KUHLE himself has done some new experimental work concerning the edge effect of Sillan SP 120. He showed that the edge effect is reduced, if the edges of the sample are lined with broad vertical planks. This experiment gives a good indication as to the existence of diffraction phenomena at the edge. KUHLE and later afterwards TEN WOLDE [1967] found b_{stat} to be a function of the frequency and, of course, to be dependent on the type of acoustical material. The constant b_{stat} has a maximum value of the order of 0.25 m somewhere in the neighbourhood of 500 Hz (Fig. 1.5).

For small areas, E is large, the linearity of the relation between a_E and E is not so good. It is then perhaps better to speak of the "area effect".

Theoretical aspects have been studied by many authors. Most of these investigations concern the sound absorption of an acoustic strip. The results of these investigations will be discussed in the introduction of Chapter III.

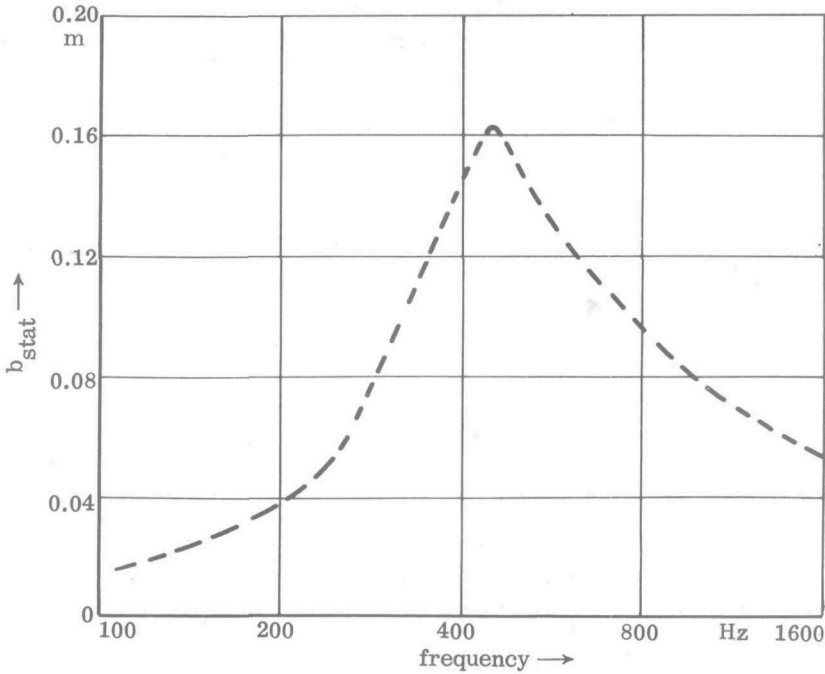


Fig. 1.5. The edge effect constant b_{stat} as a function of frequency for the sound absorbing material Sillan SP 100, 5 cm thick (after TEN WOLDE [1967]).

In this thesis we deal with the scattering and absorption of a plane wave by:

- (1) a semi-infinite absorbing plane supplemented to an infinite hard plane;
- (2) an absorbing acoustic strip lying on an infinite hard plane;
- (3) absorbing acoustic strips lying in a periodic arrangement.

All three absorbing configurations are assumed to coincide with the x, y -plane of a rectangular co-ordinate system and to extend indefinitely in the y -direction and to be uniform in this direction. The representation of the incident wave is given by Eq. (1.10).

For the sake of convenience we introduce the direction cosines

$$\alpha_0 = k \sin(\theta) \cos(\varphi), \quad \beta_0 = k \sin(\theta) \sin(\varphi) \quad \text{and} \quad \gamma_0 = k \cos(\theta).$$

In terms of these quantities we have

$$(1.24) \quad p^i = \exp \left[j \alpha_0 x + j \beta_0 y + j \gamma_0 z \right]$$

Without any loss of generality the amplitude of p^i is assumed to be unity.

Because of the fact that the absorbing configurations extend to infinity in the y -direction without any discontinuity and that the incident wave is assumed to be a plane wave, it is obvious that the boundary conditions and the wave equation are invariant under a translation in the y -direction. Consequently, the

y-dependence of the incident and the scattered fields are the same. Accordingly, let us write for the pressure

$$(1.25) \quad p(x, y, z) = \exp(j\beta_0 y) \Phi(x, z),$$

where Φ is a function related to the sound pressure.

In this notation the incident field becomes

$$(1.26) \quad \Phi^i = \exp \left[j\alpha_0 x + j\gamma_0 z \right].$$

Inserting Eq. (1.25) into Eq. (1.9) we obtain the two-dimensional Helmholtz equation

$$(1.27) \quad \partial^2 \Phi / \partial x^2 + \partial^2 \Phi / \partial z^2 + \kappa^2 \Phi = 0,$$

where $\kappa^2 = k^2 - \beta_0^2$.

All problems, encountered in the next chapters are solved by taking the simplified expression for the pressure given in Eq. (1.25).

The reasons for considering the three mathematical models listed above are given in the introductions to the different chapters.

CHAPTER II

Diffraction and absorption by an absorbing half-plane

2.1 Introduction

In the previous chapter we discussed the fact that the additional absorption due to diffraction of the waves at the edge was approximately proportional to the relative edge length of the sample. The shape of the sample was not important to the effect if the sample were not too small in respect to the wave length. The observed changes in the absorption coefficient can be attributed to sound scattered by the sample in such a way that the part of the absorbing surface near the edge generally absorbs more sound power than an equally large area near the centre. The additionally absorbed power near the edge of a large sample will be greatest near the edge and will decrease away from the edge falling off to a negligible value in a distance of several wavelengths. DANIEL [1963] showed this fact in an experiment concerning one straight edge of a large fiber glass blanket lying on the floor of a reverberation chamber.

It seems to be reasonable that the diffraction by a large sample of rectangular shape can be constructed as the diffraction for four separate half-planes. For this reason, the present chapter will be devoted to the calculation of the diffraction and absorption by an absorbing semi-infinite plane lying on an infinite acoustically hard plane, when a plane wave is incident from an arbitrary direction.

Many authors have given attention to diffraction by a half-plane. The oldest investigation is due to SOMMERFELD [1896] who considered the conducting half-plane. SOMMERFELD's basic concept was a multivalued solution of the wave equation. COPSON [1946] and SCHWINGER formulated the problem in terms of an integral equation, which they solved by the Wiener-Hopf method (NOBLE [1958a]).

SENIOR [1951] extended the method to a metallic sheet of finite conductivity. He derived explicit expressions containing Fresnel integrals for the distant field. The difficulty in extending the Sommerfeld problem to a finitely conducting half-plane lies in the so-called factorization of the Fourier transformed kernel function. This explains why it is difficult for the problem considered by SENIOR to obtain simple expressions for the diffracted field.

HEINS and FESHBACH [1954] investigated the effect of a plane wave incident upon an infinite plane divided into two half-planes by a straight line. Each of the two half-planes is assumed to have acoustic properties which can be expressed by an acoustic admittance. The solution found by these authors, obtained by solving the relevant integral equation, is very complicated due to the great difficulties met in the process of factorization. In general, the integral equation method needs the choice of a suitable Green's function, the formulation of the integral equation and the application of integral transforms in order to

solve the integral equation. The Green's function method for formulating an integral equation is sometimes cumbersome (HEINS & FESHBACH [1954]). Often it is far from obvious which Green's function should be chosen. The main advantage of the integral equation method of approach seems to be that it is easy to recognize whether the problems can be solved by the Wiener-Hopf technique or not.

All the problems just mentioned are amenable to a simpler treatment based on representation of the scattered field as an angular spectrum of plane waves (CLEMMOW [1966a]). This directly leads to a pair of dual integral equations which replace the single integral equation. The distinction lies in the choice of a plane wave as the fundamental field rather than the field due to a line source.

The concept of a field built up out of elementary waves generated by a source is directly employed in Huygens' principle and the classical Kirchhoff diffraction theory. That the alternative concept of a plane wave spectrum may be more convenient in the theory of diffraction has been recognized for a long time.

The technique has originally been developed in connection with the theory of radio propagation over a non-homogeneous earth (BOOKER & CLEMMOW [1950a, b]). In the present chapter we apply it to the two-dimensional problem of a plane wave incident upon a half-plane. The dual integral equations obtained through an application of the boundary conditions at the half-plane can be solved with the aid of complex function theory through a technique which uses the same arguments as the Wiener-Hopf method. From the expression for the scattered field we derive a quantity for the additional power absorbed by the edge. In the case of a diffuse sound field we define a quantity b_{stat} being the ratio of the additional power per unit edge length and the incident intensity. The dimension of this quantity is a length so we expect this quantity to be the same as the one which is experimentally detected in the reverberation chamber. Comparison of theoretical and experimental results is now possible.

2.2 Mathematical formulation of the problem

Let a plane wave be incident upon the structure, which is located in the x, y -plane (Fig. 2.1). In the domain $-\infty < x < 0, -\infty < y < \infty, z = 0$ this plane is acoustically hard, in the domain $0 < x < \infty, -\infty < y < \infty, z = 0$ this plane consists of sound absorbing material, whose properties are characterized by a reduced specific acoustic admittance η .

The space dependence of the incident wave is specified in Eq. (1.24).

As explained in Chapter I, this three-dimensional scattering problem can be reduced to a two-dimensional one.

The total sound pressure is written as the superposition of three contributions: the incident field Φ^i , a field Φ^r reflected against an acoustically hard boundary of infinite extent and a scattered field Φ^s . The expression for the total field therefore can be written as

$$(2.1) \quad \Phi^t(x, z) = \exp(j\alpha_0 x + j\gamma_0 z) + \exp(j\alpha_0 x - j\gamma_0 z) + \Phi^s.$$

We first seek a suitable representation for Φ^s .

An elementary solution of the Helmholtz equation is the plane wave:

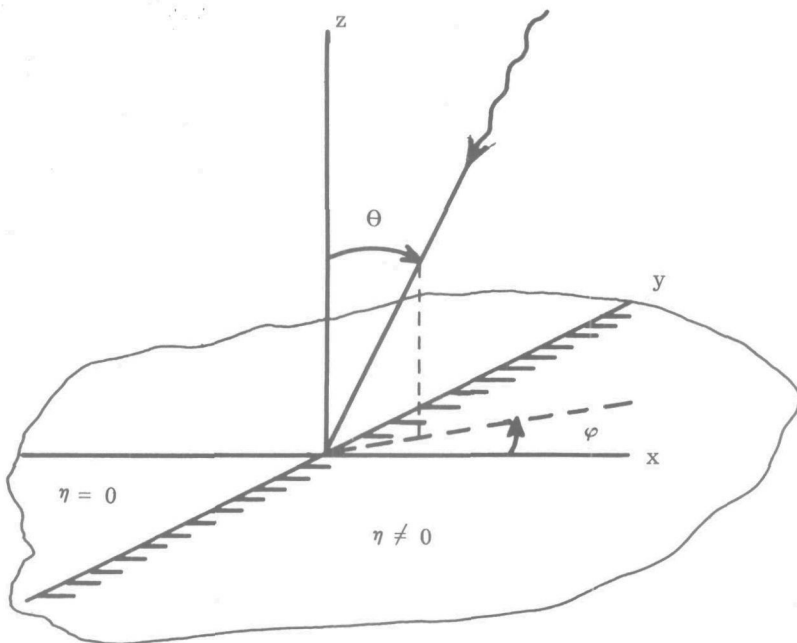


Fig. 2.1. Geometry of the diffraction problem.

$$(2.2) \quad \exp \left[-j\alpha x \pm j(\kappa^2 - \alpha^2)^{\frac{1}{2}} z \right].$$

If $(\kappa^2 - \alpha^2)^{\frac{1}{2}}$ is real (2.2) represents an uniform plane wave; if on the other hand $(\kappa^2 - \alpha^2)^{\frac{1}{2}}$ is imaginary or complex (2.2) represents a non-uniform plane wave. Now it can be shown that any solution of the Helmholtz equation can be brought into the form of an angular spectrum of plane waves:

$$(2.3) \quad \frac{1}{2\pi j} \int_{\mathcal{L}} f(\alpha) \exp \left[-j\alpha x \pm j(\kappa^2 - \alpha^2)^{\frac{1}{2}} z \right] d\alpha,$$

by a suitable choice of the path of integration \mathcal{L} and the function $f(\alpha)$ (CLEMMOW [1966 b]). Such a representation is closely linked with the expression of an arbitrary function by means of a Fourier integral. The function $f(\alpha)$ is the spectrum function which specifies in terms of amplitude and phase, the "weight" attached to each plane wave of the spectrum. Without loss of generality a suitable fixed path of integration can be selected so that the problem under consideration becomes a matter of determining the appropriate spectrum function $f(\alpha)$.

The first condition to be imposed on the scattered field is founded on the Sommerfeld radiation condition and this implies that this field consists solely of

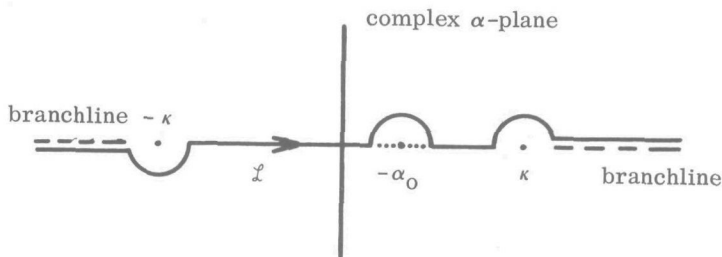


Fig. 2.2. The path of integration \mathcal{L} in the complex α -plane.

either plane waves travelling in the direction of the positive z -axis or waves decreasing exponentially in this direction. If the sign of the square root $(\kappa^2 - \alpha^2)^{\frac{1}{2}}$ is chosen such that $\text{Re}(\kappa^2 - \alpha^2)^{\frac{1}{2}} > 0$ in the entire α -plane then only the solution

$$(2.4) \quad \frac{1}{2\pi j} \int_{\mathcal{L}} f(\alpha) \exp \left[-j\alpha x - j(\kappa^2 - \alpha^2)^{\frac{1}{2}} z \right] d\alpha$$

satisfies this requirement. The choice of the square root implies that the branch cuts are situated at $\text{Im}(\alpha) = 0$ and $\kappa < |\text{Re}(\alpha)| < \infty$ (Fig. 2.2.).

The path of integration in the complex α -plane must run the full range from $-\infty$ to ∞ as shown in Fig. 2.2. The reason for this choice of the limits of the integral is that we expect in the plane $z = 0$ different field representations for $x < 0$ and $x > 0$, respectively, on account of the discontinuity in the boundary conditions at $x = 0, z = 0$. For a precise determination of the contour \mathcal{L} in the complex α -plane we must determine the behaviour of the square root $(\kappa^2 - \alpha^2)^{\frac{1}{2}}$ in the complex α -plane.

Let

$$(2.5) \quad (\kappa^2 - \alpha^2)^{\frac{1}{2}} = \kappa_1 + j\kappa_2$$

in which κ_1 and κ_2 are real, and let $\alpha = \alpha_1 + j\alpha_2$

then by squaring both sides of Eq. (2.5) we obtain $\kappa^2 - \alpha_1^2 + \alpha_2^2 = \kappa_1^2 - \kappa_2^2$

and $-\alpha_1\alpha_2 = \kappa_1\kappa_2$

Since Φ^S is bounded as $z \rightarrow \infty$ we must assume that $\kappa_2 \leq 0$ on the path of integration. Consequently, $\kappa_1\kappa_2 \leq 0$, or since $\kappa_1 > 0$ (see above) we have $\alpha_1\alpha_2 > 0$. This situation occurs only in the first and the third quadrants. For this reason the path of integration \mathcal{L} is located in these regions of the complex α -plane. Further the contour may not extend to infinity in a direction other than along the real axis because of the boundedness of the field at any finite x . Therefore, the path of integration must pass along the real axis to infinity in the first or third quadrant.

The boundary conditions from which the spectrum function is to be determined are

$$(2.6) \quad \partial \Phi^t / \partial z = j k \eta \Phi^t, \quad 0 < x < \infty, \quad z = 0,$$

$$(2.7) \quad \partial \Phi^t / \partial z = 0, \quad -\infty < x < 0, \quad z = 0.$$

With the aid of Eqs. (2.1), (2.4), (2.6) and (2.7) we have

$$(2.8) \quad \frac{1}{2\pi j} \int_{\mathcal{L}} f(\alpha) \left[k \eta + (\kappa^2 - \alpha^2)^{\frac{1}{2}} \right] \exp(-j\alpha x) d\alpha = -2k\eta \exp(j\alpha_0 x), \quad 0 < x < \infty;$$

$$(2.9) \quad \frac{1}{2\pi j} \int_{\mathcal{L}} f(\alpha) (\kappa^2 - \alpha^2)^{\frac{1}{2}} \exp(-j\alpha x) d\alpha = 0, \quad -\infty < x < 0.$$

Eqs. (2.8) and (2.9) are dual integral equations in the unknown spectrum function $f(\alpha)$.

2.3 The solution of the dual integral equations

It is convenient to introduce the following notations:

The domain of the complex α -plane above the path of integration (the upper half-plane) will be referred to as D^+ and the domain below the path of integration \mathcal{L} (the lower half-plane) as to D^- . Further, functions which are free of singularities and zeros in D^+ and of algebraic growth at infinity therein will be denoted by the subscript + and those free of singularities and zeros in D^- and of algebraic growth at infinity therein will be denoted by the subscript -.

The dual integral equations Eqs. (2.8) and (2.9) may be solved as follows. If we bear in mind that x is negative in the left-hand side of Eq. (2.9), we may close the path of integration with a semicircle at infinity in D^+ provided that this procedure does not lead to any additional contribution to the integral.

This latter requirement is only fulfilled if $f(\alpha) \cdot (\kappa^2 - \alpha^2)^{\frac{1}{2}}$ tends to zero as $|\alpha| \rightarrow \infty$ in D^+ by virtue of Jordan's lemma (WHITTAKER & WATSON [1927a]). Let $g_+(\alpha)$ be any function which is regular in D^+ and of algebraic growth at infinity therein, and let $g_+(\alpha) \rightarrow 0$ as $|\alpha| \rightarrow \infty$ in D^+ , then the integral equation of Eq. (2.9) is clearly satisfied by:

$$(2.10) \quad g_+(\alpha) = f(\alpha) (\kappa^2 - \alpha^2)^{\frac{1}{2}}$$

The function $g_+(\alpha)$ is now substituted into the first integral equation of Eq. (2.8). We then obtain

$$(2.11) \quad \frac{1}{2\pi j} \int_{\mathcal{L}} g_+(\alpha) \left[1 + k\eta (\kappa^2 - \alpha^2)^{-\frac{1}{2}} \right] \exp(-j\alpha x) d\alpha = -2k\eta \exp(j\alpha_0 x),$$

$0 < x < \infty.$

We introduce the function $K(\alpha) \stackrel{\text{def}}{=} 1 + k\eta(\kappa^2 - \alpha^2)^{-\frac{1}{2}}$. This function has two singularities in the complex α -plane:

- (1) a branch point $\alpha = -\kappa$ in D^+ ;
- (2) a branch point $\alpha = \kappa$ in D^- .

We now assume that $K(\alpha)$ can be written as a product of two functions $K_+(\alpha)$ and $K_-(\alpha)$ which have the following properties:

- (1) $K_+(\alpha) K_-(\alpha) = K(\alpha)$ on \mathcal{L} ;
- (2) $K_+(\alpha)$ is regular in D^+ and has the behaviour $K_+(\alpha) \rightarrow 1$ as $|\alpha| \rightarrow \infty$ in D^+ ;
- (3) $K_-(\alpha)$ is regular in D^- and has the behaviour $K_-(\alpha) \rightarrow 1$ as $|\alpha| \rightarrow \infty$ in D^- .

That such a factorization is possible is known from the general Wiener-Hopf theory (NOBLE [1958b]) and explicit expressions for $K_+(\alpha)$ and $K_-(\alpha)$ are given in the next section.

The integral equation can be written as

$$(2.12) \quad \frac{1}{2\pi j} \int_{\mathcal{L}} g_+(\alpha) K_+(\alpha) K_-(\alpha) \exp(-j\alpha x) d\alpha = 2k\eta \exp(j\alpha_0 x), \quad 0 < x < \infty.$$

By virtue of Cauchy's theorem we may write for the right-hand side of Eq. (2.12)

$$(2.13) \quad -2k\eta \exp(j\alpha_0 x) = \frac{2k\eta}{2\pi j} \int_{\mathcal{L}} \frac{\exp(-j\alpha x)}{(\alpha + \alpha_0)} d\alpha,$$

provided that the path of integration \mathcal{L} is indented above the pole $\alpha = -\alpha_0$. This leads to the integral equation

$$(2.14) \quad \frac{1}{2\pi j} \int_{\mathcal{L}} \left[g_+(\alpha) K_+(\alpha) K_-(\alpha) - \frac{2k\eta}{(\alpha + \alpha_0)} \right] \exp(-j\alpha x) d\alpha = 0, \quad 0 < x < \infty.$$

Likewise in the integral for $x > 0$ we can close the path of integration with a semicircle at infinity in D^- without making any additional contribution to the integral on the assumption that a function $h_-(\alpha)$ exists which is regular in D^- and of algebraic growth at infinity therein and satisfies the following requirements:

- (1) $h_-(\alpha) = g_+(\alpha) (\alpha + \alpha_0) K_+(\alpha)$;
- (2) $h_-(\alpha) = 2k\eta / K_-(\alpha)$;
- (3) $h_-(\alpha) / (\alpha + \alpha_0) = O(\alpha^{-1})$ as $|\alpha| \rightarrow \infty$ in D^- .

Substitution of this function $h_-(\alpha)$ in the integral equation leads to

$$(2.15) \quad \frac{1}{2\pi j} \int_{\mathcal{L}} \left[\frac{h_-(\alpha)}{(\alpha + \alpha_0)} K_-(\alpha) - \frac{2k\eta}{(\alpha + \alpha_0)} \right] \exp(-j\alpha x) d\alpha = 0, \quad 0 < x < \infty.$$

It is clear from the second requirement for $h_-(\alpha)$ that the non-exponential part of the integrand of Eq. (2.15) is regular in D^- . The function $h_-(\alpha)$ is a product of three functions which are regular in D^+ . Moreover, $h_-(\alpha)$ is regular in D^- , hence this function is regular in the entire α -plane and has algebraic

behaviour as α tends to infinity. Accordingly, we denote $h_-(\alpha)$ by $h(\alpha)$. Such functions are called integral functions. We proceed to examine the behaviour of $h(\alpha)$ as α tends to infinity in order to apply the extended form of Liouville's theorem (NOBLE [1958c]). From the third requirement we conclude that $h(\alpha) = O(|\alpha|^{+q})$, $q < 1$ as $|\alpha| \rightarrow \infty$. From Liouville's theorem $h(\alpha)$ must be a polynomial of degree less than or equal to $[q]$ where $[q]$ is the integral part of q . From the fact that $q < 1$ we state that the polynomial contains only a constant, viz. $h(-\alpha_0) = h_-(\alpha_0)$.

From all this we obtain

$$(2.16) \quad f(\alpha) = 2k\eta \left[(\kappa^2 - \alpha^2)^{\frac{1}{2}} K_-(-\alpha_0) K_+(\alpha) (\alpha + \alpha_0) \right]^{-1}$$

and

$$(2.17) \quad \begin{aligned} \phi^t(x, z) &= \exp(j\alpha_0 x + j\gamma_0 z) + \exp(j\alpha_0 x - j\gamma_0 z) \\ &+ \frac{2k\eta}{2\pi j} \int_{\mathcal{L}} \frac{\exp[-j\alpha x - j(\kappa^2 - \alpha^2)^{\frac{1}{2}} z] d\alpha}{(\alpha + \alpha_0) (\kappa^2 - \alpha^2)^{\frac{1}{2}} K_-(-\alpha_0) K_+(\alpha)}. \end{aligned}$$

Applying once more the boundary condition at $x > 0$, $z = 0$, Eq (2.6), we obtain for the field distribution at the absorbing half-plane

$$(2.18) \quad \phi^t(x, 0) = \frac{-2}{2\pi j} \int_{\mathcal{L}} \frac{\exp(-j\alpha x) d\alpha}{K_-(-\alpha_0) K_+(\alpha) (\alpha + \alpha_0)}, \quad 0 < x < \infty, \quad z = 0.$$

2.4 The factorization of $K(\alpha)$.

The required factorization of $K(\alpha)$ may be carried out with the aid of Cauchy's integral theorem. In order to accomplish this we note that the multiplicative decomposition of $K(\alpha)$ is essentially equivalent to the additive decomposition of the logarithm of $K(\alpha)$. For convenience' sake we introduce the following notation:

$$(2.19) \quad L(\alpha) = \ln [K(\alpha)]$$

The function $L(\alpha)$ satisfies the Hölder condition

$$(2.20) \quad |L(\alpha_1) - L(\alpha_2)| < A |\alpha_1 - \alpha_2|^\mu$$

with $A > 0$ and $\mu > 0$ and has the behaviour at infinity

$$(2.21) \quad L(\alpha) = O(|\alpha|^{-1}), \text{ for } |\alpha| \rightarrow \infty$$

We now define two functions

$$(2.22) \quad L_+(\alpha) \stackrel{\text{def}}{=} \frac{1}{2\pi j} \int_{\mathcal{L}} \frac{L(s) ds}{(s-\alpha)}, \quad \alpha \text{ in } D^+;$$

$$(2.23) \quad L_-(\alpha) \stackrel{\text{def}}{=} -\frac{1}{2\pi j} \int_{\mathcal{L}} \frac{L(s) ds}{(s-\alpha)}, \quad \alpha \text{ in } D^-.$$

These integrals are absolutely convergent by virtue of Eqs. (2.20) and (2.21), provided that α does not lie on the path of integration \mathcal{L} . The function $L_+(\alpha)$ is regular in D^+ , the function $L_-(\alpha)$ is regular in D^- (NOBLE [1958b]). For a point α_1 on the contour we define

$$(2.24) \quad L_+(\alpha_1) \stackrel{\text{def}}{=} \lim_{\alpha \rightarrow \alpha_1} L_+(\alpha)$$

where $\alpha \rightarrow \alpha_1$ along values in D^+ ;

$$(2.25) \quad L_-(\alpha_1) \stackrel{\text{def}}{=} \lim_{\alpha \rightarrow \alpha_1} L_-(\alpha)$$

where $\alpha \rightarrow \alpha_1$ along values in D^- .

we now state that

$$(2.26) \quad L_+(\alpha_1) + L_-(\alpha_1) = L(\alpha_1).$$

In order to prove this statement the limits in Eqs. (2.24) and (2.25) have to be determined with the aid of Eqs. (2.22) and (2.23) (DE HOOP [1963]). After some manipulations with the integrals in Eqs. (2.22) and (2.23) we obtain

$$(2.27) \quad L_+(\alpha_1) = \frac{1}{2} L(\alpha_1) + \frac{1}{2\pi j} \mathcal{P} \int_{\mathcal{L}} \frac{L(s) ds}{(s-\alpha_1)}$$

$$(2.28) \quad L_-(\alpha_1) = \frac{1}{2} L(\alpha_1) - \frac{1}{2\pi j} \mathcal{P} \int_{\mathcal{L}} \frac{L(s) ds}{(s-\alpha_1)}$$

where \mathcal{P} denotes the Cauchy principal value (WHITTAKER & WATSON [1927b]). 'Addition of these formulae yields Eq. (2.26). The formulae (2.27) and (2.28) are a special case of PLEMELJ's formulae. (MUSKHELISHVILI [1953]).

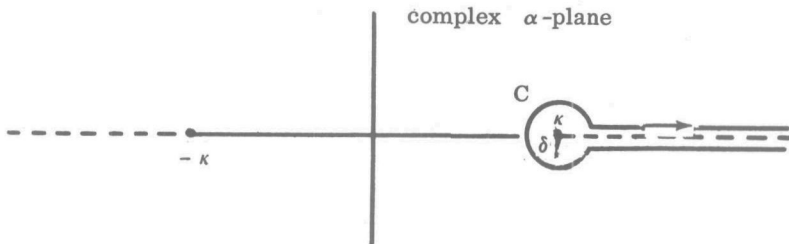


Fig. 2.3. The deformation of the contour \mathcal{L} in order to calculate the function $K_+(\alpha)$.

From a calculational point of view we deform the path of integration \mathcal{L} , as shown in Fig. 2.3. The loop integral around the branch line gives three contributions:

$$(2.29) \quad L_+(\alpha) = \frac{1}{2\pi j} \int_C \frac{L(s) ds}{(s-\alpha)} + \frac{1}{2\pi j} \int_{\kappa-\delta}^{\infty} \frac{L(s) ds}{(s-\alpha)} + \frac{-1}{2\pi j} \int_{\kappa-\delta}^{\infty} \frac{L_1(s) ds}{(s-\alpha)}.$$

$L_1(s)$ is obtained from $L(s)$ by replacing $-j(s^2 - \kappa^2)^{\frac{1}{2}}$ by $(s^2 - \kappa^2)^{\frac{1}{2}}$.

The contribution from the circular arc C around the branch point κ can be shown to vanish in the limit of vanishing radius. Thus we obtain

$$(2.30) \quad L_+(\alpha) = \frac{1}{2\pi j} \int_{\kappa}^{\infty} \frac{L(s) ds}{(s-\alpha)} - \frac{1}{2\pi j} \int_{\kappa}^{\infty} \frac{L_1(s) ds}{(s-\alpha)}$$

or

$$(2.31) \quad \ln [K_+(\alpha)] = \frac{1}{2\pi j} \int_{\kappa}^{\infty} \ln \left[\frac{-j(s^2 - \kappa^2)^{\frac{1}{2}} + k\eta}{-j(s^2 - \kappa^2)^{\frac{1}{2}} - k\eta} \right] \frac{ds}{(s-\alpha)}$$

or

$$(2.32) \quad K_+(\alpha) = \exp \left[\frac{1}{2\pi j} \int_{\kappa}^{\infty} \ln \left\{ \frac{-j(s^2 - \kappa^2)^{\frac{1}{2}} + k\eta}{-j(s^2 - \kappa^2)^{\frac{1}{2}} - k\eta} \right\} \frac{ds}{(s-\alpha)} \right].$$

In a similar way we find

$$(2.33) \quad K_-(\alpha) = \exp \left[\frac{1}{2\pi j} \int_{\kappa}^{\infty} \ln \left\{ \frac{-j(s^2 - \kappa^2)^{\frac{1}{2}} + k\eta}{-j(s^2 - \kappa^2)^{\frac{1}{2}} - k\eta} \right\} \frac{ds}{s+\alpha} \right].$$

These expressions for $K_+(\alpha)$ and $K_-(\alpha)$ can be used everywhere in the α -plane, except on the path of integration.

2.5 Asymptotic evaluation of the scattered field

Consider Eq. (2.18) for the field directly above the absorbing surface ($x > 0, z = 0$). We may supplement the contour by a semicircle at infinity in the lower half-plane D^- . There are two singularities of the integrand: the pole $\alpha = -\alpha_0$ and the branch point $\alpha = \kappa$.

The contribution from the pole is :

$$(2.34) \quad \Phi^{\text{as}}(x, 0) = \frac{2 \exp(j\alpha_0 x)}{K_-(-\alpha_0)K_+(-\alpha_0)} = \psi^{\text{as}} \exp(j\alpha_0 x), \quad 0 < x < \infty$$

where

$$(2.35) \quad \psi^{\text{as}} = \frac{2\gamma_0}{\gamma_0 + k\eta}.$$

The conclusion is that the contribution from the pole gives a term which exactly agrees with the field just above the absorbing surface far from the discontinuity at $x = 0$. We should also say that Φ^{as} represents the field above the x, y -plane as if there were no discontinuity in the admittance and the entire x, y -plane were to consist of sound absorbing material (cf. Chapter I).

The loop integral around the branch line gives:

$$(2.36) \quad \Phi^{\text{dif}}(x, 0) = \int_{\kappa}^{\infty} \psi^{\text{dif}}(\alpha) \exp(-j\alpha x) d\alpha$$

where

$$(2.37) \quad \psi^{\text{dif}}(\alpha) = -\frac{2K_-(\alpha)}{2\pi j(\alpha + \alpha_0)K_-(-\alpha_0)} \left[\frac{1}{K(\alpha)} - \frac{1}{M(\alpha)} \right].$$

$M(\alpha)$ is obtained from $K(\alpha)$ by replacing $-j(s^2 - \kappa^2)^{\frac{1}{2}}$ by $j(s^2 - \kappa^2)^{\frac{1}{2}}$.

Thus Φ^{dif} is the field component that indicates the scattering of the plane wave by the discontinuity in the boundary conditions at $x = 0, z = 0$.

The approximation of this integral for the case $x \rightarrow \infty$ can be carried out with the aid of an asymptotic expansion of the integral (ERDELYI [1956]). In order to perform the integration required by Eq. (2.36) the behaviour of ψ^{dif} in the vicinity of the branch point κ is important. It turns out that $\psi^{\text{dif}} = O(\alpha - \kappa)^{\frac{1}{2}}$ as $\alpha \rightarrow \kappa$. For a Fourier integral whose integrand has a singularity of this simple type at an end point of the interval, it can be shown that

$$(2.38) \quad \int_{\kappa}^{\infty} \psi^{\text{dif}}(\alpha) \exp(-j\alpha x) d\alpha = A x^{-\frac{3}{2}} \exp(-j\kappa x).$$

This solution, where A is some constant, has the character of a wave with decreasing amplitude in the positive x-direction.

Eq.(2.38) is usually called the "edge wave" approximation (CLEMMOW [1966c]).

2.6 The quantities P_{edge} , b and b_{stat}

We must derive a quantity which indicates the additional absorption due to diffraction of the waves in the neighbourhood of the edge. Therefore, we introduce P_{edge} being the additional power absorbed by an infinitely long strip of the absorbing half-plane with unit width in the y-direction. In the previous section we pointed out that the total field consists of two contributions: Φ^{as} and Φ^{dif} ; Φ^{dif} is the field that gives rise to an additional absorption. For the derivation of P_{edge} we refer to the general formula for sound absorption, Eq. (1.18). For P_{edge} this leads to:

$$(2.39) \quad P_{edge} = \frac{1}{2} \frac{\text{Re}(\eta)}{\rho_0 c} \lim_{X \rightarrow \infty} \int_0^1 dy \int_0^X \left\{ |p^t(x, y, 0)|^2 - |p^{as}(x, y, 0)|^2 \right\} dx$$

Note that P_{edge} has been expressed as the difference of the true absorbed power and the extrapolated asymptotic value of the absorbed power. The integration with respect to the variable y is very simple being unity since

$$|p^t(x, y, z)|^2 = |\Phi^t(x, z)|^2$$

and

$$|p^{as}(x, y, 0)|^2 = |\Phi^{as}(x, 0)|^2.$$

Hence we obtain:

$$(2.40) \quad P_{edge} = \frac{1}{2} \frac{\text{Re}(\eta)}{\rho_0 c} \lim_{X \rightarrow \infty} \int_0^X \left\{ |\Phi^t(x, 0)|^2 - |\Phi^{as}(x, 0)|^2 \right\} dx$$

$$= \frac{1}{2} \frac{\text{Re}(\eta)}{\rho_0 c} \lim_{X \rightarrow \infty} \int_0^X \left\{ |\Phi^{dif}(x, 0)|^2 + \Phi^{dif}(x, 0) \Phi^{as*}(x, 0) \right.$$

$$\left. + \Phi^{dif*}(x, 0) \Phi^{as}(x, 0) \right\} dx.$$

We have introduced an upper limit since $\int_0^{\infty} |\Phi^t(x,0)|^2 dx$ and $\int_0^{\infty} |\Phi^{as}(x,0)|^2 dx$ are not convergent.

The difference between these integrals does converge on account of the fact that ψ^{dif} approaches zero strongly enough as $x \rightarrow \infty$. We now have a sum of three integrals:

$$\begin{aligned}
 (2.41.I) \quad & \lim_{X \rightarrow \infty} \int_0^X dx \int_{\kappa}^{\infty} \psi^{dif}(\alpha) \exp(-j\alpha x) d\alpha \int_{\kappa}^{\infty} \psi^{dif*}(\beta) \exp(j\beta x) d\beta \\
 &= \lim_{X \rightarrow \infty} \int_0^X dx \int_{\kappa}^{\infty} \psi^{dif}(\alpha) d\alpha \int_{\kappa}^{\infty} \psi^{dif*}(\beta) \exp[-j(\alpha - \beta)x] d\beta \\
 &= \lim_{X \rightarrow \infty} \int_{\kappa}^{\infty} \psi^{dif}(\alpha) d\alpha \int_{\kappa}^{\infty} \psi^{dif*}(\beta) \frac{\exp[-j(\alpha - \beta)X] - 1}{-j(\alpha - \beta)} d\beta;
 \end{aligned}$$

$$\begin{aligned}
 (2.41.II) \quad & \lim_{X \rightarrow \infty} \psi^{as*} \int_0^X \exp(-j\alpha_0 x) dx \int_{\kappa}^{\infty} \psi^{dif}(\alpha) \exp(-j\alpha x) d\alpha \\
 &= \lim_{X \rightarrow \infty} \psi^{as*} \int_{\kappa}^{\infty} \psi^{dif}(\alpha) \frac{\exp[-j(\alpha + \alpha_0)X] - 1}{-j(\alpha + \alpha_0)} d\alpha;
 \end{aligned}$$

$$\begin{aligned}
 (2.41.III) \quad & \lim_{X \rightarrow \infty} \psi^{as} \int_0^X \exp(j\alpha_0 x) dx \int_{\kappa}^{\infty} \psi^{dif*}(\alpha) \exp(j\alpha x) d\alpha \\
 &= \lim_{X \rightarrow \infty} \psi^{as} \int_{\kappa}^{\infty} \psi^{dif*}(\alpha) \frac{\exp[j(\alpha + \alpha_0)X] - 1}{j(\alpha + \alpha_0)} d\alpha
 \end{aligned}$$

The terms containing X in the last two integrals (Eqs. (2.41.II) & (2.41.III)) approach zero in the limit $X \rightarrow \infty$ by virtue of the Riemann-Lesbesgue lemma (WHITTAKER & WATSON [1927 c]), since we exclude the case $\alpha_0 = -\kappa$. In the first integral (Eq. (2.41.I)) a difficulty arises as $\alpha \rightarrow \beta$. For this reason the integral with respect to β is broken up into three parts:

$$(2.42) \quad \lim_{X \rightarrow \infty} \left[\int_{\kappa}^{\alpha-\epsilon} \psi^{\text{dif}^*}(\beta) \frac{\exp[-j(\alpha-\beta)X] - 1}{-j(\alpha-\beta)} d\beta \right. \\ \left. + \int_{\alpha+\epsilon}^{\infty} \psi^{\text{dif}^*}(\beta) \frac{\exp[-j(\alpha-\beta)X] - 1}{-j(\alpha-\beta)} d\beta \right. \\ \left. + \int_{\alpha-\epsilon}^{\alpha+\epsilon} \psi^{\text{dif}^*}(\beta) \frac{\exp[-j(\alpha-\beta)X] - 1}{-j(\alpha-\beta)} d\beta \right]$$

$$(2.43) \quad = \lim_{X \rightarrow \infty} \left[\int_{\kappa}^{\alpha-\epsilon} \psi^{\text{dif}^*}(\beta) \frac{\exp[-j(\alpha-\beta)X]}{-j(\alpha-\beta)} d\beta \right. \\ \left. + \int_{\alpha+\epsilon}^{\infty} \psi^{\text{dif}^*}(\beta) \frac{\exp[-j(\alpha-\beta)X]}{-j(\alpha-\beta)} d\beta \right. \\ \left. + \int_{\kappa}^{\alpha-\epsilon} \frac{\psi^{\text{dif}^*}(\beta) d\beta}{j(\alpha-\beta)} + \int_{\alpha+\epsilon}^{\infty} \frac{\psi^{\text{dif}^*}(\beta) d\beta}{j(\alpha-\beta)} \right. \\ \left. + \int_{\alpha-\epsilon}^{\alpha+\epsilon} \psi^{\text{dif}^*}(\beta) \frac{\exp[-j(\alpha-\beta)X] - 1}{-j(\alpha-\beta)} d\beta \right].$$

The first two integrals in Eq. (2.43) approach zero by virtue of the Riemann-Lesbesgue lemma. The next two integrals can be combined:

$$(2.44) \quad \mathcal{P} \int_K^{\infty} \psi^{\text{dif}^*}(\beta) \frac{d\beta}{j(\alpha - \beta)}$$

where \mathcal{P} denotes the Cauchy principal value, The last integral can be brought into a suitable form by choosing a new variable $u = X(\alpha - \beta)$. This leads to

$$(2.45) \quad \begin{aligned} & \lim_{X \rightarrow \infty} \int_{-\varepsilon X}^{\varepsilon X} \psi^{\text{dif}^*}(\alpha - u/X) \frac{\exp(-ju) - 1}{-ju} du \\ &= \psi^{\text{dif}^*}(\alpha) \lim_{X \rightarrow \infty} \int_{-\varepsilon X}^{\varepsilon X} \frac{\exp(-ju) - 1}{-ju} du \\ &= \psi^{\text{dif}^*}(\alpha) \int_{-\infty}^{+\infty} \frac{\sin(u)}{u} du \\ &= \pi \psi^{\text{dif}^*}(\alpha), \end{aligned}$$

if ε is small, we may consider $\psi^{\text{dif}}(\beta)$ as a constant in the integration interval. Taking together all results, we obtain:

$$(2.46) \quad \begin{aligned} P_{\text{edge}} &= \frac{1}{2} \frac{\text{Re}(\eta)}{\rho_0^c} \mathcal{P} \iint_K^{\infty} \frac{\psi^{\text{dif}}(\alpha) \psi^{\text{dif}^*}(\beta)}{j(\alpha - \beta)} d\alpha d\beta \\ &+ \frac{1}{2} \frac{\text{Re}(\eta)}{\rho_0^c} \int_K^{\infty} - \frac{\psi^{\text{dif}}(\alpha) \psi^{\text{as}^*} + \psi^{\text{dif}^*}(\alpha) \psi^{\text{as}}}{-j(\alpha + \alpha_0)} d\alpha \\ &+ \frac{1}{2} \pi \frac{\text{Re}(\eta)}{\rho_0^c} \int_K^{\infty} \psi^{\text{dif}^*}(\alpha) \psi^{\text{dif}}(\alpha) d\alpha. \end{aligned}$$

We now define the quantity b to be the ratio of P_{edge} and the intensity of the incident plane wave. Since b has the dimension of a length, b may be conceived as the width of a fictitious strip of sound material (totally absorbing, however) beside the absorbing half-plane.

For a diffuse sound field we define a quantity b_{stat} as in the sound field, the statistical average of b for all angles in the hemisphere. The expression for b_{stat} can be deduced in a similar way as has been presented for the derivation of a_{stat} . Accordingly, we have

$$(2.47) \quad b_{\text{stat}} = 2 \int_0^{\pi} d\varphi \int_0^{\frac{1}{2}\pi} b \sin(\theta) \cos(\theta) d\theta.$$

2.7 Numerical results and discussion

It can be proved that b and b_{stat} are proportional to the wavelength apart from the frequency dependence of η . To this aim consider Eq. (2.46) for the additional power P_{edge} . Replacing α by α/k in the integrals of Eq. (2.46), yields an expression for the additional power P_{edge} which contains the wave number solely in the form of a factor $1/k$.

In fact, kb is a more characteristic quantity than b , since kb is a function of the admittance only and is a dimensionless quantity. For some values of η , taken from the impedance diagram of Sillan SP 100, 5 cm thick (Fig.1.2.) kb and kb_{stat} have been calculated with the aid of a digital computer.

The evaluation of the integrals occurring in the expression for P_{edge} presents no considerable difficulties, since all integrands are smooth functions of the variables involved.

Consequently, the integration with respect to the variables in the expressions for K_+ (α) and K_- (β) and with respect to the variables α and β in the expression for P_{edge} has been carried out with Simpson's rule. The integration with respect to the angle of incidence θ and the azimuth φ has been done with the trapezoid integration rule.

In Fig.2.4, the quantity b_{stat} has been plotted as a function of frequency for the values of the admittances of Sillan SP 100, 5 cm thick. The theoretical results have been plotted together with the experimental data of KUHL [1960] and TEN WOLDE [1967]. The graphs show that the theoretical curve predicts higher values than the experimentally observed ones for the major part of the frequency range. Some reasons for this behaviour can be surmised: (1) It turns out that the major part of the integral with respect to the variables φ and θ in the expression for b_{stat} results from the range where θ approaches 90° and $\varphi = 180^\circ$. See also Fig.2.5 where $kb \cos(\theta)$ has been plotted as a function of θ for two different admittances. The scattered field near the edge shows some resemblance to a wave excited by a line source at the edge. (KARP & RUSSEK [1957]). This scattered wave will be referred to as the "edge wave". The asymptotic behaviour of this wave is identical with the behaviour of Φ^{dif} in Eq.(2.38). For the values of φ and θ referred to above the wavelength of the edge wave dif-

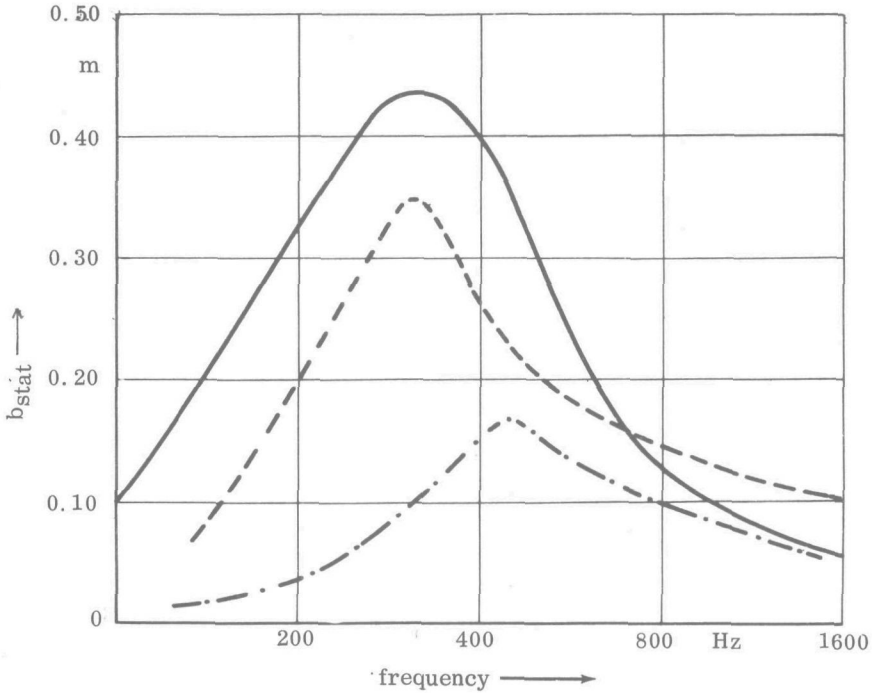


Fig. 2.4. The edge effect constant b_{stat} as a function of frequency.

————— computed,
 - - - - - after KUHL [1960],
 - · - · - after TEN WOLDE [1967].

fers but little from that of the incident wave and the directions of propagation are the same in contrast to the case where $\varphi = 0^0$. For a proof of this statement let us compare the expressions for the asymptotic behaviour of (Eq. (2.38)) and the incident wave at $z = 0$. The x -dependence enclosed in the exponential part of these expressions are $\exp(-j\kappa x)$ and $\exp(j\alpha_0 x)$, respectively. For angles referred to above $\kappa \rightarrow -\mathbf{k}$ and $\alpha_0 \rightarrow \mathbf{K}$. Thus considerable interference between the two waves is possible and may give rise to large edge effects. Stringent requirement must be imposed on the isotropy of the incident sound field if the experimental values found for the edge effect are to agree with the theoretical values, which were derived on the assumption of complete isotropy. It is a well-known experimental fact that the maintainance of isotropy for angles near grazing incidence is hard to achieve, especially at low frequencies. In a reverberation chamber having acoustically hard boundaries only, a diffuse field builds up automatically as long as non-directive sources are used, even for plane boundaries and no further measures to ensure diffusivity. If, however, a patch of highly absorptive material is applied to one of the boundaries, it will tend to

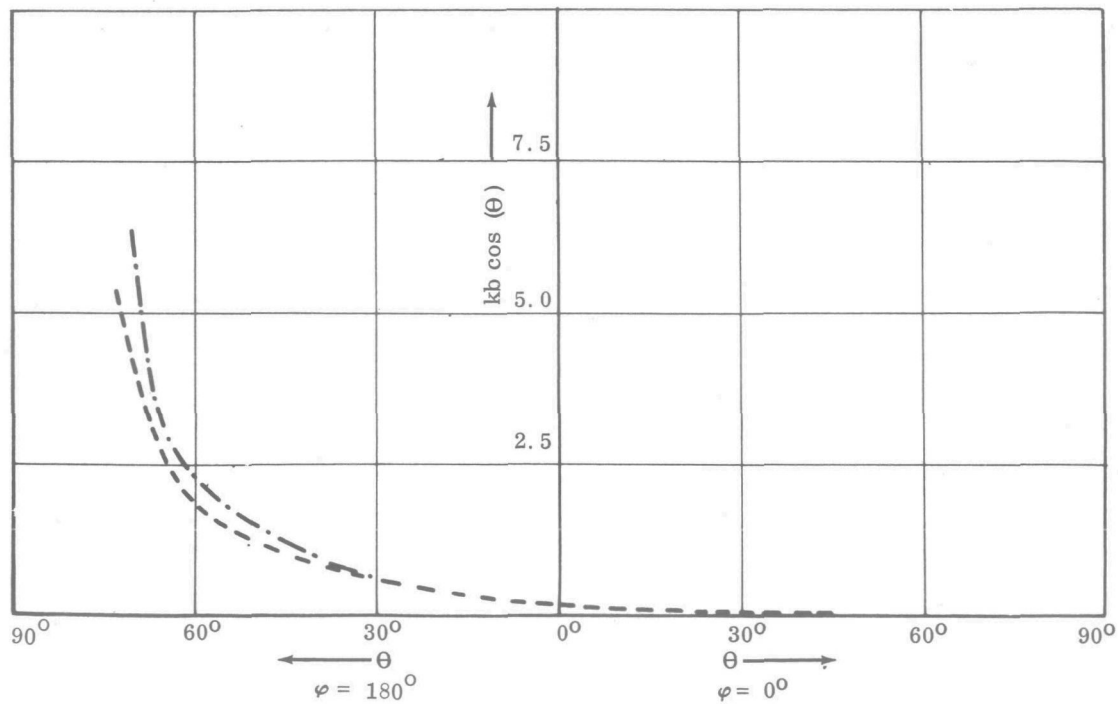


Fig. 2.5. The quantity $kb \cos(\theta)$ as a function of the angle of incidence θ .

----- $\gamma = 0.627 + j0.342$

- · - · - $\gamma = 0.265 + j0.395$

distort the diffuse sound field scattering the grazing waves and absorbing those to which it is most closely coupled. A sufficient diffusivity can be maintained in that case only by introducing diffusing elements. The larger the absorbing area is and the higher the absorption coefficient the more difficult it becomes to maintain a high rate of diffusivity. The experimental results are always a compromise between the requirements of a sufficiently large sample in order to yield accurate values of a_E and an adequate diffuse reverberant field. For this reason, as the requirements as to diffusivity are far more serious for the edge effect constant than they are for the absorption a_{stat} , the expectations for identical results obtained from different chambers and from theoretical considerations are not hopeful.

(2) In the Introduction of this chapter we noted that the mathematical model of the sound absorbing half-plane can only be a correct approximation if the dimensions of the sample are "large" with respect to the wavelength. However, at low frequencies this requirement is not fulfilled in the reverberation chamber. In that case the present analysis can not predict a correct description of the wave phenomena at the edge of the sample by virtue of the interaction between the scattered fields from the edges of the opposite "half-planes".

It is unfortunate that the experimental values presented in Fig.2.4 have been obtained from samples whose absorbing surfaces lay some 5 cm higher than the surrounding hard surface. This effect could not be incorporated in the theoretical model. Some insight into the magnitude of the possible influence may be gained from Chapter IV.

At high frequencies, η is practically constant. Hence, one would expect the same to be the case for kb_{stat} ; consequently, b_{stat} is expected to approach a hyperbola. This agrees well with experiments.

CHAPTER III

Diffraction and absorption by an absorbing strip

3.1 Introduction

In the previous chapter we have investigated the sound absorption by an absorbing half-plane. It is expected that the half-plane model predicts correct values for the edge effect for a sample of any shape as long as the frequency is high enough, since the edge effect is a local effect and in this case the interaction between different parts of the boundary can be neglected. At low frequencies however, this assumption holds no longer and therefore a refined theory has to be developed. Now the simplest case of a sample where interaction between different parts of the boundary can be taken into account mathematically, is the case where the sample has the form of an infinite strip of finite width. Accordingly, we consider the idealized problem where a single plane wave is incident upon an infinite hard plane, a part of which is covered by a straight strip of finite width. The principal purpose of this investigation is to find under which conditions the interaction between the edges of the strip becomes negligible. Again it is assumed that the strip consists of locally reacting material, the properties of which can be characterized by an acoustic admittance.

Work on the theory of diffraction of a strip has been done previously, using different techniques. MORSE and RUBINSTEIN [1938] treated diffraction of a plane wave by a perfectly hard and a perfectly weak strip by using the technique of separation of variables in the co-ordinates of the elliptic cylinder, which gives rise to an expansion of the wave function in terms of Mathieu functions. The expansion coefficients are determined from the boundary conditions. For the case of intermediate impedances the boundary conditions lead to an infinite system of linear equations in the coefficients of the expansion. PELLAM [1940] employed this procedure and solved the system of linear equations by the method of successive approximations. The major problem is that the Mathieu functions have not been tabulated for the necessary values of the arguments in the case under consideration. For this reason PELLAM restricted himself to real impedances. For real impedances his results agree with those obtained in the present chapter where the impedance may have any complex value.

LEVITAS and LAX [1951] formulated the problem in terms of an integral equation for the sound pressure on the strip, with the aid of the free space Green's function. From this integral equation a stationary (in the sense used in the calculus of variations) expression for the scattered amplitude was constructed. This variational approach gives fairly accurate estimates of the scattered amplitudes if one inserts a judicious approximation for the pressure distribution on the strip. By virtue of the scattering cross-section theorem the variational procedure also leads to a stationary expression for the total cross-section. They estimated the ratio of the scattering cross-section

to the absorption cross-section under the assumption that the pressure on the strip could be represented as the unperturbed pressure multiplied by a complex frequency-dependent factor. This is the weak point in the whole analysis. The assumption that the pressure on the strip could be represented by the unperturbed pressure times a frequency-dependent factor is only valid at low frequencies. For these frequencies the pressure above the strip equals approximately twice the incident pressure. Although the procedure yields a reasonable approximation for the absorption cross-section of the strip, the accuracy is inadequate to calculate the edge effect. This was to be expected as the model does not take into account any perturbation of the sound field near the edges. However, for normal incidence and low absorption the agreement with PELLAM's results are acceptable, for intermediate and high frequencies too.

NORTHWOOD et al. [1959] employed the same method as LEVITAS and LAX but for random incidence of sound and complex admittances. Afterwards NORTHWOOD [1963] refined the method for rectangular patches. The theoretical results have been compared with the experimental results of a round robin, reported by KOSTEN [1960]. It appears that there is a slight discrepancy at high frequencies, where reverberation chamber results are systematically higher than the calculated values. Apart from this, there is a substantial agreement and it appears that the average of results for several reverberation chambers are indeed the value that would be predicted from acoustical-impedance data.

COOK [1957] has considered both the strip and the circular patch. In order to find the sound field in the air near the absorbing surface he images the actual motion of the air to be generated by radiating "membranes" having a spatial distribution of vibrating amplitudes. The superposition of these vibrations is a Fourier series expansion for the actual motion of the absorbing surface. Each membrane radiates its own field, and the superposition of the fields gives the scattered sound field. The coefficients of the different membrane motions are then determined from the boundary condition on the patch.

MANGULIS [1965] solved the strip problem by using the Green's function formulation to obtain an integral equation for the pressure on the strip. The integral equation is then solved by the use of a Fourier series expansion for the pressure on the strip. This leads to two simultaneous sets of linear equations. The final numerical computations have been performed by solving a truncated system of equations by successive approximations.

Our method uses a plane wave spectrum representation for the scattered field. Further, the pressure on the strip is expanded in a Fourier series, which differs from the one employed by MANGULIS. Elimination of the unknown spectrum function (cf. Chapter II) then leads to a single system of linear equations which is simpler and more convenient to handle. Graphs are given in which the absorption coefficient has been plotted against the strip width with the angle of incidence and the admittance of the strip material as parameters. Comparison has been made with the absorption coefficients, obtained from the absorbing half-plane analysis.

3.2 Mathematical formulation of the problem

A plane sound wave is incident upon a perfectly rigid wall which coincides with the plane $z=0$. On this plane an acoustic strip is placed which extends

from $x = -d/2$ to $x = d/2$ and indefinitely in the y -direction. We assume that the strip consists of locally reacting sound absorbing material with a reduced specific acoustic admittance η . The spatial dependence of the incident wave has been specified in Eq. (1.24). As has been explained in Chapter I the three-dimensional diffraction problem can be reduced to a two-dimensional form. (Fig. 3.1).

The total sound pressure in the half-space $z > 0$ is written as the superposition of three contributions: the incident field Φ^i , a field Φ^r reflected against an acoustically rigid boundary of infinite extent and a scattered field Φ^s . Accordingly, the expression for the total field can be written as:

$$(3.1) \quad \Phi^t(x, z) = \exp(j\alpha_0 x + j\gamma_0 z) + \exp(j\alpha_0 x - j\gamma_0 z) + \Phi^s(x, z).$$

Again, we adopt the plane wave spectrum representation, employed in Chapter II, of the scattered field

$$(3.2) \quad \Phi^s(x, z) = \frac{1}{2\pi j} \int_{\mathcal{L}} f(\alpha) \exp[-j\alpha x - j(\kappa^2 - \alpha^2)^{\frac{1}{2}} z] d\alpha.$$

This representation satisfies the Sommerfeld radiation condition, and this implies that the field consists solely of either uniform plane waves travelling in the direction of the positive z -axis or non-uniform waves decreasing exponentially in this direction, provided that $\text{Re}(\kappa^2 - \alpha^2)^{\frac{1}{2}} > 0$ for any value of α in the complex α -plane. On the same grounds as given in Chapter II, \mathcal{L} is chosen to extend from $-\infty$ to ∞ ; hence Eq. (3.2) amounts to a Fourier integral representation of Φ^s . The points $\alpha = \pm \kappa$ are branch points and it is therefore necessary to determine how the path of integration avoids these points. The relevant problem has been solved in Chapter II. The path of integration \mathcal{L} in the complex α -plane is the one depicted in Fig. 3.2.

Furthermore, the field at the strip is assumed to have a Fourier series expansion of the form

$$(3.3) \quad \Phi^t(x, 0) = \sum_{m=0}^{\infty} A_m \cos \left[\pi m \left(x/d - \frac{1}{2} \right) \right], \text{ when } |x| < d/2, z = 0$$

where A_m is the complex strip field amplitude of order m .

We now have two representations of the total field at the strip, in which either the spectrum function $f(\alpha)$ in Eq. (3.2) or the constants A_m in Eq. (3.3) can be considered as unknowns. One of the unknowns can be eliminated with the aid of the boundary conditions in the plane $z = 0$:

$$(3.4) \quad \partial \Phi^t / \partial z = jk\eta \Phi^t, \quad |x| < d/2,$$

$$(3.5) \quad \partial \Phi^t / \partial z = 0, \quad |x| > d/2.$$

In fact, we chose to eliminate the spectrum function $f(\alpha)$; then an infinite

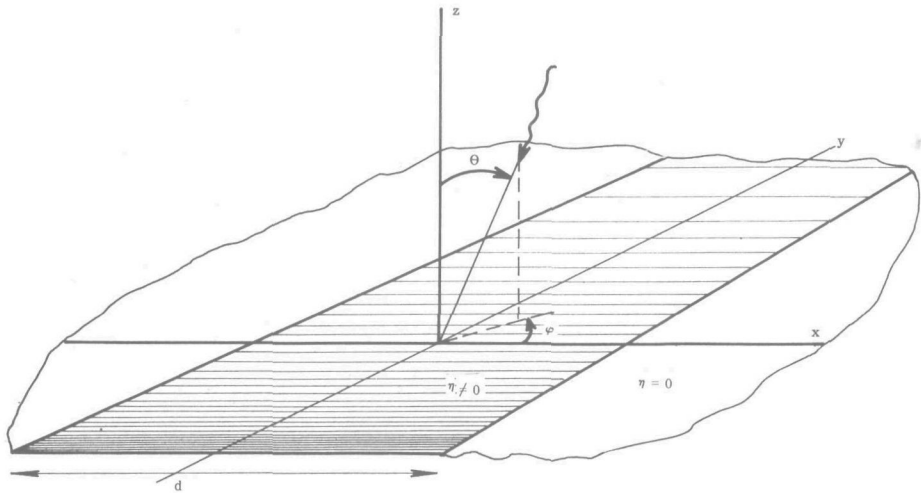


Fig. 3.1. Geometry of the diffraction by a strip.

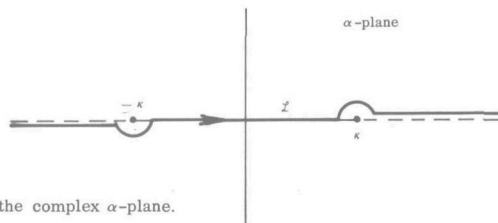


Fig. 3.2. The path of integration ζ in the complex α -plane.

system of linear equations in which the amplitudes A_m occur as unknowns, is obtained.

Using Eq. (3.1) and Eq. (3.2) at $z=0$ and equating the result to Eq. (3.3) gives

$$(3.6) \quad \sum_{m=0}^{\infty} A_m \cos \left[m \pi \left(x/d - \frac{1}{2} \right) \right] = 2 \exp(j\alpha_0 x) + \frac{1}{2\pi j} \int_{\zeta} f(\alpha) \exp(-j\alpha x) d\alpha,$$

$$\text{when } |x| < d/2.$$

By multiplying the left- and the right-hand side of this equation by $\cos[n\pi(x/d - 1/2)]$, integrating between the limits $-d/2$ and $d/2$ and using the orthogonality properties of the cosine function we obtain

$$(3.7) \quad A_m = \frac{2\varepsilon_n}{d} \int_{-d/2}^{d/2} \exp(j\alpha_0 x) \cos \left[n\pi \left(x/d - \frac{1}{2} \right) \right] dx + \frac{\varepsilon_n}{2\pi dj} \int_{\zeta} f(\alpha) d\alpha \int_{-d/2}^{d/2} \exp(-j\alpha x) \cos \left[n\pi \left(x/d - \frac{1}{2} \right) \right] dx,$$

where $\varepsilon_0=1$ and $\varepsilon_n=2$ when $n \geq 1$. This expression can be simplified by the introduction of the quantity

$$(3.8) \quad v_n(\alpha) \stackrel{\text{def}}{=} \frac{1}{d} \int_{-d/2}^{d/2} \exp(-j\alpha x) \cos \left[n\pi \left(x/d - \frac{1}{2} \right) \right] dx$$

$$= j\alpha \frac{[\exp(-j\alpha d/2) - (-1)^n \exp(j\alpha d/2)]}{d(\alpha^2 - \pi^2 n^2/d^2)}.$$

Then

$$(3.9) \quad A_n = 2\varepsilon_n v_n(-\alpha_0) + \frac{\varepsilon_n}{2\pi j} \int_{-\infty}^{\infty} v_n(\alpha) f(\alpha) d\alpha.$$

Upon substitution of Eqs. (3.1) (3.2) and (3.3) into the boundary condition Eq. (3.4) we obtain

$$(3.10) \quad k\eta \sum_{m=0}^{\infty} A_m \cos \left[m\pi \left(x/d - \frac{1}{2} \right) \right] = - \frac{1}{2\pi j} \int_{-\infty}^{\infty} f(\alpha) (\kappa^2 - \alpha^2)^{\frac{1}{2}} \exp(-j\alpha x) dx,$$

when $|x| < d/2$.

whereas the right-side of Eq. (3.10) is known to vanish outside the strip by virtue of the boundary condition Eq. (3.5). Application of Fourier's inversion theorem to Eq. (3.10) leads to

$$(3.11) \quad \int_{-d/2}^{d/2} k\eta \sum_{m=0}^{\infty} A_m \cos \left[m\pi \left(x/d - \frac{1}{2} \right) \right] \exp(j\alpha x) d\alpha = j f(\alpha) (\kappa^2 - \alpha^2)^{\frac{1}{2}}.$$

With the aid of Eq. (3.8) we obtain

$$(3.12) \quad f(\alpha) = \frac{k\eta d}{j(\kappa^2 - \alpha^2)^{\frac{1}{2}}} \sum_{m=0}^{\infty} A_m v_m^*(\alpha).$$

The substitution of this expression in Eq. (3.9) eliminates $f(\alpha)$. We then obtain an infinite system of linear equations in which the strip field amplitudes occur as unknowns

$$(3.13) \quad A_n = b_n - \sum_{m=0}^{\infty} U_{m,n} A_m \quad (n = 0, 1, 2, \dots),$$

in which

$$(3.14) \quad b_n \stackrel{\text{def}}{=} 2\varepsilon_n v_n(-\alpha_0),$$

$$(3.15) \quad U_{m,n} \stackrel{\text{def}}{=} \frac{k\eta d \varepsilon_n}{2\pi} \int_{\mathcal{L}} v_m^*(\alpha) v_n(\alpha) / (\kappa^2 - \alpha^2)^{\frac{1}{2}} d\alpha.$$

By virtue of the symmetry properties of $v_n(\alpha)$ and of the path of integration \mathcal{L} , it appears that $U_{m,n}$ equals zero, if m is even and n is odd or m is odd and n is even.

3.3 The absorption coefficient and the cross-sections

In the present section we shall show that all quantities of physical interest: the angular dependence of the scattering amplitude, the scattering cross-section, the absorption cross-section, the absorption coefficient and the extinction cross-section (i.e. the total cross-section, being the sum of the scattering and the absorption cross-section), are expressible in terms of the pressure on the strip.

For our purpose the acoustic power absorbed by the strip is of predominant interest. From the general formula for sound absorption Eq. (1.18), we determine the time-averaged power flow into the strip per unit width in the y -direction to be

$$(3.16) \quad P_a = \frac{1}{2} \frac{\text{Re}(\eta)}{\rho_0 c} \int_{-d/2}^{d/2} |\Phi^t(x, 0)|^2 dx.$$

The intensity of the incident plane wave in its direction of propagation is $\frac{1}{2}/\rho_0 c$, if the amplitude of the incident wave is assumed to be unity. We now define the absorption cross-section σ_a to be the ratio of the absorbed power to the intensity of the incident wave. Hence,

$$(3.17) \quad \sigma_a = \text{Re}(\eta) \int_{-d/2}^{d/2} |\Phi^t(x, 0)|^2 dx.$$

It is noted that this is an apparent cross-section normal to the direction of propagation of the incident wave.

Another interesting quantity is the ratio of the absorbed power to the power incident upon the strip, the latter quantity being $\frac{1}{2} d \cos(\theta)/\rho_0 c$. We now define the true absorption coefficient a_{tr} to be

$$(3.18) \quad a_{tr} = \frac{\text{Re}(\eta)}{d \cos(\theta)} \int_{-d/2}^{d/2} |\Phi^t(x, 0)|^2 dx$$

Upon substitution of the Fourier series expansion for the total field on the strip into Eq. (3.18) and evaluating the integrals, we obtain

$$(3.19) \quad a_{tr} = \frac{\text{Re}(\eta)}{\cos(\theta)} \sum_{m=0}^{\infty} |A_m|^2 / \varepsilon_m.$$

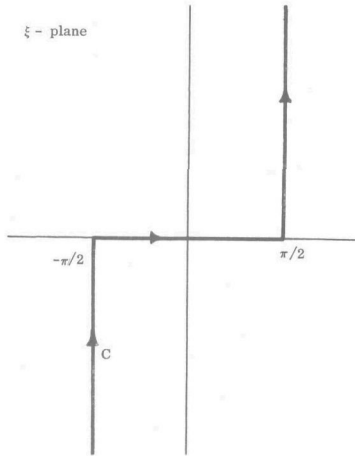


Fig. 3.3. The path of integration C in the complex ξ -plane

For the angular dependence of the scattered field we need the asymptotic behaviour of the scattered field at large distances from the strip. In order to find this behaviour from the representation Eq. (3.2) we introduce a new variable of integration ξ , related to α by $\alpha = \kappa \sin(\xi)$, and the polar co-ordinates R, ζ given in terms of x and z by the relations $x = R \sin(\zeta)$, $R = \cos(\zeta)$ ($0 \leq R < \infty$, $\frac{\pi}{2} < \text{Re}(\zeta) < \frac{\pi}{2}$). Hence,

$$(3.20) \quad \Phi^S = \frac{\kappa}{2\pi j} \int_C f[\kappa \sin(\xi)] \exp[-j\kappa R \cos(\xi - \zeta)] \cos(\xi) d\xi.$$

The contour C is depicted in Fig. 3.3. The part of C lying along the real axis corresponds to uniform plane waves fanning out into the half-space $z > 0$, whereas the arms running parallel to the imaginary axis correspond to non-uniform plane waves decaying away from $z = 0$. At sufficiently great distances from the strip it is possible to isolate a dominant part of the field, namely that part whose amplitude falls off as the inverse square root of the distance; this dominant contribution is known as the radiation field or far field of the strip. We now derive expressions for the radiation field from the plane wave representation. A heuristic argument is presented based on what is commonly called the method of stationary phase. At points where $\kappa R \gg 1$ the amplitudes of the non-uniform waves of the spectrum are very small, and such waves may be neglected. Moreover, the contributions of the uniform waves largely annul each other by destructive interference, since $\kappa R \gg 1$ the phase of the waves in general varies rapidly with ξ in the sense that a phase change of π is achieved by only a small change in ξ . Exceptionally, however, those waves for which ξ is close to ζ interfere constructively, since the variation of phase with ξ vanishes at $\xi = \zeta$. Thus it can be argued that only that part of the path of integration C in the vicinity $\xi = \zeta$ contributes significantly to Eq. (3.20) and consequently an approximation to Eq. (3.20) is

$$(3.21) \quad \Phi^S \approx \kappa f [\kappa \sin (\zeta)] \frac{\cos (\zeta)}{2 \pi j} \int_C \exp [-j \kappa R \cos (\xi - \zeta)] d \xi .$$

It is well-known that the integral in Eq. (3.21) is $\pi H_0^{(2)}(\kappa R)$ which is in turn naturally replaced by its asymptotic form for $\kappa R \gg 1$. Finally, then, the expression for Φ^S in the radiation field is

$$(3.22) \quad \Phi^S \approx \kappa (2 \pi j)^{-\frac{1}{2}} f [\kappa \sin (\zeta)] \cos (\zeta) \frac{\exp (-j \kappa R)}{(\kappa R)^{\frac{1}{2}}} \text{ as } R \rightarrow \infty .$$

With the aid of Eq. (3.12) for the spectrum function $f(\alpha)$ we obtain

$$(3.23) \quad \begin{aligned} \Phi^S &\approx \frac{k d \eta}{(2 \pi j)^{\frac{1}{2}}} \frac{\exp (-j \kappa R)}{j (\kappa R)^{\frac{1}{2}}} \sum_{m=0}^{\infty} A_m v_m^* [\kappa \sin (\zeta)] \\ &\approx \frac{k \eta}{(2 \pi j)^{\frac{1}{2}}} \frac{\exp (-j \kappa R)}{j (\kappa R)^{\frac{1}{2}}} \int_{-d/2}^{d/2} \Phi^t (x, 0) \exp [j \kappa x \sin (\zeta)] dx . \end{aligned}$$

For the sake of convenience we introduce

$$(3.24) \quad \begin{aligned} F(\zeta) &\stackrel{\text{def}}{=} k \eta \int_{-d/2}^{d/2} \Phi^t (x, 0) \exp [j \kappa x \sin (\zeta)] dx . \\ &= k d \eta \sum_{m=0}^{\infty} A_m v_m^* [\kappa \sin (\zeta)] . \end{aligned}$$

Hence

$$(3.25) \quad \Phi^S \approx \frac{\exp (-j \kappa R)}{j (2 \pi j \kappa R)^{\frac{1}{2}}} F(\zeta) .$$

This equation represents an outgoing cylindrical wave with a "polar diagram" specified by $F(\zeta)$.

The time-averaged power flow density in the x - z plane associated with the scattered field has only a radial component which can be written as $\frac{1}{2} \beta_0 |\Phi^S|^2 / \rho_0 c$. Note that the factor β_0 corrects for the power flow in the y -direction. The scattering cross-section is defined as the scattered power per unit intensity of the incident wave. Thus we obtain by integration over a semi-cylinder of large radius R

$$\begin{aligned}
 \sigma_s &= \int_{-\pi/2}^{\pi/2} R \left| \Phi^S \right|^2 d\zeta \\
 (3.26) \quad &= \frac{1}{2\pi k} \int_{-\pi/2}^{\pi/2} \left| F(\zeta) \right|^2 d\zeta.
 \end{aligned}$$

Another method for obtaining σ_s is starting directly from the knowledge of the distribution of the scattered field on the strip. In an analogous way to the derivation of σ_a we find

$$(3.27) \quad \sigma_s = -\operatorname{Re} \left[\eta \int_{-d/2}^{d/2} \Phi^S(x, 0) \Phi^{t*}(x, 0) dx \right].$$

There is a well-known theorem applicable to scattering problems that relates the total cross-section σ_t to the scattering amplitude in the forward direction, in this case specifically the amplitude in the direction of the specular reflection (DE HOOP [1959]). A direct verification of this theorem is obtained by evaluating the expression for the sum of the absorbed power P_a and the scattered power P_s per unit width in the y -direction, being

$$(3.28) \quad P_a + P_s = \frac{1}{2} \operatorname{Re} \left[\int_{-d/2}^{d/2} \left\{ \Phi^t \underline{n} \cdot \underline{u}^{t*} - \Phi^S \underline{n} \cdot \underline{u}^{S*} \right\} dx \right]$$

where \underline{n} is the inward normal to the strip. If we write

$$\Phi^S = \Phi^t - 2 \exp(j\alpha_0 x) \quad \text{at } z = 0,$$

and

$$\underline{n} \cdot \underline{u}^{S*} = \underline{u}^{t*} \quad \text{at } z = 0.$$

we find

$$(3.29) \quad P_a + P_s = \frac{1}{2} \operatorname{Re} \left[\int_{-d/2}^{d/2} \left\{ 2 \exp(j\alpha_0 x) \underline{n} \cdot \underline{u}^{t*} \right\} dx \right].$$

Eliminating $\underline{n} \cdot \underline{u}^{t*}$ by the admittance boundary condition on the strip and dividing by the intensity of the incident plane wave we obtain

$$(3.30) \quad \sigma_t = \sigma_a + \sigma_s = \operatorname{Re} \left[\eta \int_{-d/2}^{d/2} 2 \exp(-j\alpha_0 x) \Phi^t(x, 0) dx \right].$$

When the expression for σ_t is compared with representation of $F(\zeta)$, it follows by inspection that σ_t can be expressed in terms of $F(\zeta_0)$. The result is

$$(3.31) \quad \sigma_t = \frac{2}{k} \operatorname{Re} [F(-\zeta_0)] .$$

where ζ_0 's given in terms of α_0 by the relation $\zeta_0 = \arcsin(\alpha_0/\kappa)$.

3.4 Numerical computations

The infinite system of linear equations Eqs. (3.15) can be solved by truncating the infinite system to a finite one. The solution will evidently be acceptable provided that the error involved in solving N equations approaches zero as N tends to infinity. For this reason we evaluate $U_{m,n}$ for large values of m and n . For large values of m and n we have from Eq. (3.15):

$$U_{m,n} = O(1/mn) \quad \text{as } m, n \rightarrow \infty .$$

A sufficient condition for the uniqueness of the solution is that the matrix coefficients satisfy the Koch condition (KANTOROVICH & KRYLOV [1964]):

$$\sum_{m,n} |U_{m,n}|^2 < \infty .$$

Our system obviously satisfies this condition.

The truncated system is best solved by the method of successive approximations. In the zero order approximation we take $U_{m,n} = 0$ for $m \neq n$. Then in the matrix only the diagonal elements remain. Consequently, the zero-order solution is

$$A_n^{(0)} = b_n / (1 + U_{n,n}) .$$

Substituting this zero order approximation into Eqs. (3.13) we obtain a recurrence relation for any approximation of higher order s

$$A_n^{(s+1)} (1 + U_{n,n}) = b_n - \sum_{\substack{m=0 \\ m \neq n}}^{\infty} U_{m,n} A_m^{(s)} .$$

This process of numerical computation is called "Jacobi iteration" (FOX [1964]). A sufficient condition for its convergence is that the diagonal elements are predominant, which implies

$$|1 + U_{n,n}| > \sum_{\substack{m=0 \\ m \neq n}}^{\infty} |U_{m,n}| .$$

For our problem the diagonal elements are predominant.

The main difficulty in the numerical computations lies in the evaluation of the integrals in the matrix coefficients. This evaluation can most appropriately be done with Simpson's integration rule with a step width adapted to the variations in the function. For the sake of numerical convenience we rewrite $v_m(\alpha)$ as

$$v_m(\alpha) = \frac{2\alpha \sin(\frac{1}{2}\alpha d)}{d(\alpha^2 - \pi^2 m^2/d^2)}, \text{ if } m \text{ is even,}$$

$$v_m(\alpha) = \frac{2j\alpha \cos(\frac{1}{2}\alpha d)}{d(\alpha^2 - \pi^2 m^2/d^2)}, \text{ if } m \text{ is odd}$$

and by virtue of the symmetry of the path of integration \mathcal{L} in α we rewrite $U_{m,n}$ as

$$\begin{aligned} U_{m,n} &= \frac{2k\eta\varepsilon_n}{2\pi d} \int_0^\infty \frac{4\alpha^2 \sin^2(\frac{1}{2}\alpha d) d\alpha}{(\alpha^2 - \pi^2 m^2/d^2)(\alpha^2 - \pi^2 n^2/d^2)(\kappa^2 - \alpha^2)^{\frac{1}{2}}} \\ &= \frac{2k\eta\varepsilon_n}{2\pi d} \left[\int_0^\kappa \frac{4\alpha^2 \sin^2(\frac{1}{2}\alpha d) d\alpha}{(\alpha^2 - \pi^2 m^2/d^2)(\alpha^2 - \pi^2 n^2/d^2)(\kappa^2 - \alpha^2)^{\frac{1}{2}}} \right. \\ &\quad \left. + j \int_\kappa^\infty \frac{4\alpha^2 \sin^2(\frac{1}{2}\alpha d) d\alpha}{(\alpha^2 - \pi^2 m^2/d^2)(\alpha^2 - \pi^2 n^2/d^2)(\alpha^2 - \kappa^2)^{\frac{1}{2}}} \right], \text{ if } m,n \text{ is even;} \\ U_{m,n} &= \frac{2k\eta\varepsilon_n}{2\pi d} \int_0^\infty \frac{4\alpha^2 \cos^2(\frac{1}{2}\alpha d) d\alpha}{(\alpha^2 - \pi^2 m^2/d^2)(\alpha^2 - \pi^2 n^2/d^2)(\kappa^2 - \alpha^2)^{\frac{1}{2}}} \\ &= \frac{2k\eta\varepsilon_n}{2\pi d} \left[\int_0^\kappa \frac{4\alpha^2 \cos^2(\frac{1}{2}\alpha d) d\alpha}{(\alpha^2 - \pi^2 m^2/d^2)(\alpha^2 - \pi^2 n^2/d^2)(\kappa^2 - \alpha^2)^{\frac{1}{2}}} \right. \\ &\quad \left. + j \int_\kappa^\infty \frac{4\alpha^2 \cos^2(\frac{1}{2}\alpha d) d\alpha}{(\alpha^2 - \pi^2 m^2/d^2)(\alpha^2 - \pi^2 n^2/d^2)(\alpha^2 - \kappa^2)^{\frac{1}{2}}} \right], \text{ if } m,n \text{ is odd.} \end{aligned}$$

Difficulties could be expected as $\alpha = m\pi/d$ or $\alpha = n\pi/d$. However, at these values both numerator and denominator vanish, and the integrand remains bounded and continuous. In the integrals containing the infinite range of integration the upper limit has been taken to be $\alpha = 50$. The convergence of the integrals is very good, as the integrand is of order $O(\alpha^{-3})$ as $\alpha \rightarrow \infty$.

In Section 3.3 we have considered the cross-section theorem. This theorem provides an excellent tool as to the correctness of the numerical computations. Computing the scattering cross-section from Eq. (3.26) by integration with respect to the angle θ , adding the computed absorption cross-section from Eq; (3.17), we obtain a value for the total cross-section. This value must be equal to the value obtained for the right-hand side of Eq. (3.31). One of the most important results of the application of this theorem is the determination of the number of equations of the truncated system required in order to yield correct values of the strip field constants. In the present instance about fifteen equations were adequate to ensure the theorems being satisfied to within a relative error of 10^{-4} .

3.5 Discussion of the results

We shall discuss the graphs where the absorption coefficient a_{tr} has been plotted as a function of the strip width with the angle of incidence θ and the admittance of the sample as parameters. We have chosen two values for the admittance, corresponding to a medium and a high value of the absorption coefficient of the strip material. All plots show a large increase of the absorption coefficient for small strip widths. This is easily understood if we bear in mind that for these values of the strip width the pressure above the strip deviates little from its undisturbed value over the acoustically hard part of the plane; in other words, the pressure on the strip is twice the pressure of the incident wave. It is now simple to see from Eq. (1.20) that $a_{tr} = 4 \operatorname{Re}(\eta) / \cos(\theta)$. Of course, this equation is only valid in the limiting case of small values of kd approaching zero. From this equation we can understand why the absorption coefficient can exceed 100%. If the strip width is increased then the pressure distribution on the strip will no longer be uniform but the pressure in the centre of the strip will decrease. The expectation is then that the absorption coefficient also decreases for increasing strip width until the limiting value a_{θ} has been reached. The extent to which a_{tr} approach a_{θ} depends to a large extent on the angle of incidence. At $\theta = 0^\circ$ the limiting value a_{θ} is reached rapidly, but at $\theta = 60^\circ$ several tens of units of kd are necessary to reach this limiting value.

An important aspect of the graphs is that they yield information as to the interaction between the edges of the strip. In order to extract this information we introduce a_{sep} , being the absorption coefficient for a strip of given width, taking the edge effects to be resulting from two-separate, non-interacting half-planes. If interaction between the edges of the strip does not occur, a_{sep} will equal a_{tr} . The discrepancy between these two quantities is thus a measure for the interaction of the edges. We can determine a_{sep} from the following equation:

(3.3.)

$$a_{\text{sep}} = a_{\theta} + (b' + b'') / \cos(\theta) d$$

where b' is the coefficient, defined in section 2.7, relevant to a plane wave incident under an angle θ , while b'' is the coefficient belonging to a plane wave incident under an angle $-\theta$. It may be seen from Eq. (3.33) that a_{sep} as a function of kd is a displaced hyperbola. This function has been compared with the true absorption coefficient obtained from the exact analysis. It is evident from Figs. 3.4 - 3.9 that the approximate analysis for a_{sep} yields acceptable results for intermediate and large strip widths. The absorption coefficient a_{sep} equals a_{tr} within 10%, when $kd > 10$. In Chapter II it was stated that the additional absorption due to diffraction can be considered as a result of a local field in the neighbourhood of the edges of the patch. This is also confirmed by the experimental results of DANIEL [1963], who found that for $kd > 5$ interaction does not occur.

For a diffuse sound field, we assume that the same analysis holds as such a field may be expanded in a set of superimposed plane waves. The plane waves, incident under the angles $\theta = 0^\circ, 30^\circ$ und 60° are expected to give a good indication as to the behaviour of a strip in a diffuse sound field.

That the whole problem can be treated as a real edge effect and not as an area effect is a favourable fact for the further refinement of reverberation techniques. The statement of KOSTEN [1960] that a_E is proportional to the relative edge length is not only confirmed experimentally but also theoretically. The validity of this result is confined, of course, to intermediate and large patches.

For the sake of completeness we present twelve "polar diagrams" (Fig. 3.10 - 3.13). The basic principles governing the polar diagram can be learned from studying combinations of simple line sources. For small strip width we may consider the strip to radiate as a single line source and we expect a circular polar diagrams. With increasing strip width more line sources may be considered to be present on the strip; the pressures arriving from these sources will differ in phase and consequently, the polar diagram will not longer be a circle. In other words, the strip will radiate sound in some directions better than in others. The wider the extent of the strip the more lobes are present in the polar diagram. The principal lobe lies in the direction of the specularly reflected wave which is surrounded by a number of side lobes.

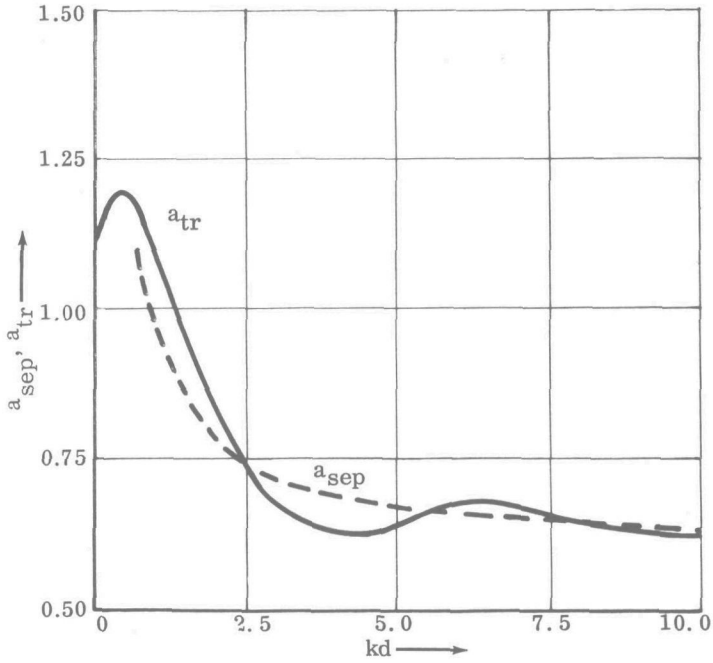


Fig. 3.4.
 The absorption coefficient a_{tr} and a_{sep} as a function
 of the strip width kd at $\varphi = 0^\circ$, $\theta = 0^\circ$,
 $\eta = 0.264 + j 0.395$.

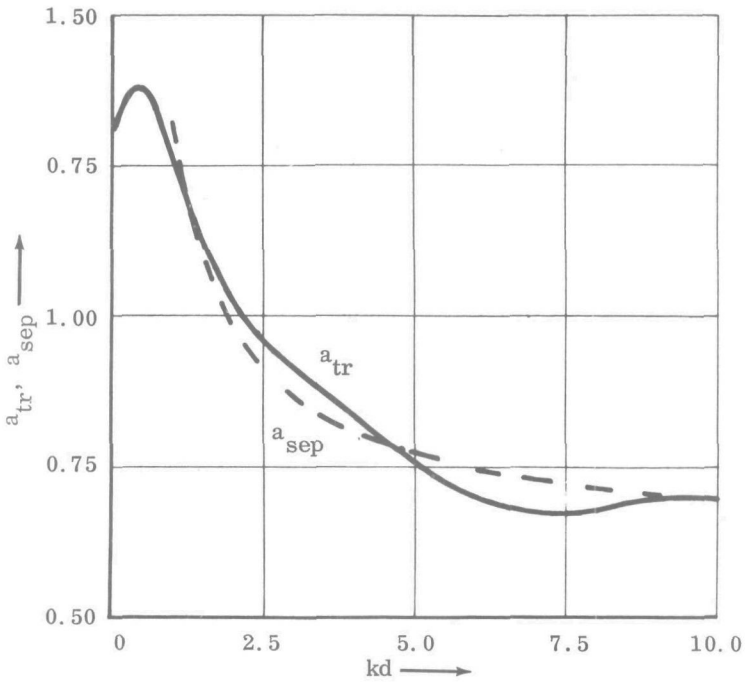


Fig. 3.5. The absorption coefficients a_{tr} and a_{sep} as a function of the strip width kd , at $\varphi = 0^\circ$, $\theta = 30^\circ$, $\eta = 0.264 + j 0.395$.

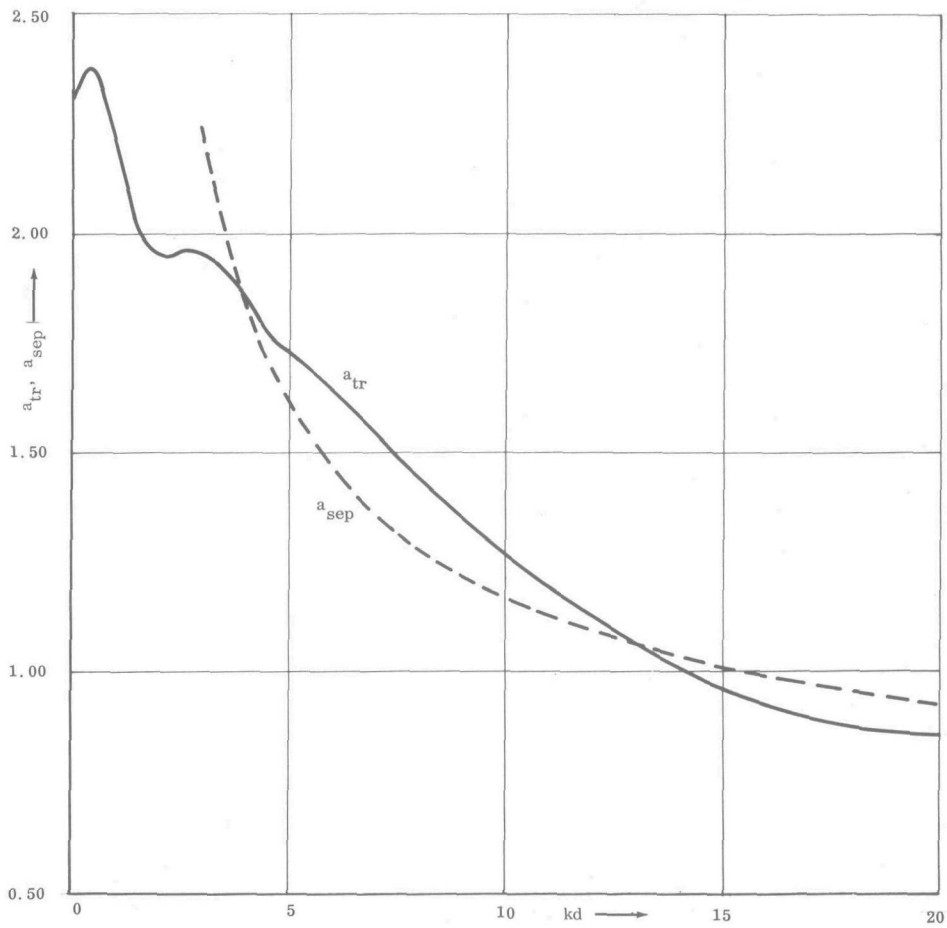


Fig. 3.6. The absorption coefficients a_{tr} and a_{sep} as a function of the strip width kd at $\varphi = 0^\circ$; $\theta = 60^\circ$, $\eta = 0.264 + j 0.395$.

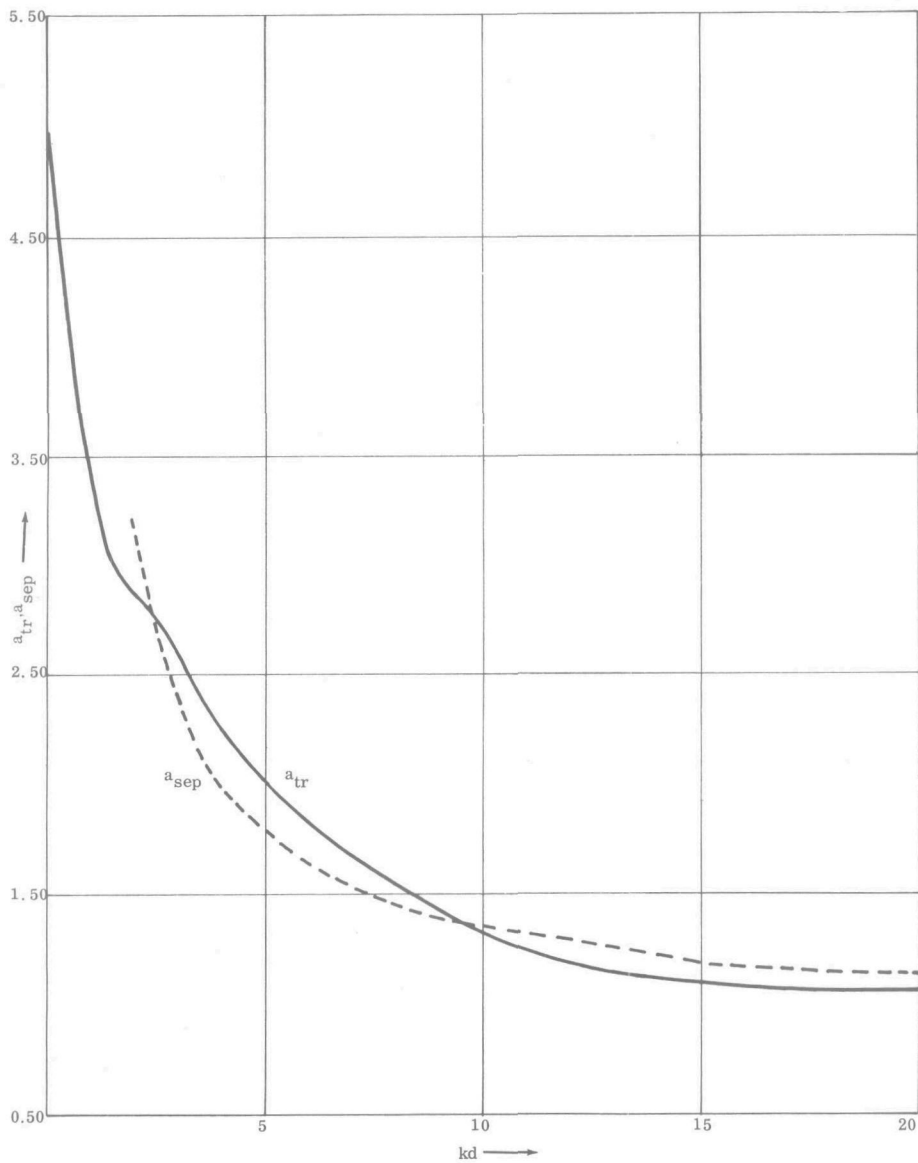


Fig. 3.7. The absorption coefficients a_{tr} and a_{sep} as a function of the strip width kd at $\varphi = 0^\circ$, $\theta = 60^\circ$, $\eta = 0.627 + j 0.342$.

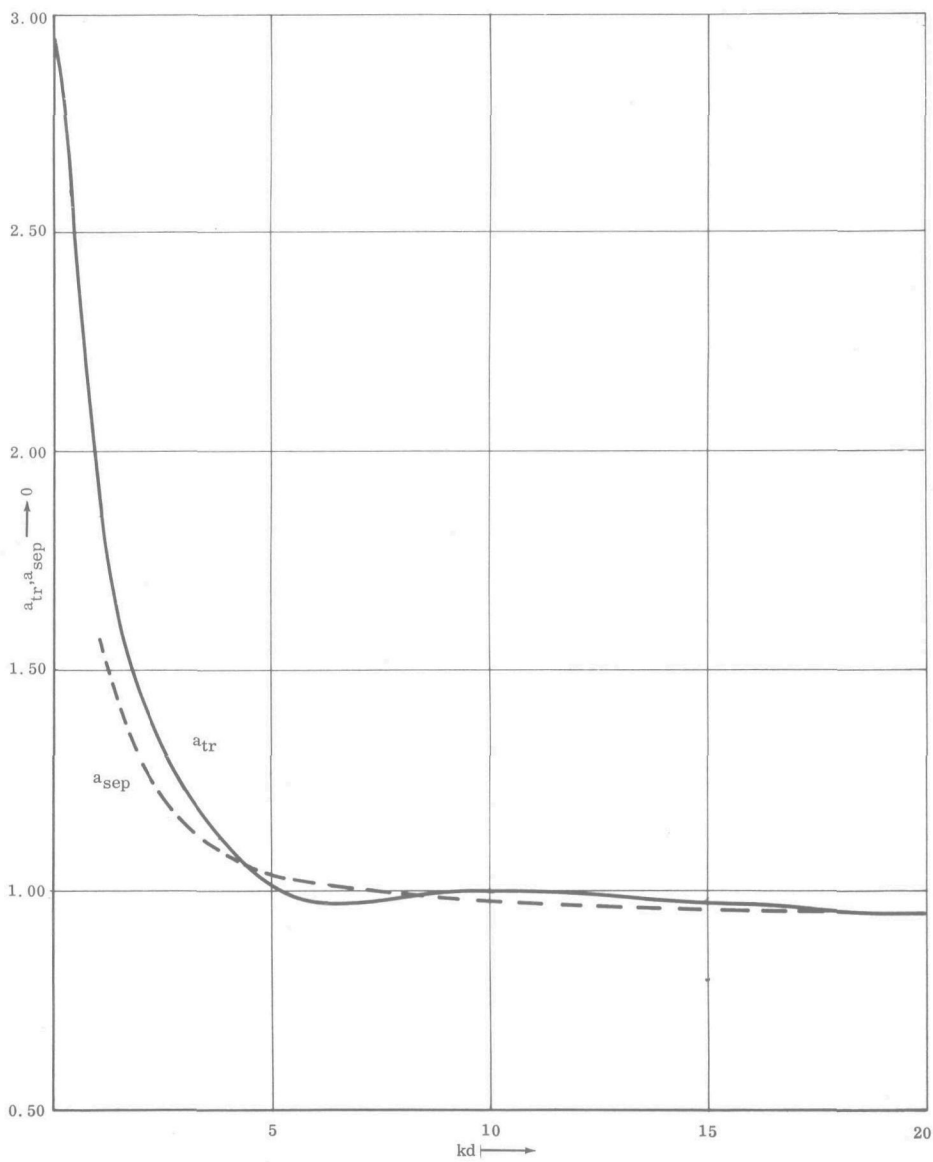


Fig. 3.8. The absorption coefficients a_{tr} and a_{sep} as a function of the strip width kd , at $\varphi = 0^\circ$, $\theta = 30^\circ$; $\eta = 0.627 + j 0.342$.

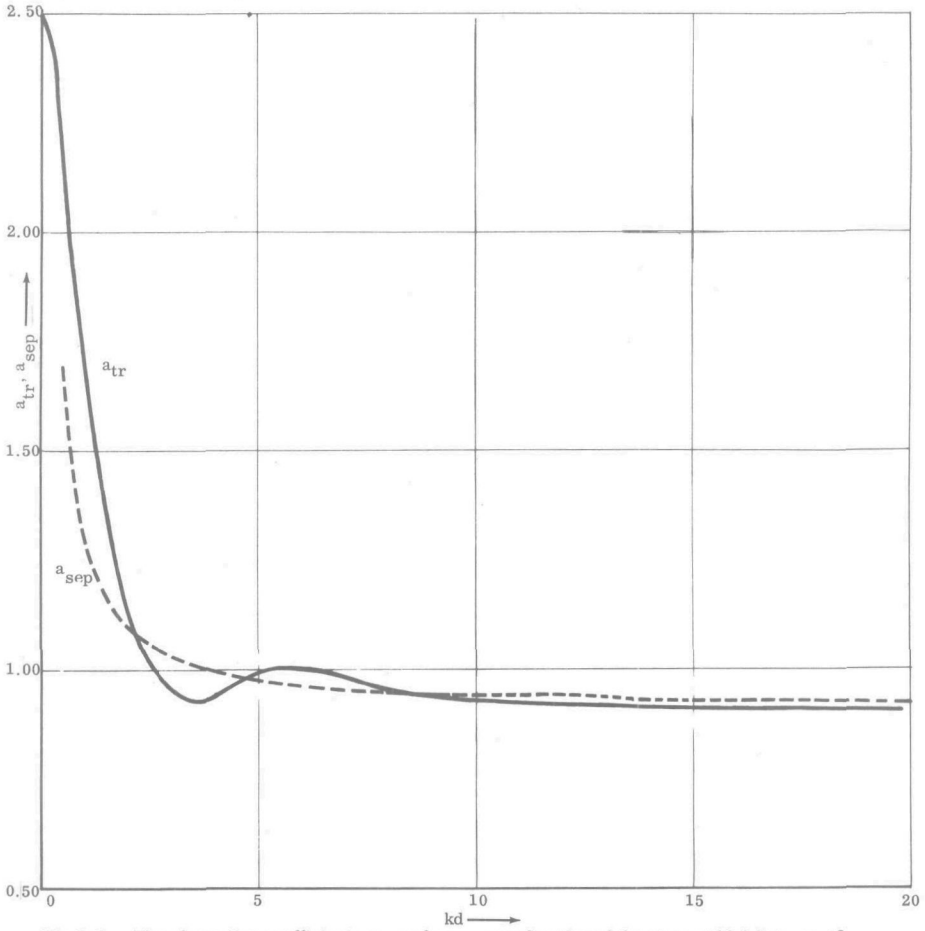
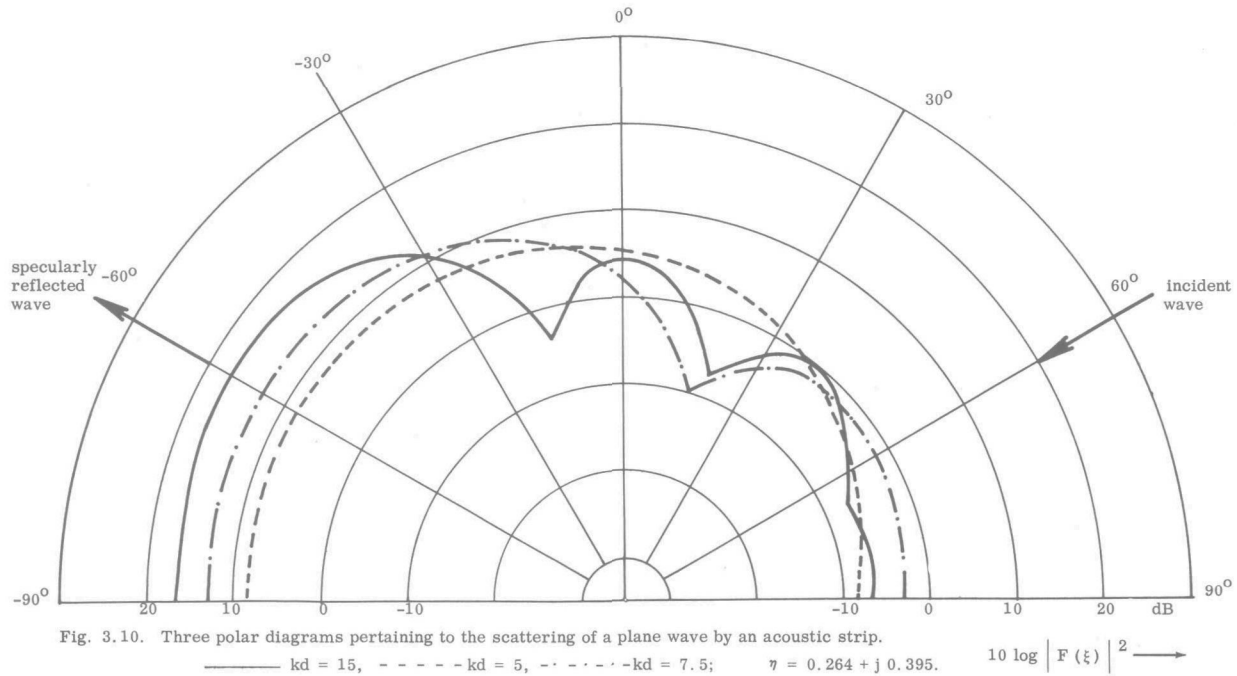
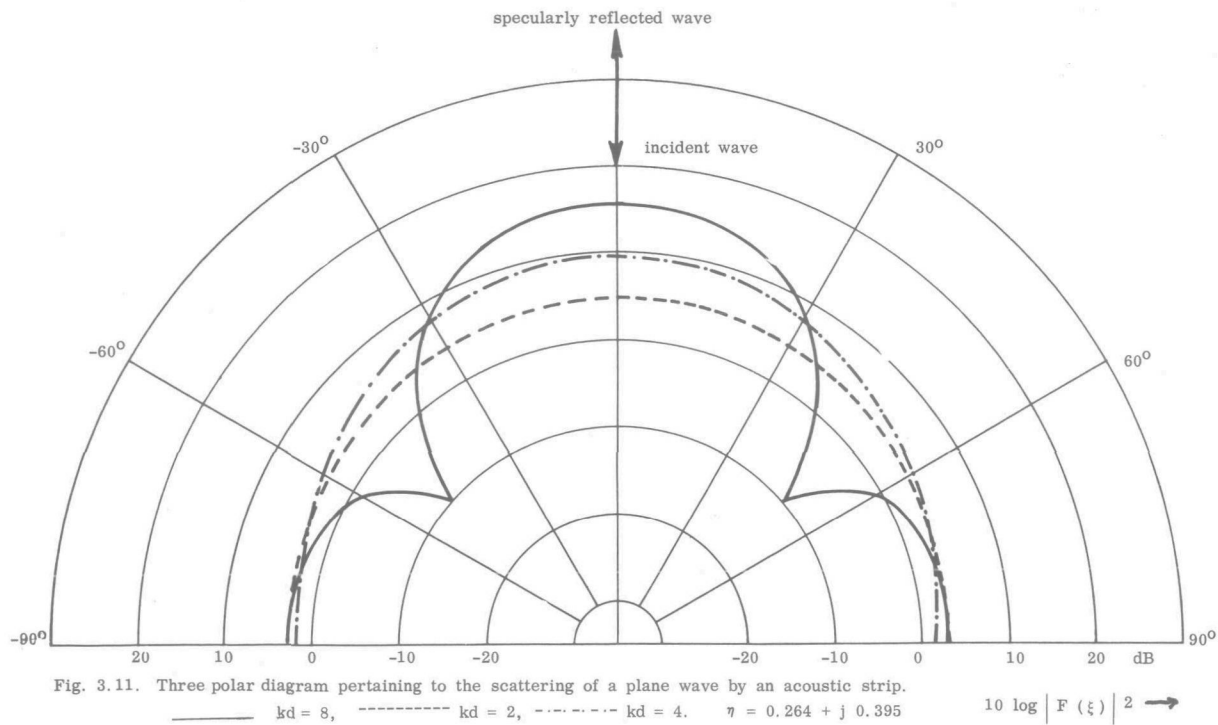


Fig. 3.9. The absorption coefficients a_{tr} and a_{sep} as a function of the strip width kd at $\varphi = 0^\circ$, $\theta = 0^\circ$; $\eta = 0.627 + j 0.342$.





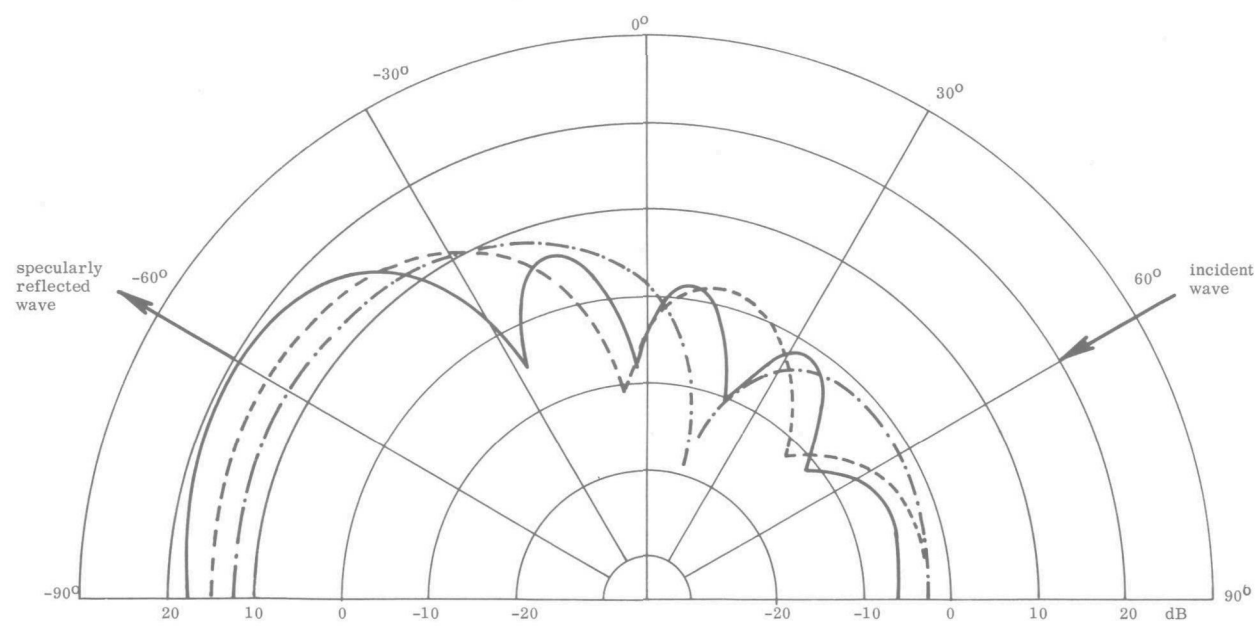


Fig. 3.12. • Three polar diagrams pertaining to the scattering of a plane wave by an acoustic strip.
 ——— $kd = 10$ - - - - $kd = 7.5$ - · - · - $kd = 5$ $\eta = 0.627 + j 0.342$.

$10 \log |F(\xi)|^2 \rightarrow$

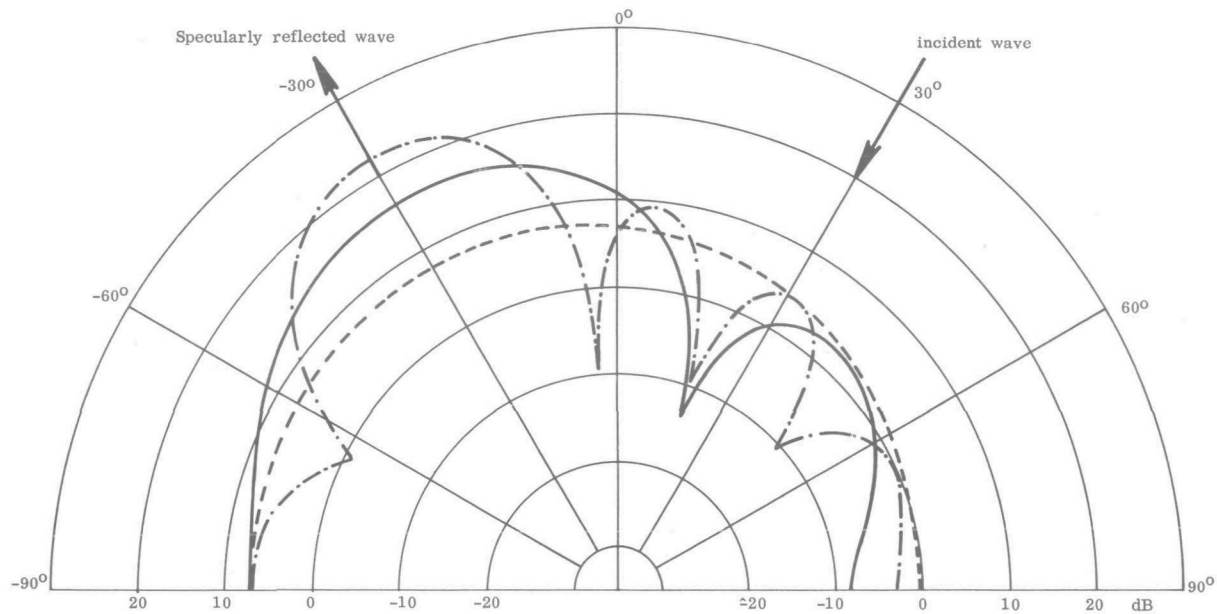


Fig. 3.13. Three polar diagrams pertaining to the scattering of a plane wave by an acoustic strip.

- · - · - · - $kd = 15$ - - - - - $kd = 2.5$ ———— $kd = 7.5$ $\eta = 0.627 + j 0.342$. $10 \log |F(\xi)|^2 \rightarrow$

CHAPTER IV

Diffraction and absorption by an absorbing periodically uneven surface of rectangular profile

4.1 Introduction

In Chapter III we have described the wave phenomena associated with the diffraction of a plane wave by a sound absorbing strip, lying in an acoustically rigid plane.

However, this mathematical model presents an oversimplified view upon the determination of b_{stat} . When b_{stat} is determined in the reverberation chamber with the aid of Eq. (1.23):

$$a_E = a_{\text{stat}} + b_{\text{stat}} E,$$

we use a sample consisting of several rectangular patches, which in various arrangements yield various values of the relative edge length E of the sample. In this way we obtain, for each value of E , a value of the absorption coefficient a_E . We now compose a graph of a_E as a function of E . This plot should be a straight line and its slope with the E -axis yields the edge effect constant b_{stat} . It turns out that this constant, thus determined, depends not only upon frequency and the nature of the acoustical material, but also upon the distance between the patches under test. The latter effect can be explained by the fact that the scattered waves from the edges interact with each other resulting in a diminution of the edge effect and thus introducing an experimental error. If the free edges of the patches are separated by about three wavelengths then the interaction becomes negligible and we obtain a correct value for b_{stat} .

Consequently, a refinement of the theory is needed if the edges are close to each other. One of the possibilities for studying the interaction of the edges is to consider a periodic arrangement of absorbing strips. The influence of the edges upon each other is then rigorously taken into account. The periodic structure is also attractive from an architectural-acoustic point of view. In many halls for public assembly periodic structures of this kind have been applied. The quantity of major importance is now the absorption coefficient of the entire structure. The present chapter is devoted to an investigation of a periodically uneven structure of rectangular profile of either sound absorbing ridges or sound absorbing grooves.

The method used here has been employed before by DERYUGIN [1952, 1953, 1960a, 1960b] who solved the problem of the reflection of a normally or obliquely incident plane wave, by an uneven surface with rectangular non-absorbing grooves. The essence of the method consists of finding solutions in both the upper half-space and the region containing the grooves by means of separation of variables. The imposition of the boundary conditions at the plane

common to the two regions then leads to two infinite systems of linear algebraic equations in which the amplitudes of the reflected waves and the groove field amplitudes occur as unknowns, respectively. The form of the wave field is different for the two regions involved. In the upper half-space the solution consists of plane waves which are either propagating or evanescent in a direction away from the interface. In the grooves the wave motion is a superposition of waveguide modes either travelling or evanescent in opposite directions.

In order to obtain numerical results the two infinite systems of equations are solved by successive approximation; through this method any desired degree of accuracy can be acquired.

The principle of the method resembles the one employed by RAYLEIGH [1907] in that the field is expressed as the superposition of plane waves with unknown coefficients, while the boundary conditions then lead to linear, algebraic equations from which the coefficients in the corresponding expansions can be determined. However, DERYUGIN's method differs from RAYLEIGH's method in this respect, that it first determines the exact structure of the field in the grooves, while afterwards the field in the space above the corrugations is coupled to the field in the grooves by imposing the conditions of continuity in the interface. This method is exact; as far as RAYLEIGH's method is concerned, this is at least doubtful.

Anomalies in the wave field have been observed when one of the reflected spectral plane waves travels along the grating. In that case repeated perturbations from all corresponding elements of the surface add in phase and may produce intense waves of glancing spectral order. It is interesting to note that anomalies due to diffraction at a grating have been detected experimentally a long time ago by WOOD [1902]. The first theoretical treatment of these anomalies is due to RAYLEIGH [1907]. In addition to this "Wood anomaly" OLINER and HESSEL [1965] found a resonance type of behaviour in the amplitudes of the reflected wave (cf. section 4.5). Another interesting feature of the uneven surface is the waveguide type of resonance, which is related to the depth of the groove: at special values of this depth an unusually large or unusually small absorption is found.

4.2 Diffraction by a periodically uneven surface of rectangular profile

In the present section we deal with the diffraction of a plane sound wave by the configuration, shown in Fig. 4.1. The uneven surface is composed of a periodic structure of infinitely long grooves parallel to the y -axis of a cartesian co-ordinate system. We assume that the upper side of the ridges consists of locally reacting sound absorbing material with reduced specific acoustic admittance η_1 , and that the bottom of the grooves consists of locally reacting sound absorbing material with reduced specific acoustic admittance η_2 . The side walls of the grooves are assumed to be acoustically hard. The plane $z = 0$ coincides with the upper side of the ridges. The width of the grooves is d , the period of the grooves is ℓ , and the depth of the grooves is h .

The spatial dependence of the incident wave is specified in Eq. (1.24).

As has been explained in Chapter I we may reduce this three-dimensional diffraction problem to a two-dimensional one.

We first seek representations for the total field Φ_I^t in region I (above the x, y -plane, $z > 0$) and the total field Φ_{II}^t in region II (within the groove, $-h < z < 0$).

On account of the periodicity of the structure the scattered field Φ^S in the half-space $z > 0$ can be written as a superposition of plane waves which are either uniform or propagating along the uneven surface, being evanescent in the direction normal to the surface. Accordingly, we have

$$(4.1) \quad \Phi_I^t(x, z) = \exp(j\alpha_0 x + j\gamma_0 z) + \sum_{r=-\infty}^{\infty} R_r \exp(j\alpha_r x - j\gamma_r z),$$

where R_r is the complex reflection amplitude of the plane wave of the r -th spectral order. In Eq. (4.1) the following symbols have been used

$$(4.2.) \quad \alpha_r \stackrel{\text{def}}{=} \alpha_0 + 2\pi r/\ell,$$

$$(4.3) \quad \gamma_r \stackrel{\text{def}}{=} \begin{cases} (\kappa^2 - \alpha_r^2)^{\frac{1}{2}} \geq 0, & \text{when } \kappa^2 \geq \alpha_r^2; \\ -j(\alpha_r^2 - \kappa^2)^{\frac{1}{2}} & \text{with } (\alpha_r^2 - \kappa^2)^{\frac{1}{2}} \geq 0, & \text{when } \alpha_r^2 \geq \kappa^2. \end{cases}$$

The sign of the square roots has been chosen such that the reflected waves either travel in the positive z -direction or are evanescent in this direction.

The field in the grooves can be written as a superposition of waveguide modes considering the direction of the z -axis as axial direction. By virtue of the boundary condition $\partial\Phi_{II}^t/\partial x = 0$ at the waveguide walls, the appropriate eigenfunctions in the transverse direction are $\cos[m\pi(x/d - \frac{1}{2})]$, where m is an arbitrary integer. Separation of variables in the Helmholtz equation then leads to the following representation for the field in the ν -th groove

$$(4.4) \quad \Phi_{II}^t(x, z) = \exp(j\alpha_0 \nu \ell) \sum_{m=0}^{\infty} \left[A_m \exp(jx_m z) + B_m \exp(-jx_m z) \right] \times \\ \times \cos \left[m\pi(x_\nu/d - \frac{1}{2}) \right],$$

where

$$\text{when } -d/2 < x_\nu < d/2, \quad -h < z < 0;$$

$$(4.5) \quad x_m \stackrel{\text{def}}{=} \begin{cases} (\kappa^2 - \pi^2 m^2/d^2)^{\frac{1}{2}} \geq 0, & \text{when } \kappa^2 > \pi^2 m^2/d^2; \\ -j(\pi^2 m^2/d^2 - \kappa^2)^{\frac{1}{2}} & \text{with } (\pi^2 m^2/d^2 - \kappa^2)^{\frac{1}{2}} \geq 0 \\ & \text{when } \pi^2 m^2/d^2 \geq \kappa^2. \end{cases}$$

A_m and B_m are the groove field amplitudes and x_ν is the co-ordinate in the x -direction in the ν -th period ($\nu = 0, \pm 1, \pm 2, \dots$).

From the definition of the incident field we see that it satisfies the difference equation

$$(4.6) \quad \Phi^i(x + \ell, \nu, z) = \exp(j\alpha_\nu \ell) \Phi^i(x, z),$$

where ν is an integer. In Eqs. (4.1) and (4.4) we have made the customary assumption that the total field in both domains satisfies the same difference equation.

4.3 The infinite systems of linear equations

From the boundary condition in the grooves at $z = -h$

$$(4.7) \quad \partial \Phi_{II}^t / \partial z = jk\eta_2 \Phi_{II}^t$$

we have

$$(4.8) \quad \begin{aligned} & jA_m \chi_m \exp(-jh\chi_m) - jB_m \chi_m \exp(jh\chi_m) = \\ & = jk\eta_2 [A_m \exp(-jh\chi_m) + B_m \exp(jh\chi_m)], \end{aligned}$$

from which we express B_m in terms of A_m through

$$(4.9) \quad B_m = \Gamma_m A_m$$

in which the coefficient Γ_m is given by

$$(4.10) \quad \Gamma_m \stackrel{\text{def}}{=} \frac{\chi_m - k\eta_2}{\chi_m + k\eta_2} \exp(-2jh\chi_m).$$

Substitution of this result in Eq. (4.4) gives

$$(4.11) \quad \Phi_{II}^t = \exp(j\alpha_\nu \ell) \sum_{m=0}^{\infty} A_m [\exp(j\chi_m z) + \Gamma_m \exp(-j\chi_m z)] \cos[m\pi(x_\nu/d - \frac{1}{2})].$$

We now have two sets of unknown coefficients, viz. A_m and R_r . We can eliminate one of these sets with the aid of the condition of continuity at the interface where the grooves are linked to the half-space $z > 0$:

$$(4.12) \quad \left. \begin{aligned} \partial \Phi_I^t / \partial z - j k \eta_1 \Phi_I^t &= \partial \Phi_{II}^t / \partial z - j k \eta_1 \Phi_{II}^t \\ \Phi_I^t &= \Phi_{II}^t \end{aligned} \right\} \begin{array}{l} \text{at } z = 0, \\ \nu \ell - d/2 < x < \\ \nu \ell + d/2 \end{array}$$

and the boundary condition on the ridges

$$(4.14) \quad \partial \Phi_I^t / \partial z - j k \eta_1 \Phi_I^t = 0, \text{ at } z = 0, \ell \nu + d/2 < x < \ell(\nu + 1) - d/2.$$

Substitution of Eqs. (4.1) and (4.11) in Eq. (4.12) gives

$$(4.15) \quad \begin{aligned} j(\gamma_0 - k\eta_1) \exp(j\alpha_0 x) - j \sum_{r=-\infty}^{\infty} R_r \exp(j\alpha_r x) (\gamma_r + k\eta_1) = \\ j \exp(j\alpha_0 \nu \ell) \sum_{m=0}^{\infty} A_m [\chi(1 - \Gamma_m) - k\eta_1(1 + \Gamma_m)] \cos[m\pi(x_\nu/d - \frac{1}{2})]. \end{aligned}$$

Replacing x by $x_\nu + \ell \nu$ in the left-hand side of Eq. (4.15), we may cancel the common factor $\exp(j\alpha_0 \ell \nu)$. Multiplying the left- and the right-hand sides of the resulting equation by $\exp(-j\alpha_r x_\nu)$, integrating between the limits $-\ell/2$ and $\ell/2$, using the orthogonality properties of the exponential function and the boundary condition Eq. (4.14), we obtain an expression for the reflection coefficient R_r in terms of A_m :

$$(4.16) \quad R_r = - \frac{1}{\ell(\gamma_r + k\eta_1)} \int_{-d/2}^{d/2} \sum_{m=0}^{\infty} A_m [\chi_m(1 - \Gamma_m) - k\eta_1(1 + \Gamma_m)] \times \\ \times \cos[m\pi(x_\nu/d - \frac{1}{2})] \exp(-j\alpha_r x_\nu) dx_\nu + \\ + \frac{\gamma_0 - k\eta_1}{\ell(\gamma_r + k\eta_1)} \int_{-\ell/2}^{\ell/2} \exp[jx_\nu(\alpha_0 - \alpha_r)] dx_\nu, r = 0, \pm 1, \pm 2, \dots$$

We now introduce the coefficients

$$\begin{aligned}
 v_{m,r} &\stackrel{\text{def}}{=} \frac{1}{d} \int_{-d/2}^{d/2} \cos [m\pi (x_\nu/d - \frac{1}{2})] \exp (j\alpha_r x_\nu) dx_\nu \\
 (4.17) \quad &= -j\alpha_r \frac{[\exp (j\alpha_r d/2) - (-1)^m \exp (-j\alpha_r d/2)]}{d (\alpha_r^2 - \pi^2 m^2/d^2)}.
 \end{aligned}$$

Eq. (4.16) can then be written as

$$(4.18) \quad R_0 = \frac{\gamma_0 - k\eta_1}{\gamma_0 + k\eta_1} - \left(\frac{d}{\ell}\right) \sum_{m=0}^{\infty} A_m [x_m (1 - \Gamma_m) - k\eta_1 (1 + \Gamma_m)] \frac{v_{m,0}^*}{\gamma_0 + k\eta_1};$$

$$R_r = -\left(\frac{d}{\ell}\right) \sum_{m=0}^{\infty} A_m [x_m (1 - \Gamma_m) - k\eta_1 (1 + \Gamma_m)] \frac{v_{m,r}^*}{(\gamma_r + k\eta_1)};$$

$$r = \pm 1, \pm 2, \dots$$

The asterisk attached to $v_{m,r}$ and $v_{m,0}$ indicates the complex conjugate. Substituting Eqs. (4.1) and (4.11) in the condition of continuity Eq. (4.13) we obtain

$$\begin{aligned}
 &\sum_{m=0}^{\infty} A_m (1 + \Gamma_m) \cos [m\pi (x_\nu/d - \frac{1}{2})] = \\
 (4.19) \quad &\sum_{r=-\infty}^{\infty} R_r \exp (j\alpha_r x_\nu) + \exp (j\alpha_0 x_\nu), \text{ when } -d/2 < x_\nu < d/2.
 \end{aligned}$$

Using the orthogonality properties of the cosine function over the period d , we obtain from Eq. (4.19) an expression for A_m in terms of R_r

$$\begin{aligned}
 A_m (1 + \Gamma_m) &= \left(\frac{\epsilon_m}{d}\right) \int_{-d/2}^{d/2} \exp (j\alpha_0 x_\nu) \cos [m\pi (x_\nu/d - \frac{1}{2})] dx_\nu \\
 (4.20) \quad &+ \left(\frac{\epsilon_m}{d}\right) \int_{-d/2}^{d/2} \sum_{r=-\infty}^{\infty} R_r \exp (j\alpha_r x_\nu) \cos [m\pi (x_\nu/d - \frac{1}{2})] dx_\nu. \\
 &\quad (m = 0, 1, 2, \dots),
 \end{aligned}$$

where $\varepsilon_0 = 1$ and $\varepsilon_m = 2$ when $m \geq 1$. Making use of Eq. (4.17), Eq. (4.20) can be written as

$$(4.21) \quad A_m (1 + \Gamma_m) = \varepsilon_m V_{m,0} + \varepsilon_m \sum_{r=-\infty}^{\infty} V_{m,r} R_r, \quad (m = 0, 1, 2, \dots).$$

By eliminating the reflection amplitudes with the aid of Eq. (4.18) we obtain an infinite system of linear equations in which the groove field amplitudes A_n occur as unknowns

$$(4.22) \quad (1 + \Gamma_n) A_n = b_n - \sum_{m=0}^{\infty} U_{m,n} A_m, \quad (n = 0, 1, 2, \dots),$$

where

$$(4.23) \quad b_n \stackrel{\text{def}}{=} 2 \varepsilon_n v_{n,0} \gamma_0 / (\gamma_0 + k \eta_1),$$

$$(4.24) \quad U_{m,n} \stackrel{\text{def}}{=} \varepsilon_n \left(\frac{d}{l} \right) [\chi_m (1 - \Gamma_m) - k \eta_1 (1 + \Gamma_m)] \times \\ \times \sum_{r=-\infty}^{\infty} v_{m,r}^* v_{n,r} / (\gamma_r + k \eta_1).$$

In a similar way we can first eliminate the groove field amplitudes; then we obtain an infinite system of linear equations in which the reflection coefficients R_r occur as unknowns:

$$(4.25) \quad (\gamma_n + k \eta_1) R_n = c_n - \sum_{r=-\infty}^{\infty} V_{r,n} R_r, \quad (n = 0, \pm 1, \pm 2, \dots),$$

where

$$(4.26) \quad c_0 \stackrel{\text{def}}{=} + \gamma_0 - k \eta_1 - \left(\frac{d}{l} \right) \sum_{m=0}^{\infty} \varepsilon_m \frac{[\chi_m (1 - \Gamma_m) - k \eta_1 (1 + \Gamma_m)]}{(1 + \Gamma_m)} v_{m,0}^* v_{m,0};$$

(4.27)

$$c_n \stackrel{\text{def}}{=} - \left(\frac{d}{l} \right) \sum_{m=0}^{\infty} \epsilon_m \frac{[x_m (1 - \Gamma_m) - k \eta_1 (1 + \Gamma_m)]}{(1 + \Gamma_m)} v_{m,n} v_{m,0}^*$$

(4.28)

 $(n = \pm 1, \pm 2, \dots),$

$$v_{r,n} \stackrel{\text{def}}{=} \left(\frac{d}{l} \right) \sum_{m=0}^{\infty} \epsilon_m \frac{[x_m (1 - \Gamma_m) - k \eta_1 (1 + \Gamma_m)]}{(1 + \Gamma_m)} v_{m,n}^* v_{m,r}$$

 $(n, r = 0, \pm 1, \pm 2, \dots)$

4.4 Considerations concerning the scattered and absorbed power by the uneven surface

In the first place we shall prove that of the reflected spectrum only the uniform plane waves contribute to the power radiated into the half-space $z > 0$ and that the evanescent waves do not carry any power into this domain. In order to substantiate this statement we start with the general formula for power transport across a surface. The power P_s scattered across one period of the uneven surface and per unit length in the y -direction is given by

$$(4.29) \quad P_s = \frac{1}{2} \operatorname{Re} \left[\int_{-l/2}^{l/2} \Phi^S(x, 0) \underline{u}^{S*} \cdot \underline{n} \, dx \right]$$

where $\underline{u}^S \cdot \underline{n}$ represents the particle velocity associated with the scattered field in the direction normal to the interface. With the aid of the equation of motion we eliminate this particle velocity, through

$$(4.30) \quad \underline{u}^S \cdot \underline{n} = - (j \omega \rho_0)^{-1} \partial \Phi^S / \partial \underline{n}.$$

We then obtain, if we insert at the same time the plane wave representation for Φ^S into Eq. (4.29),

$$(4.31) \quad P_s = \frac{1}{2} (\omega \rho_0)^{-1} \operatorname{Re} \left[\int_{-l/2}^{l/2} \left\{ \sum_{r=-\infty}^{\infty} R_r \exp(j \alpha_r x) \right\} \times \right. \\ \left. \times \left\{ \sum_{n=-\infty}^{\infty} R_n^* (\kappa^2 - \alpha_n^2)^{\frac{1}{2}} \exp(-j \alpha_n x) \right\} dx \right].$$

By evaluating the occurring integrals we obtain by virtue of the orthogonality properties of the exponential function

$$(4.32) \quad P_S = \frac{1}{2} \ell (\omega \rho_0)^{-1} \operatorname{Re} \left[\sum_{r=-\infty}^{\infty} |R_r|^2 (\kappa^2 - \alpha_r^2)^{\frac{1}{2}} \right].$$

However, only for a finite number of values of r , viz. those corresponding to the uniform plane waves, the square root $(\kappa^2 - \alpha_r^2)^{\frac{1}{2}}$ is a real quantity. For all remaining values of r , $(\kappa^2 - \alpha_r^2)^{\frac{1}{2}}$ is imaginary; these terms do not contribute to P_S because of the operation of taking the real part. The quantity P_S is, therefore, built up solely from the contributions of the uniform plane waves, travelling without damping into the half-space $z > 0$.

In addition the power P_a absorbed by one period of the uneven surface is immediately given by the difference between the incident power P_i , i.e., $\frac{1}{2} \cos(\theta) \ell / \rho_0 c$, and P_S .

A different method for calculating P_a employs the field directly above the boundary of the periodic structure. The absorbed power P_a may then be derived from the general formula for sound absorption Eq. (1.10). Accordingly, we have

$$(4.33) \quad P_a = \frac{\frac{1}{2} \operatorname{Re}(\eta_2)}{(\rho_0 c)} \int_{-d/2}^{d/2} \left| \Phi_{II}^t(x_\nu, -h) \right|^2 dx_\nu + \frac{\frac{1}{2} \operatorname{Re}(\eta_1)}{\rho_0 c} \int_{d/2}^{l-d/2} \left| \Phi_I^t(x, 0) \right|^2 dx.$$

The first term of this equation represents the sound absorption by the groove, while the second term represents the absorption by the ridge. We now define the true absorption coefficient a_{tr} as the ratio of P_a to P_i , i.e. $a_{tr} = P_a / P_i$.

We also distinguish another absorption coefficient, the so-called equivalent absorption coefficient a_{eq} , representing the sound absorption as if there were no diffraction of the waves at the edges of the grooves. Consequently,

$$(4.34) \quad a_{eq} = (d/\ell) a_{2,\theta} + [(l-d)/\ell] a_{1,\theta},$$

where $a_{1,\theta}$ and $a_{2,\theta}$ are the absorption coefficients for an infinite sample of the sound absorbing materials of which the upper side of the ridges and the bottom of the grooves, respectively, are consisting.

Still another interesting quantity is the shape factor Q defined as the ratio of a_{tr} and a_{eq} ; this quantity is a measure for the edge effect in the periodic structure.

4.5 Considerations concerning the Wood anomaly, the surface resonance and the waveguide resonance

The Wood anomaly is related to the occurrence of zeros among the coefficients γ_n . When this occurs one of the plane waves is travelling exactly along the uneven surface. This event is mathematically accompanied by a singularity in the scattered field. This singularity in the wave field is also experimentally observed in the investigation of light diffraction by an optical reflection grating. In 1902 WOOD discovered the presence of unexpected narrow bright and dark bands in the spectrum of an optical reflection grating illuminated by a light source with a slowly varying spectral intensity distribution. He noticed, in addition, that the occurrence of these bands was dependent upon the state of polarization of the incident light. Since these effects could not be explained by means of ordinary grating theory, WOOD termed them "anomalies".

The first theoretical treatment of these anomalies has been given by RAYLEIGH [1907]. His "dynamical theory of the grating" was based on an expansion of the scattered field in terms of outgoing waves only in the entire domain up to the corrugated surface. With this assumption he found that the scattered field is singular at wavelengths or angles of incidence for which one of the spectral orders emerges from the grating at the grazing angle. If by variation of θ , φ and k one of the γ_n 's changes from real to imaginary values, or vice versa, the corresponding reflection amplitudes show an anomalous behaviour. An indication for this anomalous behaviour of the reflection coefficients is that the reflected power distributes itself over one more or one less spectral order when passing a zero of γ_n .

One of the limitations in RAYLEIGH's results is that it does not yield the shape of the bands associated with the anomaly. In an attempt to overcome this difficulty FANO [1938], and afterwards ARTMANN [1942] derived approximate expansions in the vicinity of the singularities, of which only ARTMANN's representation of the field exhibits some characteristic properties of the shape of the Wood anomalies.

For a period of several years, therefore, the theory was essentially in agreement with the basic experimental observations, even though many of the finer points, such as the detailed shape of the anomalies, could not be calculated.

A careful re-examination of RAYLEIGH's initial assumption of including outgoing waves only was conducted by LIPPMANN [1953] and he concluded that RAYLEIGH's approximation to be a valid one for shallow grooves only. For this reason RAYLEIGH's theory is clearly incompetent to predict the finer details of the Wood anomalies.

In recent years, with the advance of sophistication in the treatment of scattering from various obstacles, a different approach to the explanation of the Wood anomalies has been adopted. This approach is based on the multiple-scattering point of view. In most of the relevant treatments, the total scattered field is expressed in terms of the single-scattering amplitude of one scatterer within the grating. The expression for the multiple-scattering amplitude takes into account all the coupling effects between the various scatterers. Such analyses have been applied by a number of writers to a variety of periodic arrays of scatterers. In particular, we mention KARP AND RADLOW [1956], MILLAR [1963a, b] and TWERSKY [1952, 1956]. This method can predict satisfactorily the location and shape of the anomalies in the case of certain

simple geometries of the basic scatterer in the grating. The results, however, have been limited to gratings of relatively shallow groove depth.

A new theoretical approach is presented by OLINER and HESSEL [1965] which yields a new insight into the character of Wood's anomalies. It is not an extension of the multiple-scattering approach, but it may be viewed upon as an extension of RAYLEIGH's work containing a number of new elements. If the intensity variations of a Wood anomaly are examined carefully, it is seen that the appearance of a next undamped spectral order is in itself not sufficient for a description of the form of variation. There is, in addition, a resonance effect present. The resonance condition can be seen from the second system of equations (Eq. (4.25)) involving the reflection amplitudes R_r , by inspecting the diagonal elements. The resonance is expected to occur when one of these elements takes a small value, viz. if $|\gamma_n + k\eta_1 + V_{n,n}| \rightarrow 0$. For some structures these resonance effects can occur at wavelengths or angles of incidence far removed from the values predicted by the Rayleigh condition. If $V_{n,n}$ is viewed upon as an admittance, representing the influence of the grooves, the above condition is related to the total surface admittance. The phenomenon is, therefore, called the surface resonance. Especially, if γ_n is negative imaginary and the quantity $k\eta_1 + V_{n,n}$ has a positive imaginary part together with a small real part, we could expect a sharp resonance type of behaviour in the reflection coefficients. In the special case of vanishing groove depth the quantity $k\eta_1 + V_{n,n}$ turns out to approach the value η_{av} of the admittance, averaged over one period of the surface.

In a similar way we can disclose a resonance type of behaviour in the groove field amplitudes by inspecting the diagonal elements of the first system of equations (Eqs. (4.22)), involving the unknown groove field amplitudes. The corresponding "waveguide resonance" is associated with the existence of minimum values of these diagonal elements.

Especially the minimum values of the zero-order diagonal element turns out to exert considerable influence upon the calculated value of the absorption coefficient. Roughly speaking, resonances associated to the plane-wave mode in the groove are simply given by the relation

$$|1 + \Gamma_0| \rightarrow 0$$

or

$$\left| 1 + \frac{\kappa - k\eta_2}{\kappa + k\eta_2} \exp(-2j\kappa h) \right| \rightarrow 0.$$

In the case of a non-absorbing groove bottom ($\eta_2 = 0$) the left-hand side in the equation approaches zero for values of κh equal to $(n + \frac{1}{2})\pi$, with $n = 0, 1, 2, \dots$. In the case of non-vanishing admittance η_2 , the quantity $1 + \Gamma_0$ cannot take on the value zero, but does have a minimum. The quantity $U_{0,0}$ can be viewed upon as a detuning factor: the real resonance groove depth deviates from the values of κh obtained by an application of the condition $|1 + \Gamma_0| \rightarrow 0$. We observe a similar process in open organ pipes. The true resonance frequency does not agree with values computed from the geometrical length of the column. An end correction for the effective length of the column which is proportional to the tube radius. The pressure in the mouth of the groove at $z = 0$ has to be accounted for

$$\Phi^t(x_\nu, 0) = \exp(j\alpha_0 \ell \nu) \left[A_0 (1 + \Gamma_0) + \sum_{m=1}^{\infty} A_m (1 + \Gamma_m) \cos \left[m\pi(x_\nu/d - \frac{1}{2}) \right] \right].$$

For the sake of simplicity we confine ourselves here to the case where the zero-order term of the left-hand side of this equation expresses the dominant part of the sound pressure. Under this condition it is obvious that Φ^t approaches a minimum value at the wave guide resonance. At the bottom of the groove we have the sound pressure

$$\begin{aligned} \Phi^t(x_\nu, -h) = \exp(j\alpha_0 \ell \nu) & \left[A_0 \left\{ \exp(-j\kappa h) + \Gamma_0 \exp(j\kappa h) \right\} + \right. \\ & \left. + \sum_{m=1}^{\infty} A_m \left\{ \exp(-j\chi_m h) + \Gamma_m \exp(j\chi_m h) \right\} \right] \end{aligned}$$

It is obvious at this place that the sound pressure exhibits a maximum value at the waveguide resonance. It is now apparent why the two important types of uneven surfaces profoundly investigated in this Chapter, i.e.:

- (i) the uneven surface of rectangular profile with $\eta_1 \neq 0a$ and $\eta_2 = 0$;
- (ii) the uneven surface of rectangular profile with $\eta_1 = 0$ and $\eta_2 \neq 0$

show large differences in their behaviour as to the sound absorption in the neighbourhood of the waveguide resonance. In the first case the sound pressure above the acoustical material on the ridges beside the grooves decreases sharply as a consequence of the sharp drop in sound pressure at the mouth of the groove. In the second case a maximum pressure at the bottom of the groove leads to an unusually large sound absorption.

4.6 Numerical computations

The infinite systems of linear equations, Eqs. (4.22) and (4.25), can be most suitably solved by the method outlined in Section 3.4. Accordingly, we truncate the infinite systems to finite ones.

The solution will evidently be acceptable only if the error involved in solving N equations approaches zero as N tends to infinity. For this reason we evaluate $U_{m,n}$ and $V_{r,n}$ for large values of m , $|n|$ and $|r|$. For large values of m , n and r we have from Eqs. (4.10), (4.17) and (4.24)

$$v_{m,r} = O(m^{-2} r^{-1}) \text{ as } m \rightarrow \infty, |r| \rightarrow \infty;$$

$$1 + \Gamma_m = O(1), 1 - \Gamma_m = O(1) \text{ and } \chi_m = O(m) \text{ as } m \rightarrow \infty.$$

Hence

$$U_{m,n} = O(m^{-1} n^{-2}) \text{ as } m, n \rightarrow \infty.$$

The summations with respect to r converge very rapidly, since

$$v_{m,r} v_{n,r} / (\gamma_r + k\eta_1) = O(r^{-3}) \text{ as } |r| \rightarrow \infty$$

for all m and n .

In the same way we have

$$V_{n,r} = O(r^{-1}n^{-2})$$

For the solution to be unique it is sufficient that the matrix coefficients satisfy the Koch condition (cf. Section 3.4). Both systems under consideration obviously satisfy this condition. The truncated systems are most suitably solved by the method of the Jacobi iteration. In the zero-order approximation we neglect in the matrices of coefficients the non-diagonal elements with respect to the diagonal elements, i.e. we take $U_{m,n} = 0$ and $V_{r,n} = 0$ if $m \neq n$, $r \neq n$. Then only the diagonal elements remain and the corresponding zero-order solution is

$$A_n^{(0)} = b_n / (1 + \Gamma_n + U_{n,n});$$

$$R_n^{(0)} = c_n / (\gamma_n + k\eta_1 + V_{n,n}).$$

This zero-order approximation is the starting value in a recurrence relation for any approximation of higher order s :

$$A_n^{(s+1)} (1 + \Gamma_n + U_{n,n}) = b_n - \sum_{\substack{m=0 \\ m \neq n}}^N U_{m,n} A_m^{(s)},$$

$$R_n^{(s+1)} (\gamma_n + k\eta_1 + V_{n,n}) = c_n - \sum_{\substack{r=-N \\ r \neq n}}^N V_{r,n} R_r^{(s)}.$$

A sufficient condition for convergence is that the diagonal elements are predominant, which implies

$$|1 + \Gamma_n + U_{n,n}| > \sum_{\substack{m=0 \\ m \neq n}}^{\infty} |U_{m,n}|;$$

$$|\gamma_n + k\eta_1 + V_{n,n}| > \sum_{\substack{r=-\infty \\ r \neq n}}^{\infty} |V_{r,n}|.$$

For our problem the diagonal elements are predominant in most cases except in the three cases of anomalous behaviour.

Both systems are equally valuable for numerical computations although in some cases the successive approximation for one system will converge more rapidly than for the other. For example, for small groove widths it is advantageous to use the first system, Eqs. (4.22), in which the groove field amplitudes A_n occur as unknowns and hence the amplitude A_0 is the most important one of the coefficients A_n . The sound pressure in the groove is then almost independent of the variable x . If on the other hand we look at the reflection amplitudes R_n , we observe that the reflection coefficient R_0 does not predominate the other reflection amplitudes so strongly, as there scattering of sound in all directions takes place.

We now pay attention to the types of resonance. In the first system involving the groove amplitudes we observe that if $|\gamma_n + k\eta_1|$ approaches a minimum, all the matrix elements $U_{m,n}$ become large and the iteration process for the A_n 's fails to converge. From the second system for the reflection amplitudes it is obvious that there is no reason for any difficulty. Thus, if we require a solution of the diffraction problem under consideration for angles of incidence for which the above condition is satisfied, we have always to use the second system in order to obtain the reflection amplitudes. It is worthwhile to remark that the above condition occurs for angles of incidence in the vicinity of those, pertaining to the surface resonance which is related to a minimum of $|\gamma_n + k\eta_1 + V_{n,n}|$. It is obvious from Eq. (4.21) that, if we have solved the reflection amplitudes, we also know the groove field amplitudes. If on the other hand the quantity $|1 + \Gamma_0|$ passes through a minimum, the matrix elements $V_{r,n}$ become large and the diagonal elements in this matrix predominate no longer. The use of the first system of equations is then to be preferred.

The latter preference holds in all cases where a sharp surface resonance does not occur, for the groove field amplitudes form a sequence with index m running from zero to infinity, while the index r of the reflection amplitudes runs through all the values from $-\infty$ to ∞ , the required number for $|m|$ and $|r|$ for suitable numerical computations being roughly equal. In practical cases the second system is twice as large as the first to obtain the same accuracy; in a typical case we required 20 equations of the first system versus 36 of the second one.

4.7 Discussion of the results

Numerical computations have been carried out for a number of cases, some of these results are presented in graphical form. Let us first discuss Figs 4.2-4.12 which demonstrate the behaviour of the absorption, expressed in terms of either the true absorption coefficient a_{tr} or the shape factor Q , as well as the reflection coefficients as a function of the angle of incidence for different values of kd , $k\ell$ and kh and the admittances η_1 and η_2 . Most of the data apply to the case for which only a few propagating spectral orders are present. In the plots the most striking feature is the occurrence

of the large variation in the reflection amplitudes, which can be ascribed to the Wood anomaly or the surface resonance. The influence of the diffraction anomalies is most clearly demonstrated in the behaviour of the reflection coefficients more than in the absorption behaviour. On notes the surface resonances (Figs. 4.2b - 4.4b). For instance, the reflection coefficient R_{-1} , exhibits a sharp maximum at the surface resonance followed by a rapid fall of infinite slope at the Wood anomaly. At $k\ell = 5$ one can ascertain that the Wood anomaly is located at $\Theta_{-1} = 14^{\circ}.9$, while the spectral order $n = -1$ is the resonant one. If $kh = 0$, $kd = 2.5$ and $\eta_1 = 0.627 + j 0.342$, $\eta_2 = 0$, we can compute the average value of the admittance over the surface to be $\frac{1}{2} \eta_1 = 0.314 + j 0.171$. From this knowledge one can readily compute the location of the maximum of the curve, using the fact that $|\gamma_{-1} + k\eta_{av}| = |\gamma_{-1} + \frac{1}{2} k\eta_1|$ approaches a minimum. From this equation we obtain a maximum of $|R_{-1}|$ which is located at $\Theta = 14^{\circ}$ which is in approximative agreement with the maximum of Fig. 4.2b. If $h \neq 0$ we expect that the location of the maximum has been displaced in consequence of the different value of η_{av} . Consider to this aim Figs. 4.3b and 4.4b, where $kh = 0.5$ and $kh = 1.0$, respectively. At the angle of incidence, pertaining to the Wood anomaly, the curve exhibits an infinite slope, probably because of the fact that the derivate of the square root γ_n to Θ , $\partial\gamma_n/\partial\Theta|_{\gamma_n=0}$, becomes infinite. Although we have not been able to determine whether or not this feature is generally true, the figures suggest this occurrence of an infinite slope.

Attention is now paid to two figures which differ in their value of the parameter kh (Figs. 4.8 and 4.9). The groove depth has a value $kh = 0$ and $kh = 1.0$, respectively; the other parameters remaining unaltered, viz. $kh = 5$, $k\ell = 10$, $\eta_1 = 0.265 + j 0.395$ and $\eta_2 = 0$, $\varphi = 90^{\circ}$. There are three locations of a Wood anomaly, viz. at $\Theta_{-2} = 14^{\circ}.9$, $\Theta_{+1} = 21^{\circ}.8$ and $\Theta_{-3} = 62^{\circ}.3$. Both figures show a considerable difference of behaviour in the vicinity of these angles. The infinite slope is present, of course, but the character of the absorption coefficients being quite different in both cases. In the case $kh = 0$, a_{tr} shows a sharp dip; if, however, $kh = 1$, a_{tr} shows a sharp peak at these angles. It is strange that the anomalies of order $n = +1$ and $n = -3$ are much more important than the one of order $n = -2$.

Figs. 4.6, 4.7 and 4.8 give an impression of the dependence on the azimuth φ . As φ increases, the number of anomalies decreases, but hardly influences the general trend of the curves. This is due to the fact that the reduced wave number κ hardly influences the absorption coefficient outside the anomalies.

Figs. 4.12 a, b and c give two examples of the absorption and reflection behaviour of strips in a periodic arrangement, the admittances in the two cases being complex conjugate, viz. $\eta_1 = 0.2 - j 0.4$ and $\eta_1 = 0.2 + j 0.4$. Upon examination of the two curves of the reflection amplitude of order $n = -1$ we find, if $\text{Im}(\eta_1) < 0$, the absence of a surface resonance. We only see a sharp peak precisely at the Wood anomaly. In the alternative case, $\text{Im}(\eta_1) > 0$, we observe the usual peak of the surface resonance, which has been displaced from the Wood anomaly.

It may be useful to mention here some experimental results obtained with absorbing reflection gratings. For this purpose the results of a recent

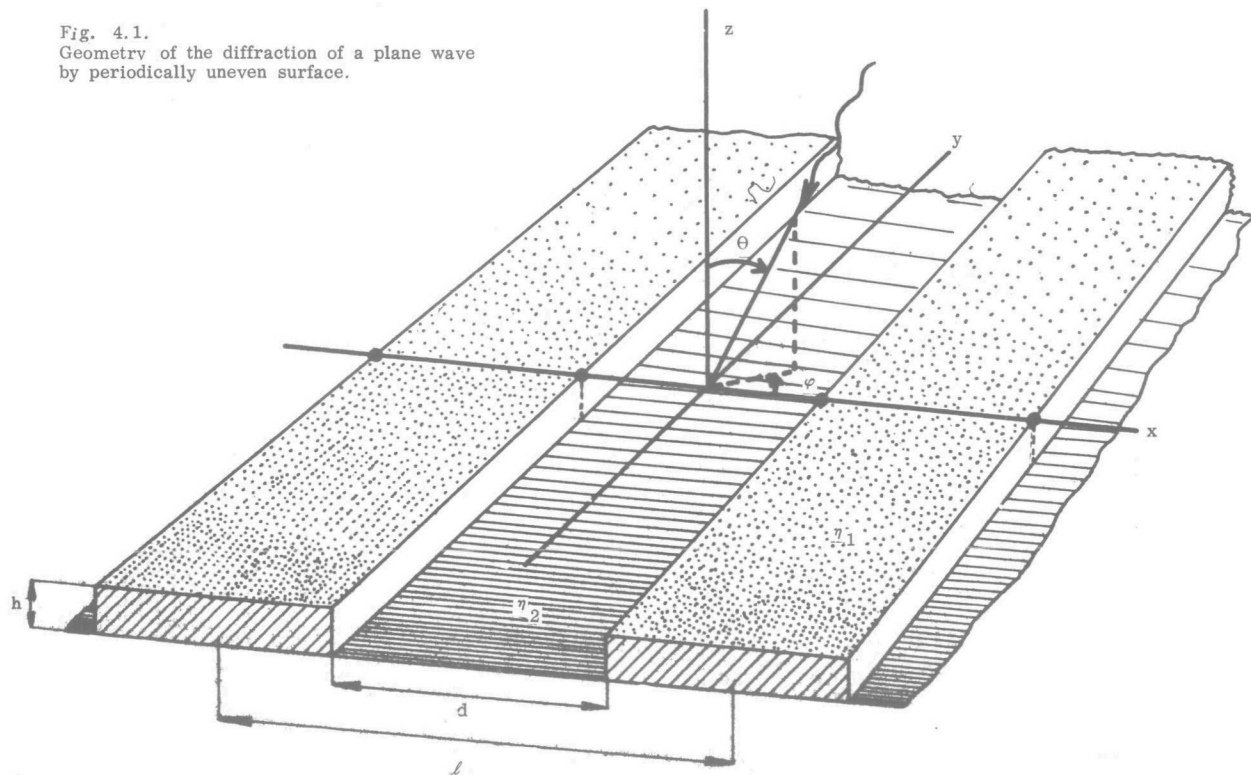
paper by HÄGGLUND and SELBERG [1966] are very suitable. These authors investigated the reflection, absorption and emission of light by an opaque optical grating, both theoretically and experimentally. Experiments and computations have been made, for instance, for aluminium gratings. With the exception of some comments published earlier by WOOD [1935] and by ARTMANN [1942], HÄGGLUND and SELBERG were the first to investigate experimentally the absorption properties at the Wood anomalies. The optical constants of aluminium in the region of visible light are well derived from the free electron model and so exhibit typical plasma properties. The losses are rather small and the imaginary part of the permittivity is smaller than the real part. Their results agree qualitatively surprisingly well with our results as far as the theory of the surface resonances is concerned. The authors found sharply peaked resonances beside the Wood anomalies. From their paper it is evident that the authors were not aware of the existence of a surface resonance as has been outlined by OLINER and HESSEL.

Other interesting features are shown in Figs. 4.13, 4.14 and 4.16 where the absorption coefficient a_{tr} or the shape factor Q has been plotted as a function of the groove depth kh . Upon examination of the curves we find a large variation in the absorption. Observe the difference between the two types of uneven surfaces mentioned in Section 4.5 as to their absorption properties. The extent of the peaks depends on the ratio d/l and the wave number k to a considerable degree. All the figures have been drawn for normal incidence. For oblique incidence the same type of figures is found. The consequence of these waveguide resonances for practical purposes has been investigated for a periodic structure in which the absorbing material is assumed to be Sillan SP 100, 5 cm thick, which has a frequency dependent admittance (Fig. 1.1). This construction has been applied in many halls for public assembly. Fig. 4.17 shows the results for three structures of different dimensions at normal incidence. If a very good absorbing structure were needed in a narrow frequency band and with attractive architectural properties, the periodic structure would meet the requirements. This arrangement of strips is obviously also advantageous from an economic point of view. The shape factor Q usually exceeds unity to a considerable extent. As the frequency increases, a_{tr} should approach a_{eq} ; this tendency is apparent from the graph.

A question arising in the measurement of the edge effect in the reverberation chamber, is the minimum allowable distance of the free edges of the patches in order to obtain an optimum value of b_{stat} . TEN WOLDE [1967] has pointed out that this distance plays a very important role in finding an optimum value of b_{stat} . For this reason a periodic arrangement of strips of width $kd = 5$ has been investigated, where the period of the structure has been varied. The angles of incidence were $\theta = 0^\circ$ and $\theta = 60^\circ$, respectively. At the same time the absorption coefficient of a single strip has been computed by the method developed in Chapter III. At large distances between the free edges the absorption coefficient of the strip in the periodic arrangement and the single strip are expected to approach each other. For normal incidence the distance for this agreement is much smaller than one wavelength, but at oblique incidence it can amount to about three wavelengths. This agrees with the experimental results of TEN WOLDE who found a distance of three wavelengths to be acceptable for finding a correct value of b_{stat} in a diffuse

sound field. The angle of incidence 60° has been taken on account of the fact, that this value is representative for a diffuse sound field since it is most nearly equal to the average value of the angle of incidence.

Fig. 4.1.
Geometry of the diffraction of a plane wave
by periodically uneven surface.



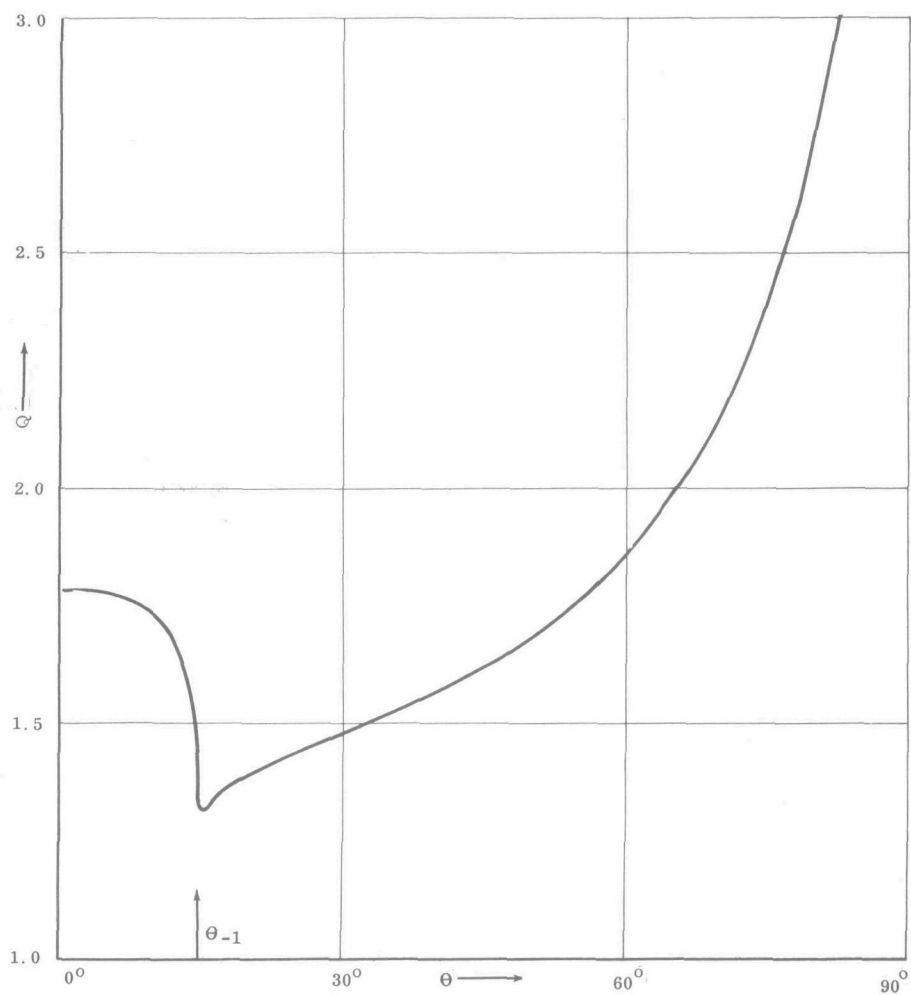


Fig. 4.2a. The shape factor Q as a function of the angle of incidence θ .
 $\eta_1 = 0.627 + j 0.342$; $\eta_2 = 0$;
 $k\ell = 5.0$; $k_d = 2.5$; $k_h = 0$.
 $\varphi = 0^\circ$.

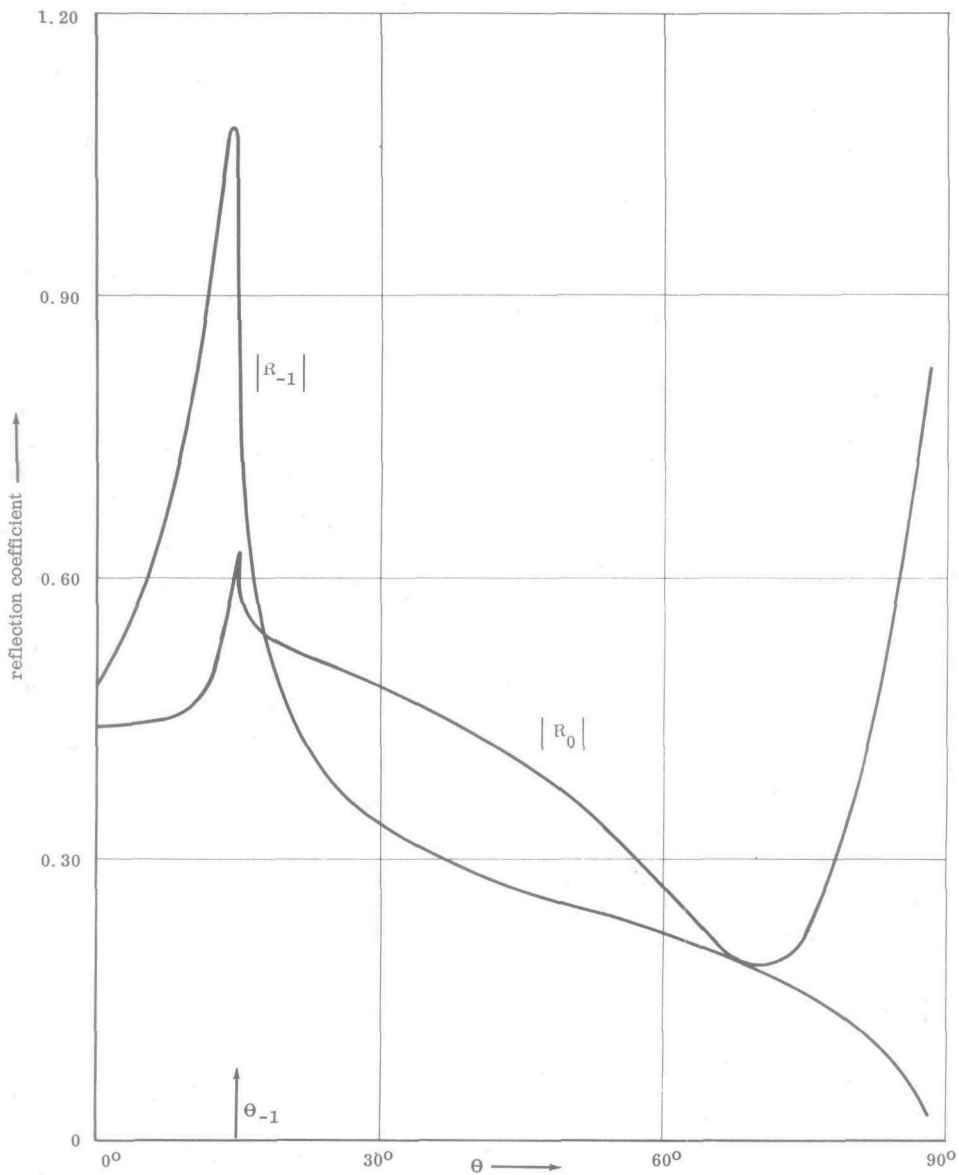


Fig. 4.2b. The modulus of the reflection coefficients R_0 and R_{-1} as a function of the angle of incidence θ . Other conditions as in Fig. 4.2a.

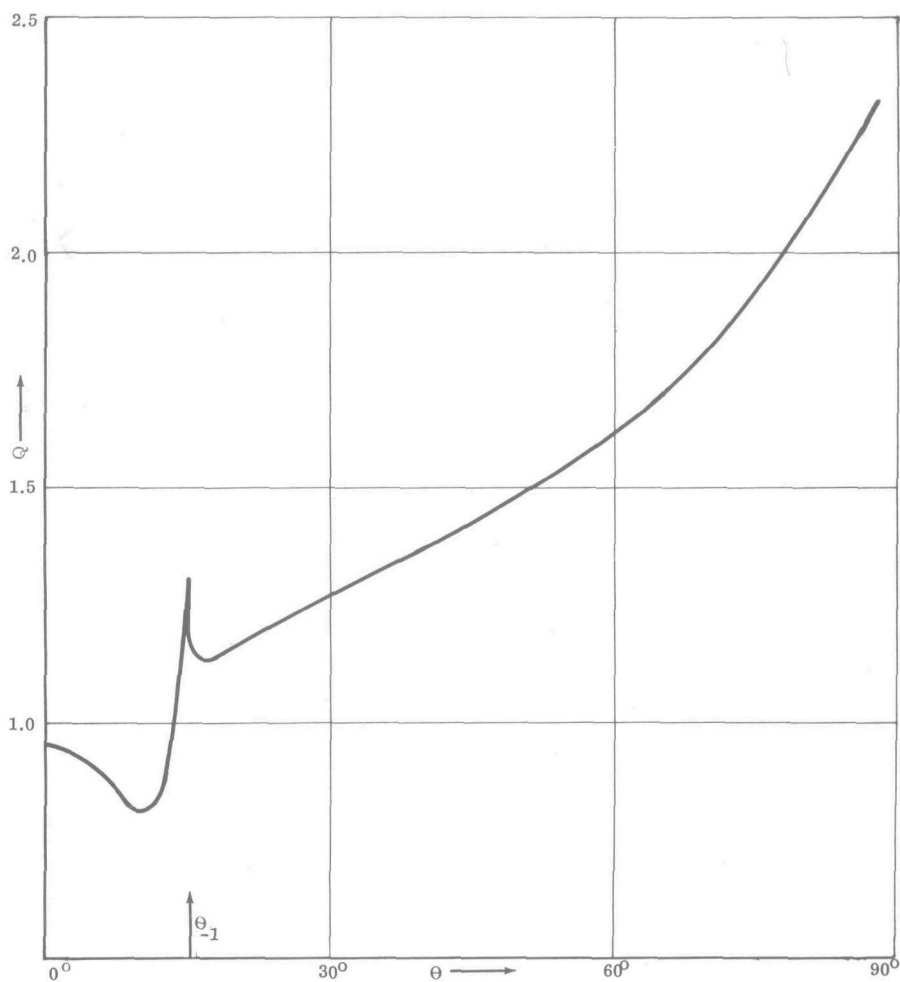


Fig. 4.3a. The shape factor Q as a function of the angle of incidence θ .

$$\eta_1 = 0.627 + j 0.342; \eta_2 = 0;$$

$$k_L = 5.0; k_d = 2.5; k_h = 0.5;$$

$$\varphi = 0^\circ.$$

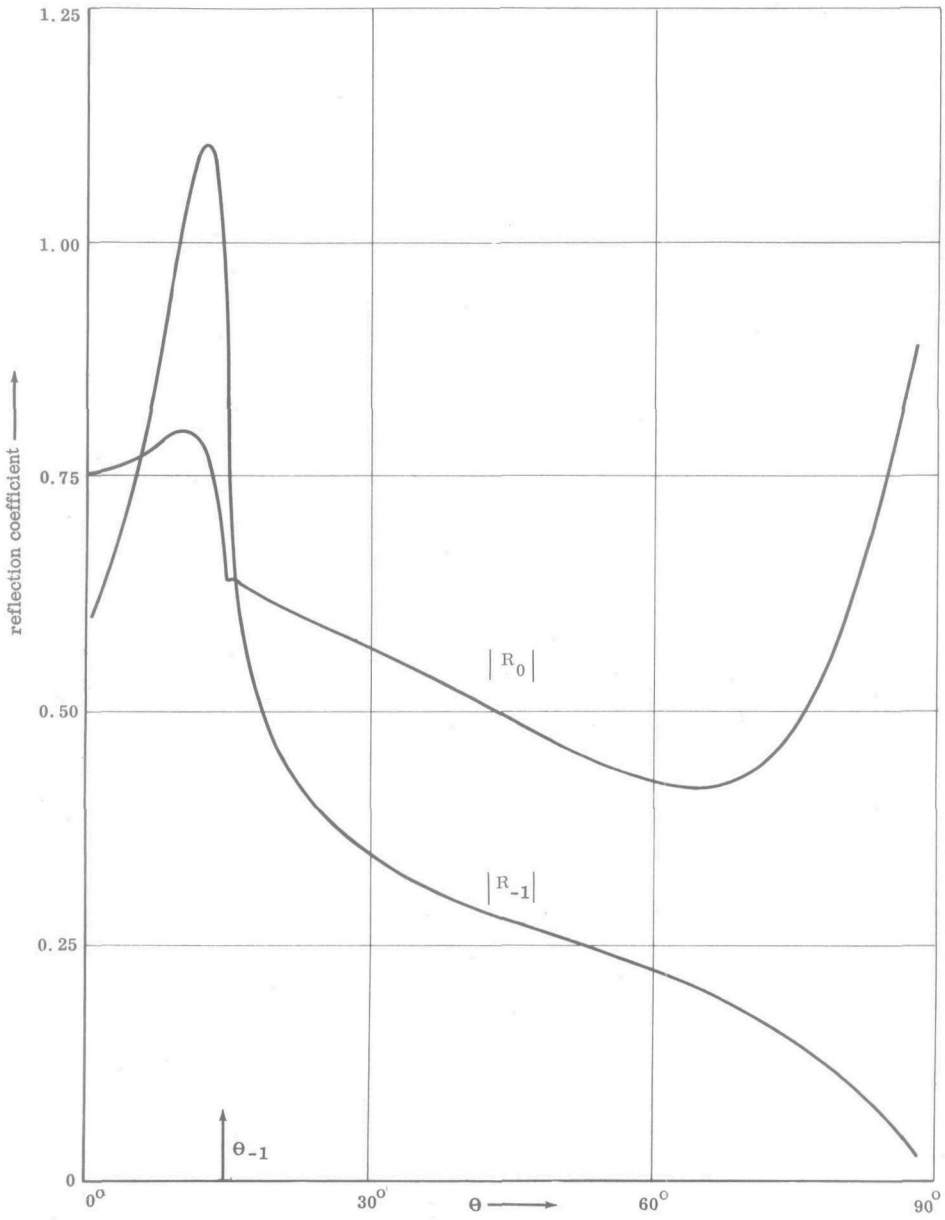


Fig. 4.3b. The modulus of the reflection coefficients R_0 and R_{-1} as a function of the angle of incidence θ . Other conditions as in Fig. 4.3a.

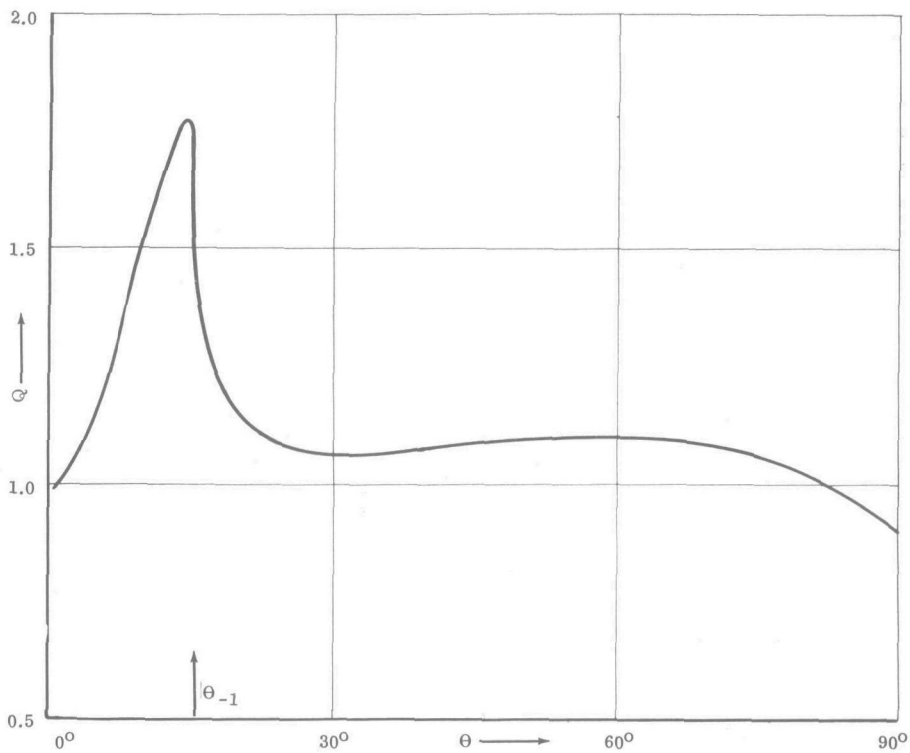


Fig. 4.4a. The shape factor Q as a function of the angle of incidence θ .

$$\eta_1 = 0.627 + j 0.342; \eta_2 = 0;$$

$$kz = 5.0; kd = 2.5; kh = 1.0;$$

$$\varphi = 0^\circ.$$

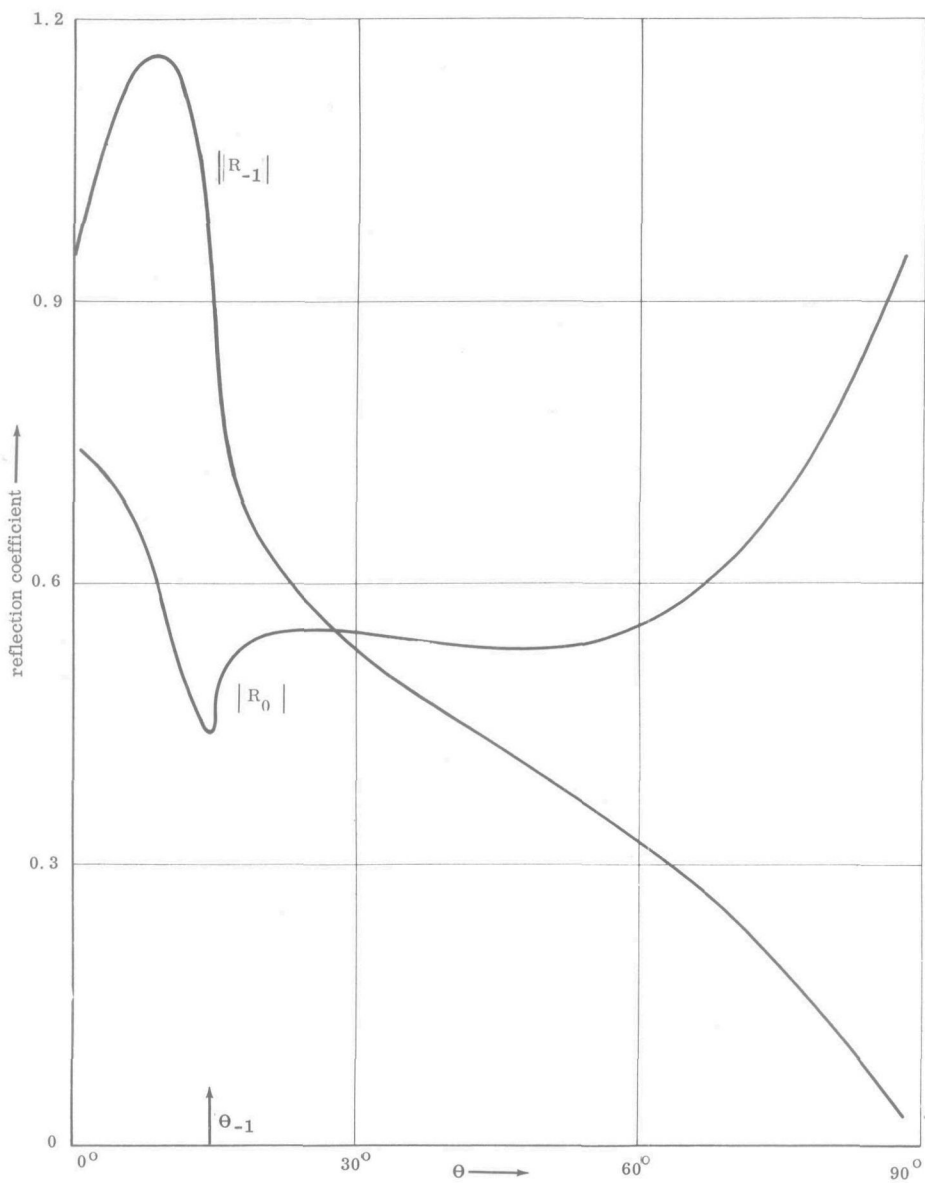


Fig. 4.4b. The modulus of the reflection coefficients R_0 and R_{-1} as a function of the angle of incidence θ . Other conditions as in Fig. 4.4a.

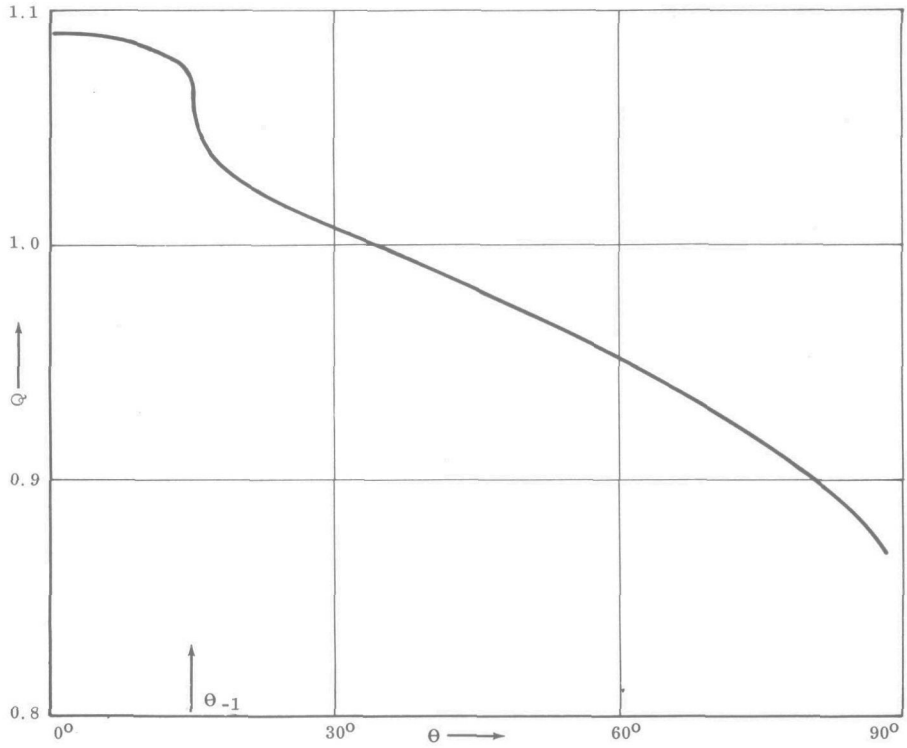


Fig. 4.5a. The shape factor Q as a function of the angle of incidence

$$\eta_1 = \eta_2 = 0.627 + j 0.342$$

$$\kappa l = 5.0; \quad \kappa d = 2.5; \quad \kappa h = 1.0;$$

$$\varphi = 0^\circ.$$

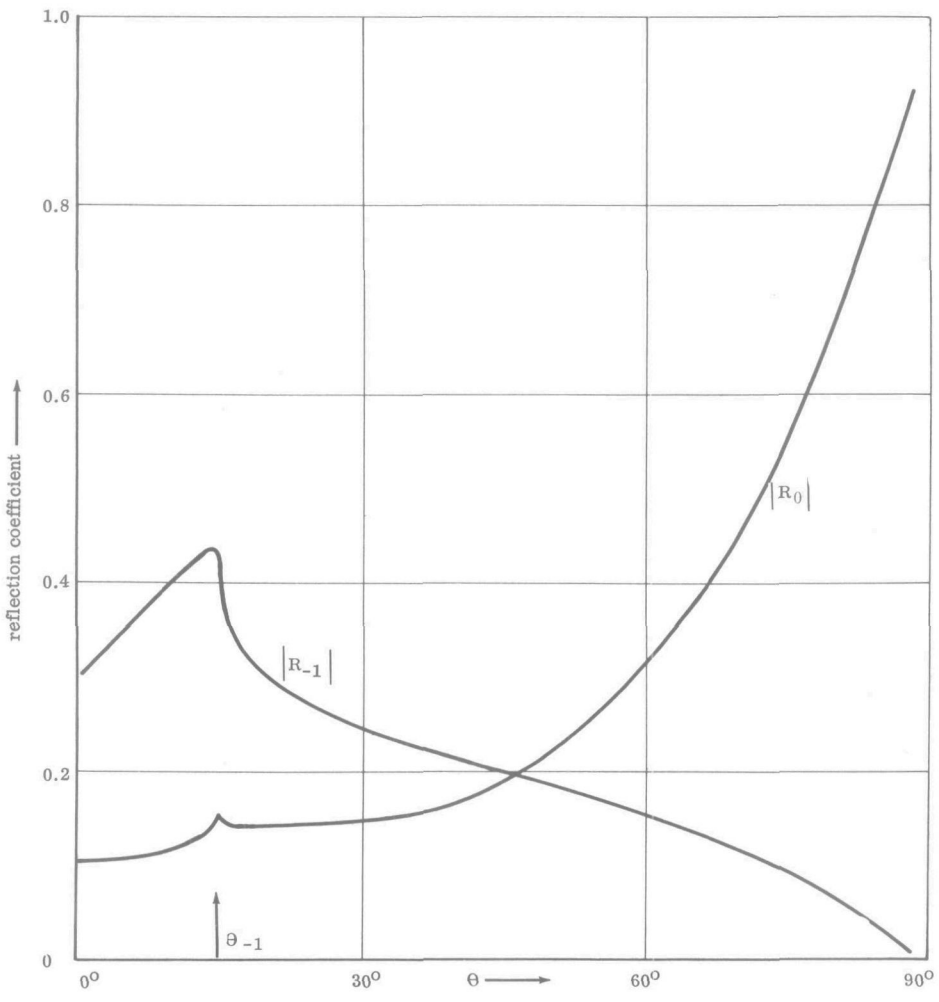


Fig. 4.5b. The modulus of the reflection coefficients R_0 and R_{-1} as a function of the angle of incidence θ . Other conditions as in Fig. 4.5a.

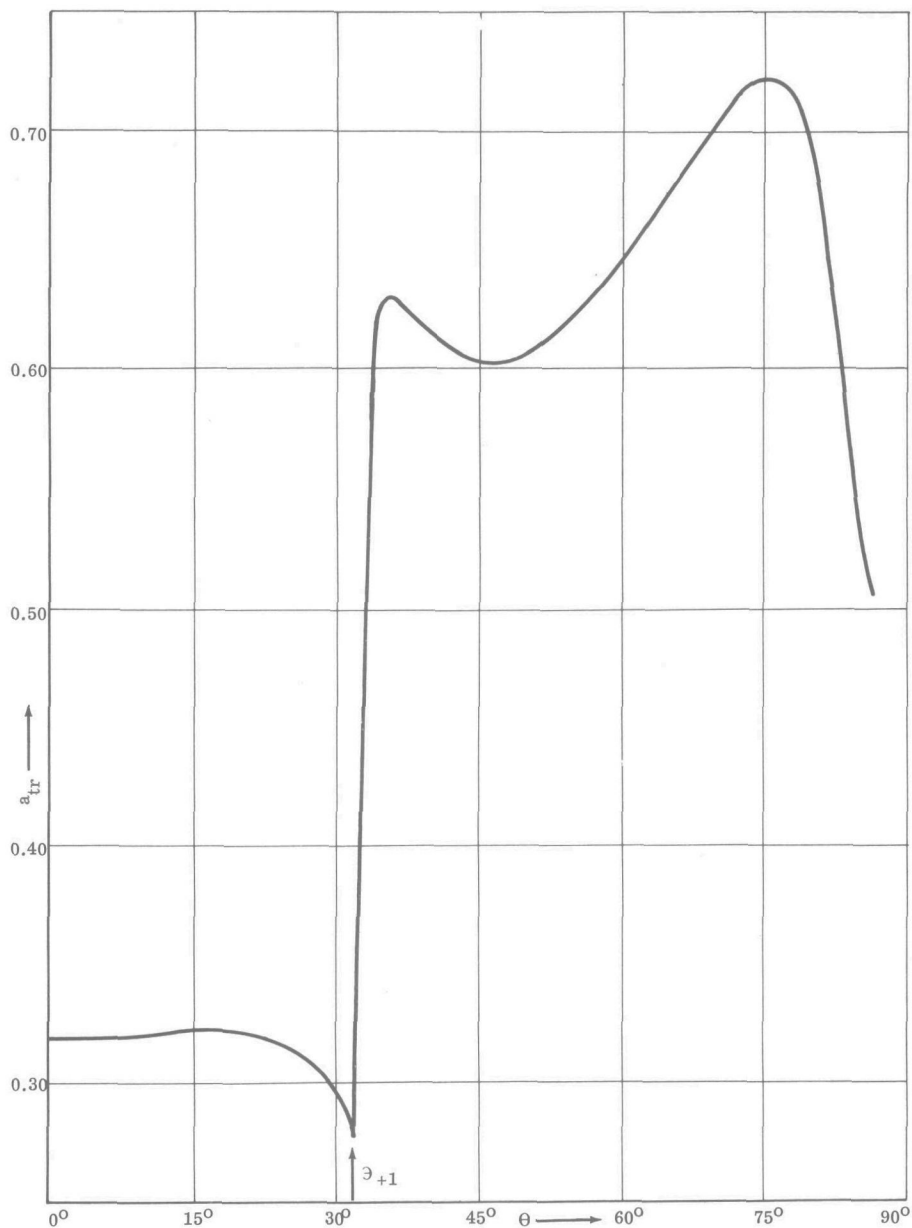


Fig. 4.6. The absorption coefficient a_{tr} as a function of the angle of incidence θ .
 $\eta_1 = 0.264 + j 0.395$; $\eta_2 = 0$;
 $k\ell = 10.0$; $kd = 5.0$; $kh = 0$;
 $\varphi = 60^\circ$.

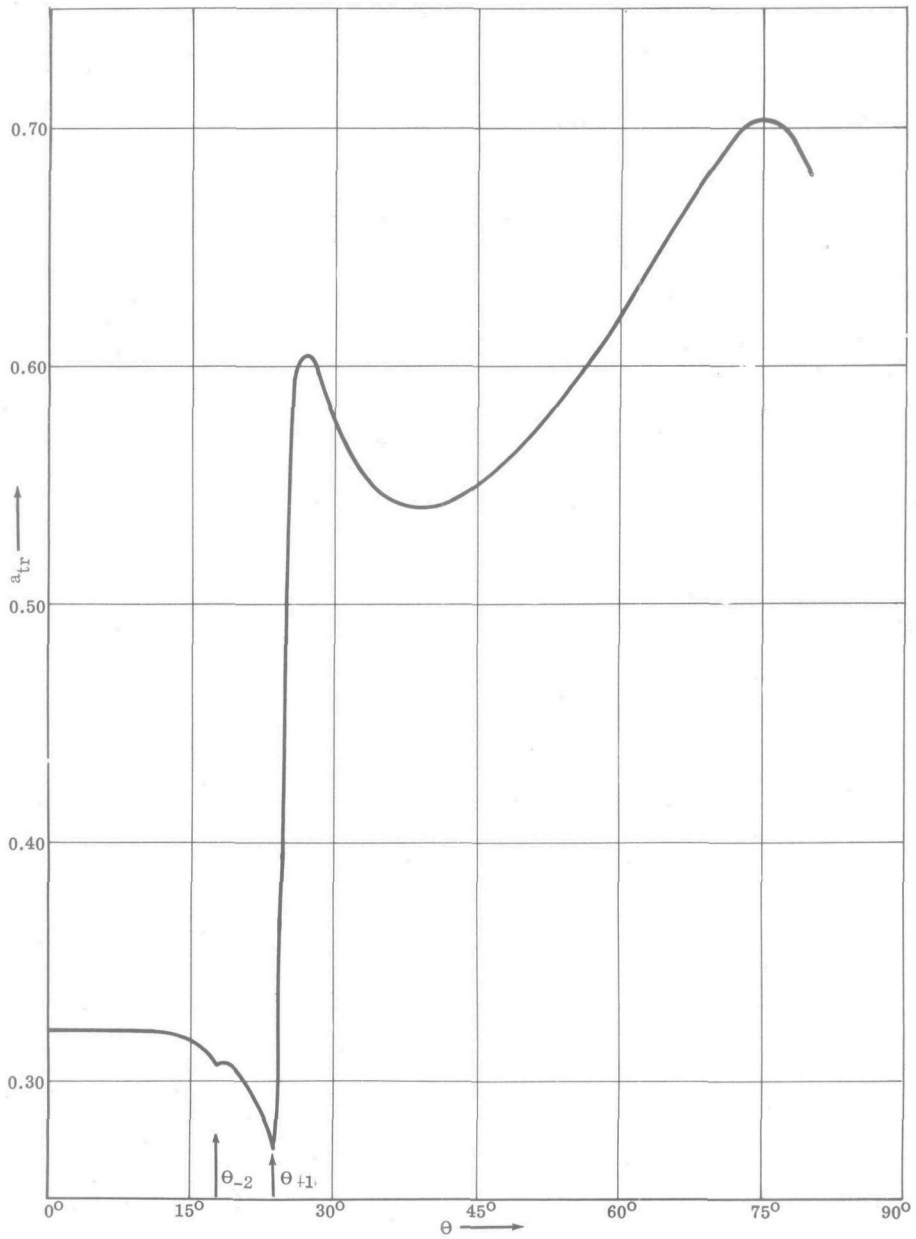


Fig. 4.7. The absorption coefficient a_{tr} as a function of the angle of incidence θ .
 $\eta_1 = 0.264 + j 0.395$; $\eta_2 = 0$;
 $kL = 10.0$; $kd = 5.0$; $kh = 0$;
 $\varphi = 30^\circ$.

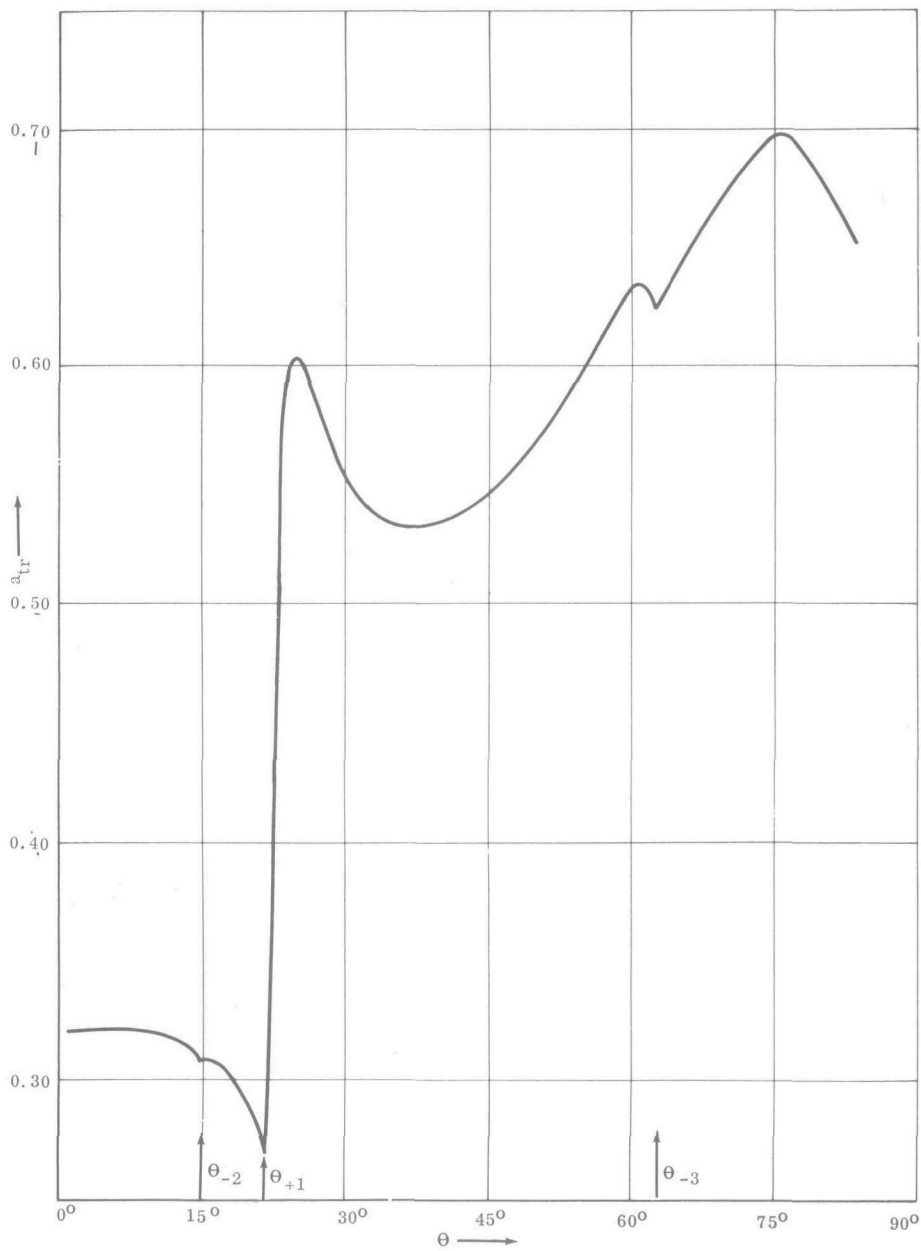


Fig. 4.8. The absorption coefficient a_{tr} as a function of the angle of incidence θ .
 $\eta_1 = 0.264 + j 0.395; \eta_2 = 0;$
 $kL = 10.0; kd = 5.0; kh = 0;$
 $\epsilon = 0$

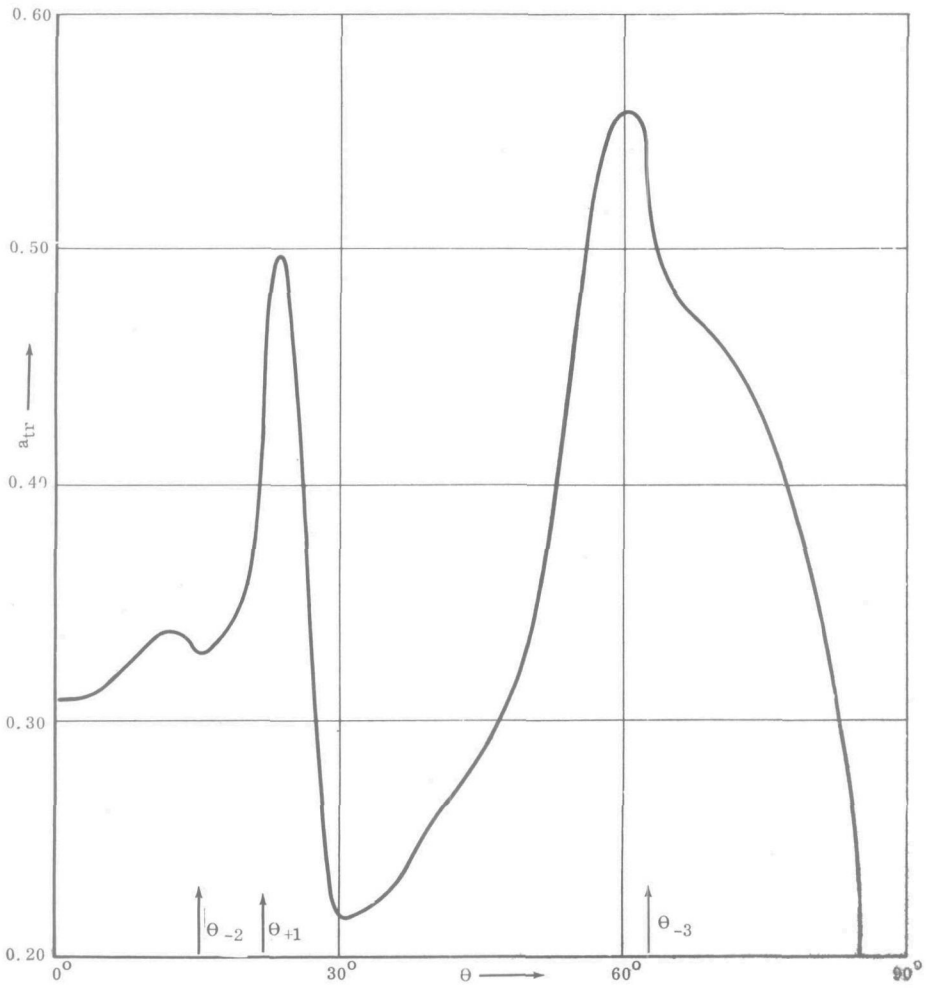


Fig. 4.9. The absorption coefficient a_{tr} as a function of the angle of incidence θ .
 $\eta_1 = 0.264 + j 0.395$; $\eta_2 = 0$;
 $kL = 10$; $kd = 5$; $kh = 1$;
 $\varphi = 0^\circ$.

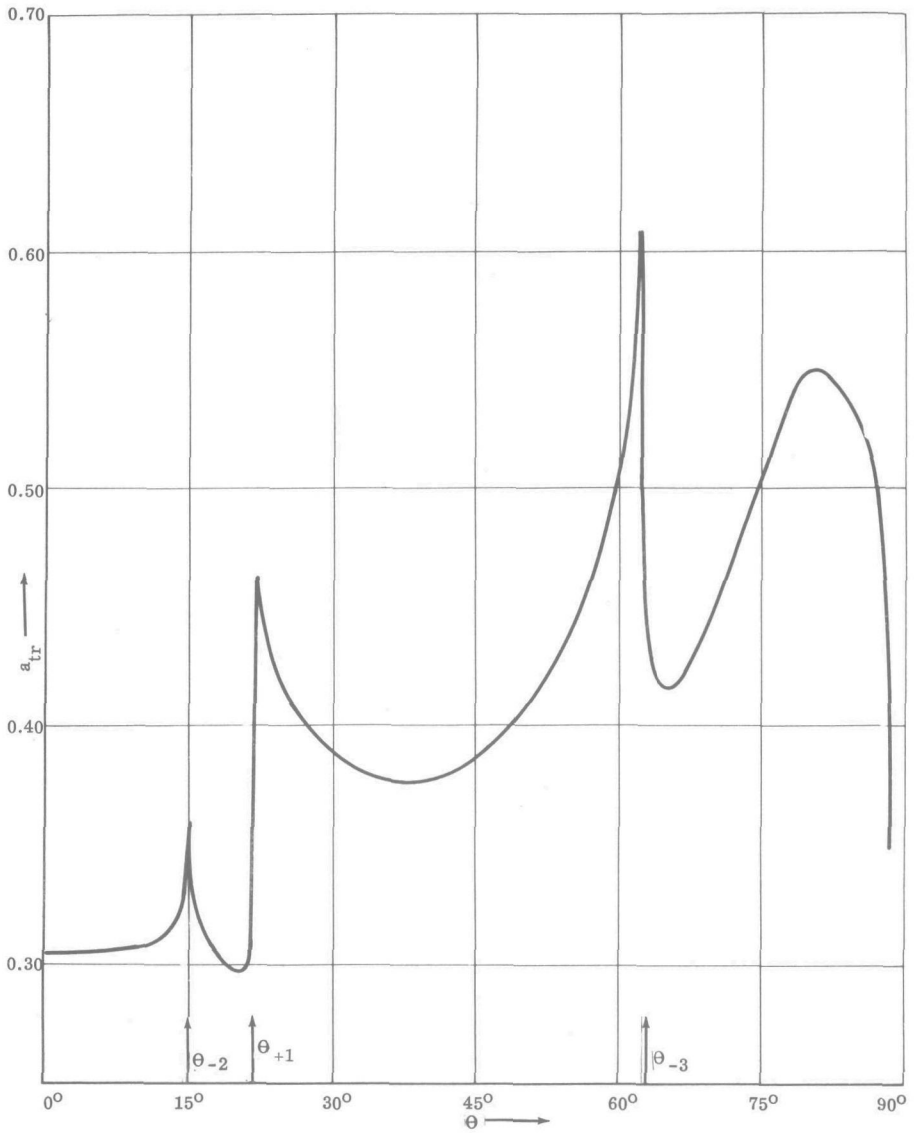


Fig. 4.10. The absorption coefficient a_{tr} as a function of the angle of incidence θ .

$$\begin{aligned} \eta_1 &= 0; \quad \eta_2 = 0.264 + j 0.395; \\ k_z &= 10.0; \quad kd = 5.0; \quad kh = 3.5; \\ \varphi &= 0^\circ. \end{aligned}$$

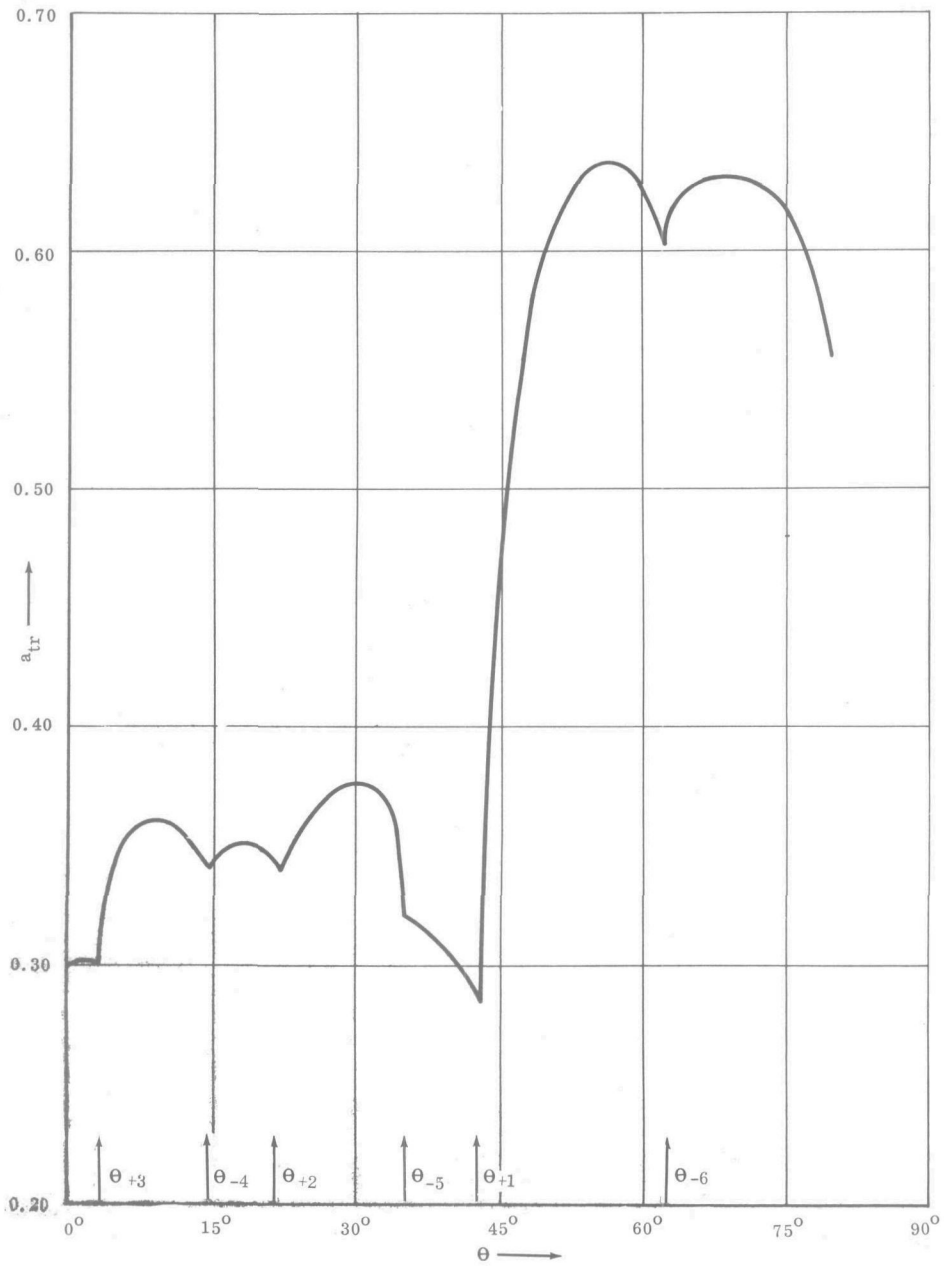


Fig. 4.11. The absorption coefficient a_{tr} as a function of the angle of incidence θ .
 $\eta_1 = 0$; $\eta_2 = 0.264 + j 0.395$;
 $k_1^2 = 20.0$; $k_d = 10.0$; $kh = 1.0$;
 $\varphi = 0^\circ$.

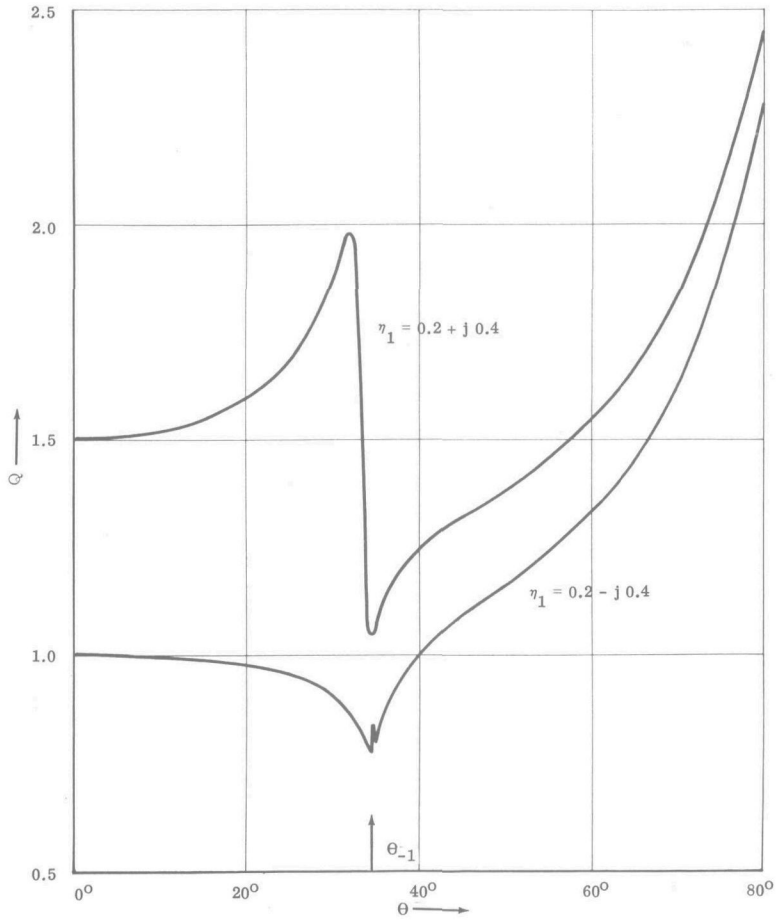


Fig. 4.12a. The shape factor Q as a function of the angle of incidence θ , for two complex conjugate values of the admittance $\eta_1, \eta_2 = 0$; $k' = 4.0$; $kd = 2.0$; $kh = 0.1$; $\varphi = 0^\circ$.

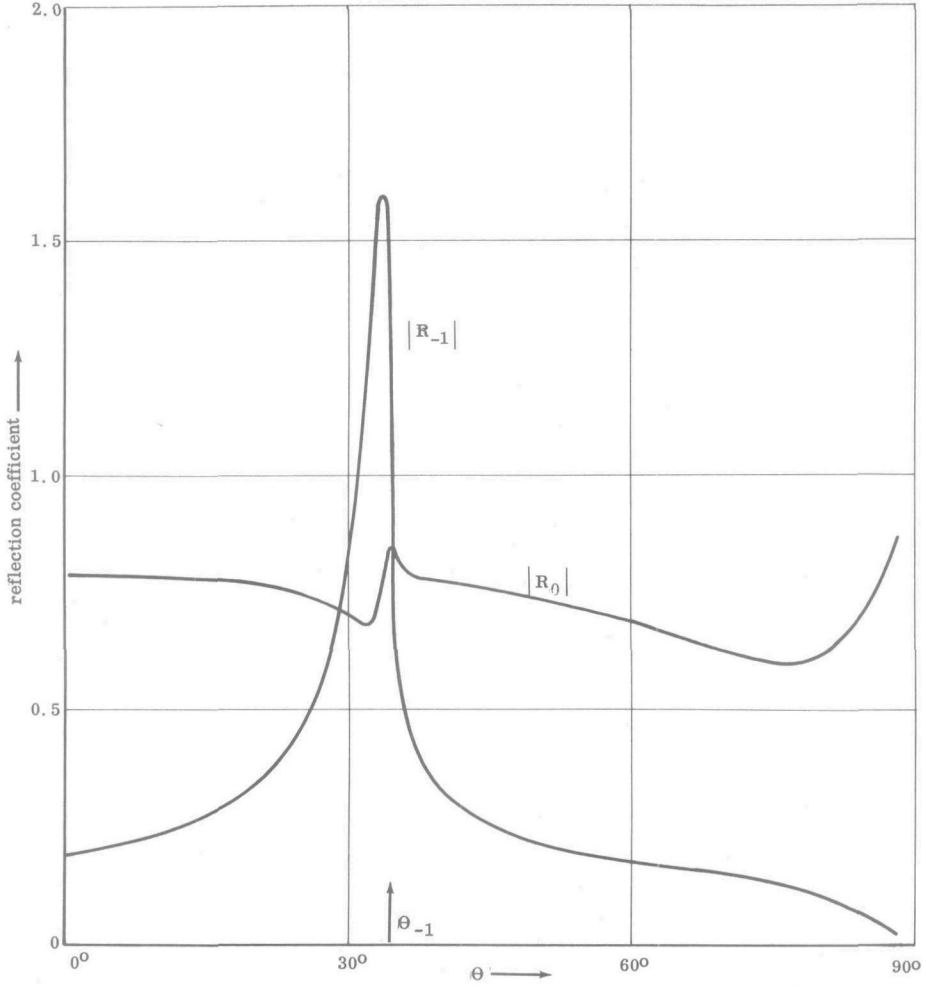


Fig. 4.12b. The modulus of the reflection coefficients R_0 and R_{-1} as a function of the angle of incidence θ . $\eta_1 = 0.2 + j 0.4$. Other conditions as in Fig. 4.12a.

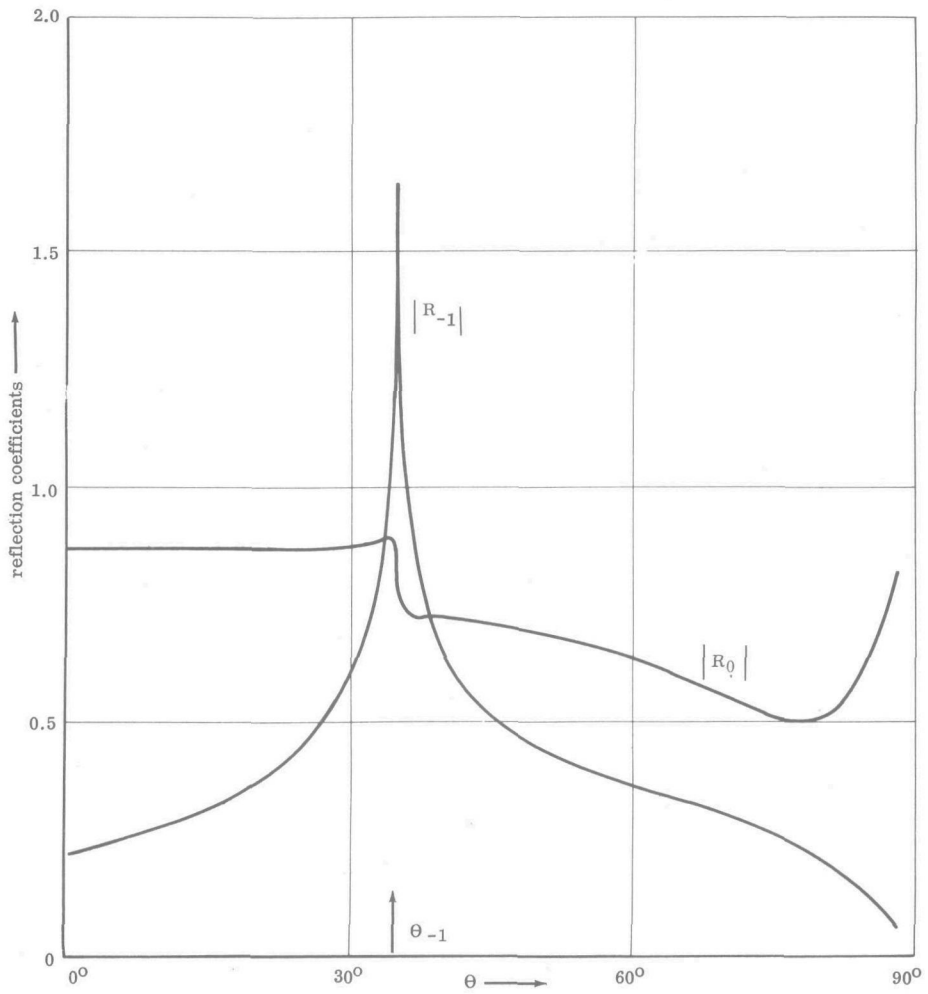


Fig.4.12c. The modulus of the reflection coefficients R_0 and R_{-1} as a function of the angle of incidence θ . $\eta_1 = 0.2 - j 0.4$. Other conditions as in Fig.4.12a.

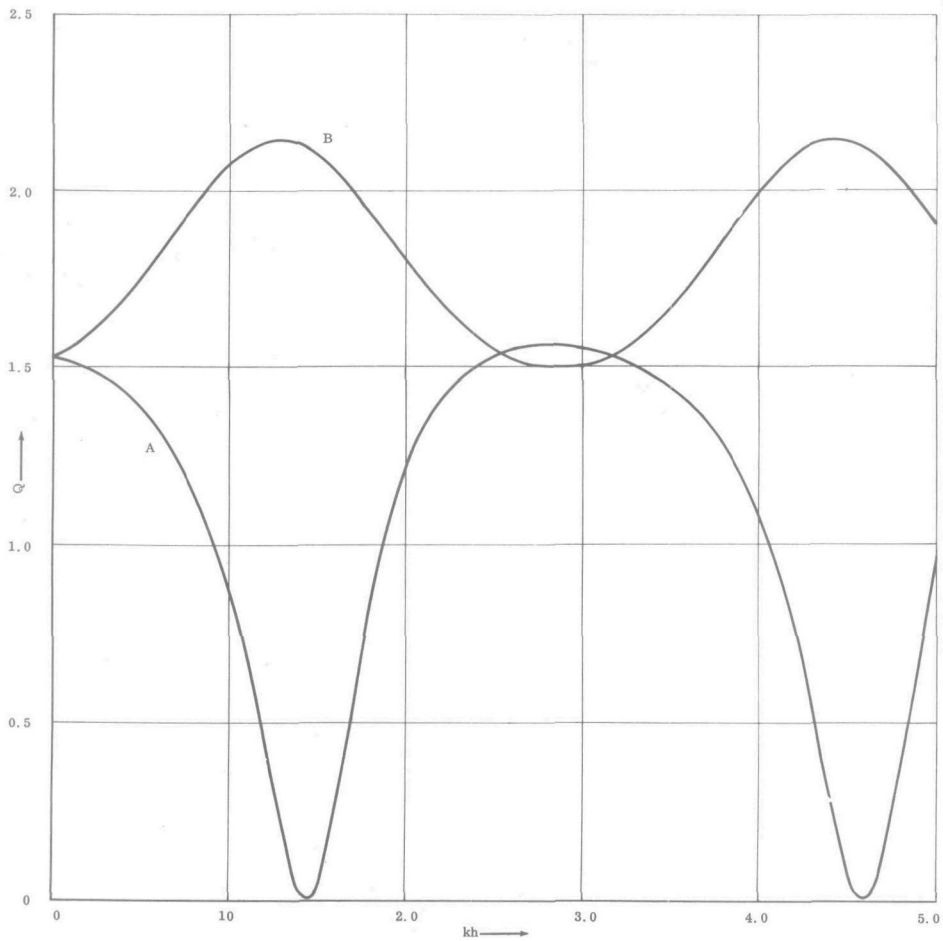


Fig. 4.13. The shape factor Q as a function of kh , where h is the groove depth and k the wave number.

(A) $\eta_1 = 0.595 + j 0.134$; $\eta_2 = 0$; $k_0 h = 1.0$; $kd = 0.5$; $\varphi = 0^\circ$; $\theta = 0^\circ$

(B) $\eta_1 = 0$; $\eta_2 = 0.595 + j 0.134$. Other conditions as in (A).

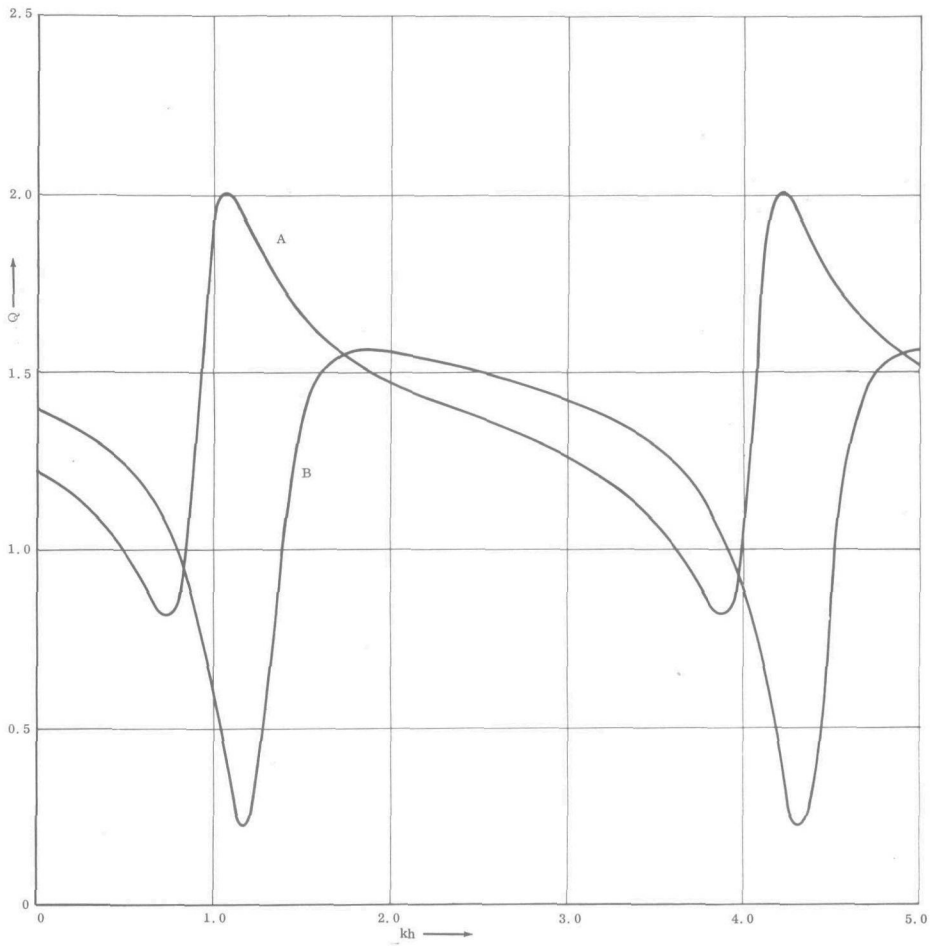


Fig. 4.14. The shape factor Q as a function of kh , where h is the groove depth and k the wave number.

(A) $\eta_1 = 0.264 + j 0.395$; $\eta_2 = 0$; $kl = 5.0$; $kd = 1.0$; $\varphi = 0^\circ$; $\theta = 0^\circ$, $a_{eq} = 0.486$.

(B) $\eta_1 = 0.627 + j 0.342$; $\eta_2 = 0$; $kl = 3.0$; $kd = 1.0$; $\varphi = 0^\circ$; $\theta = 0^\circ$, $a_{eq} = 0.605$.

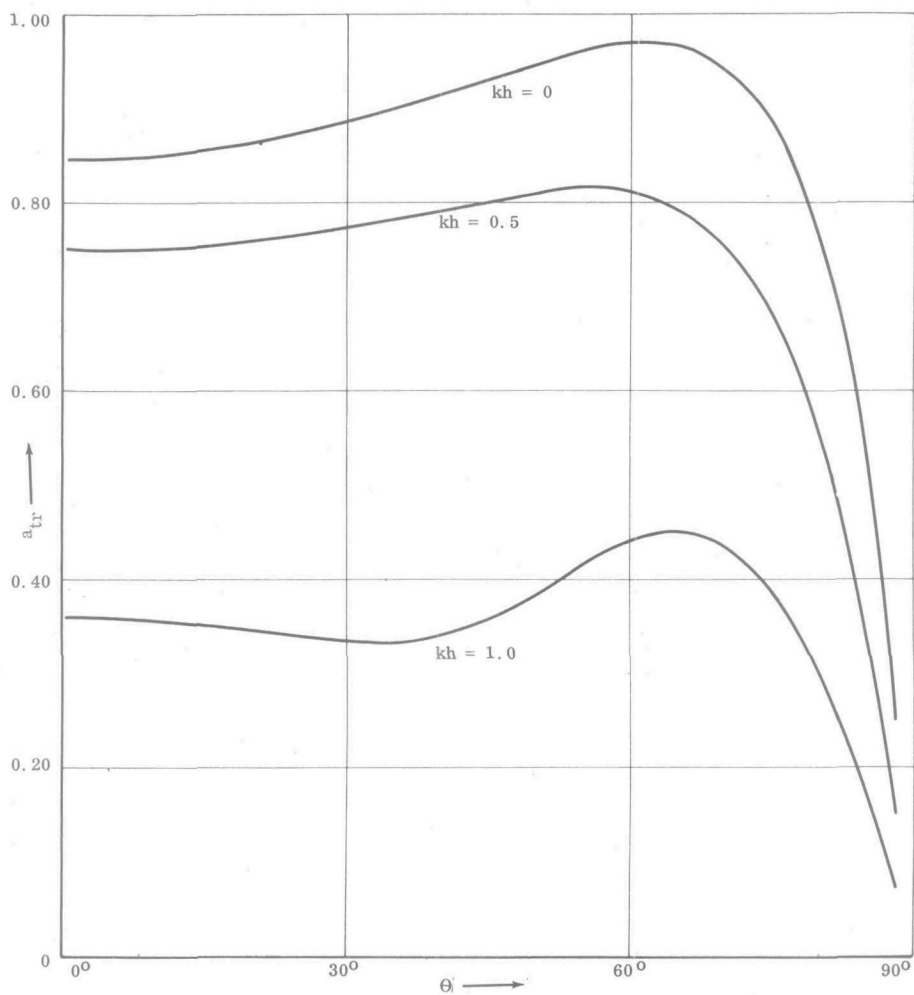


Fig. 4.15. The absorption coefficient a_{tr} as a function of the angle of incidence θ for three values of the ratio of the groove depth h and the wave number k .
 $\eta_1 = 0.627 + j 0.342$; $\eta_2 = 0$;
 $kL = 3.0$; $kd = 1.0$; $\varphi = 0^\circ$.

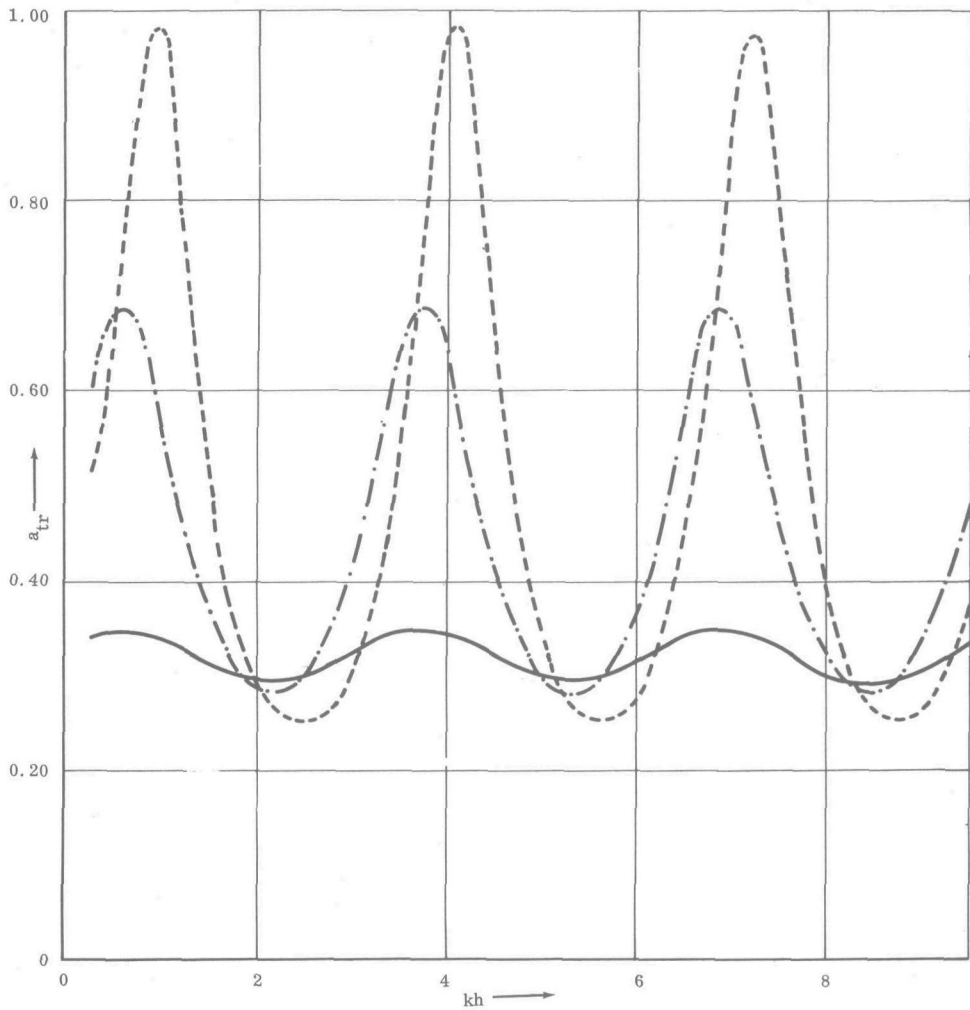


Fig. 4.16. The absorption coefficient a_{tr} as a function of the ratio of groove depth h and the wavenumber k .

- - - - $\eta_1=0; \eta_2=0.265 + j 0.395;$
 $k\ell=3.0; kd = 1.0;$
 $\varphi=0^\circ; \theta=0^\circ.$
- · - · - $\eta_1=0; \eta_2 = 0.627 + j 0.343;$
 $k\ell=5.0; kd = 1.0;$
 $\varphi = 0^\circ; \theta = 0^\circ.$
- $\eta_1=0; \eta_2 = 0.627 + j 0.343$
 $k\ell=10.0; kd = 3.0;$
 $\varphi = 0^\circ; \theta = 0^\circ.$

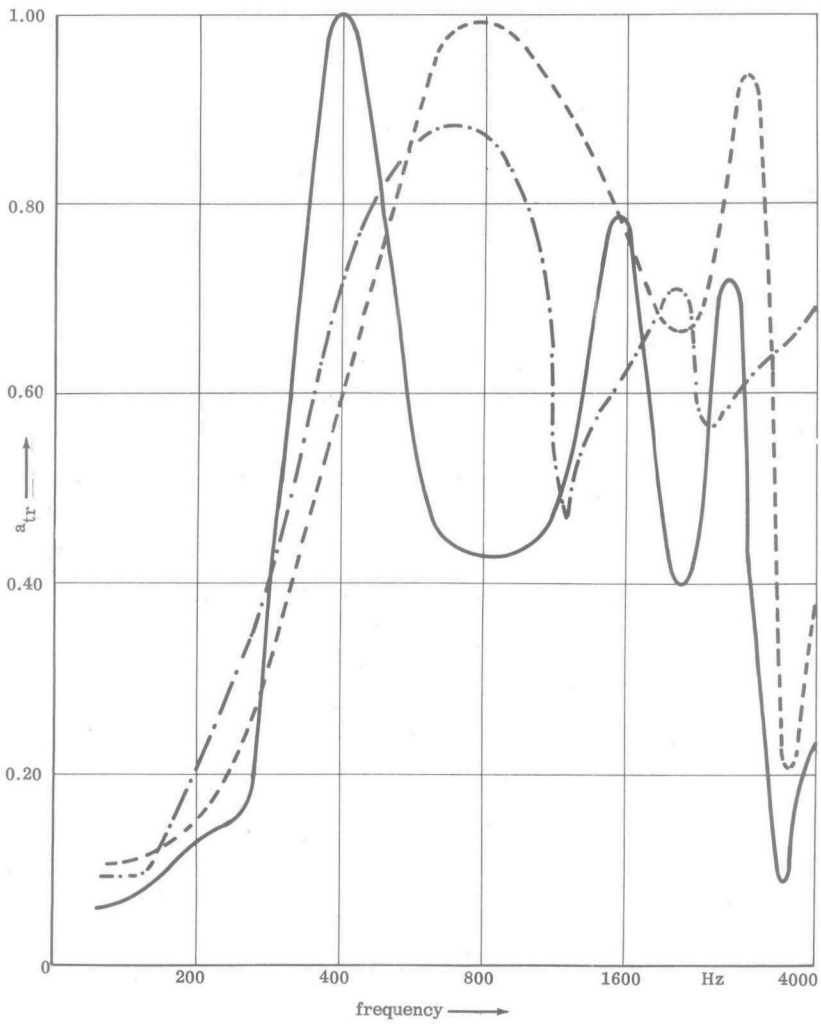


Fig. 4.17. The absorption coefficient a_{tr} as a function of frequency of a sound absorbing periodic structure of which the bottom of the grooves consists of the acoustic material Sillan SP 100, 5 cm thick, for normal incidence.

- $l = 0.15$ m; $d = 0.025$ m; $h = 0.10$ m;
 - - - $l = 0.10$ m; $d = 0.05$ m; $h = 0.075$ m;
 - · - · $l = 0.30$ m; $d = 0.20$ m; $h = 0.10$ m.
- $\varphi = 0$; $\Theta = 0^\circ$.

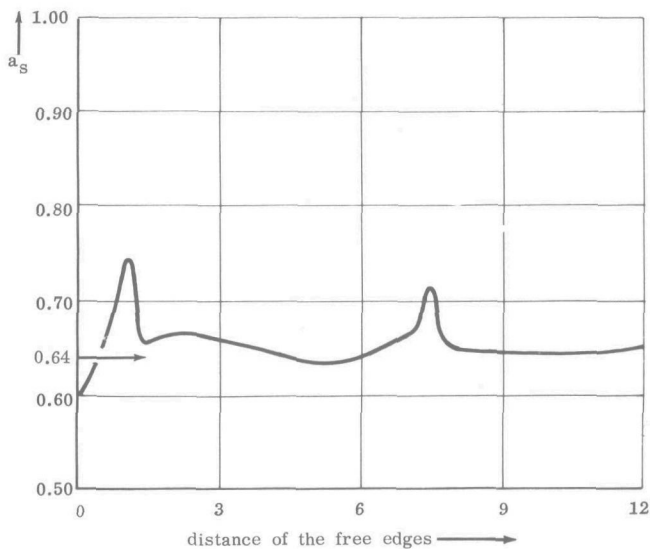


Fig. 4.18. The absorption coefficient a_s of a single sound absorbing strip with a ratio of the strip width and the wavenumber k equal to 5, lying in a periodic arrangement of identical acoustic strips, as a function of the normalized distance of the edges at normal incidence, $\eta_1 = 0.264 + j 0.395; \eta_2 = 0;$
 $kd = 5; kh = 0;$
 $\varphi = 0^\circ; \theta = 0^\circ;$

The absorption coefficient of a single sound absorbing strip with normalized width $kd = 5$, lying in an infinite hard plane at normal incidence, equals the value 0.64, as computed with the method presented in Chapter III.

The peaks in the figure are due to the surface resonance and the Wood anomaly.

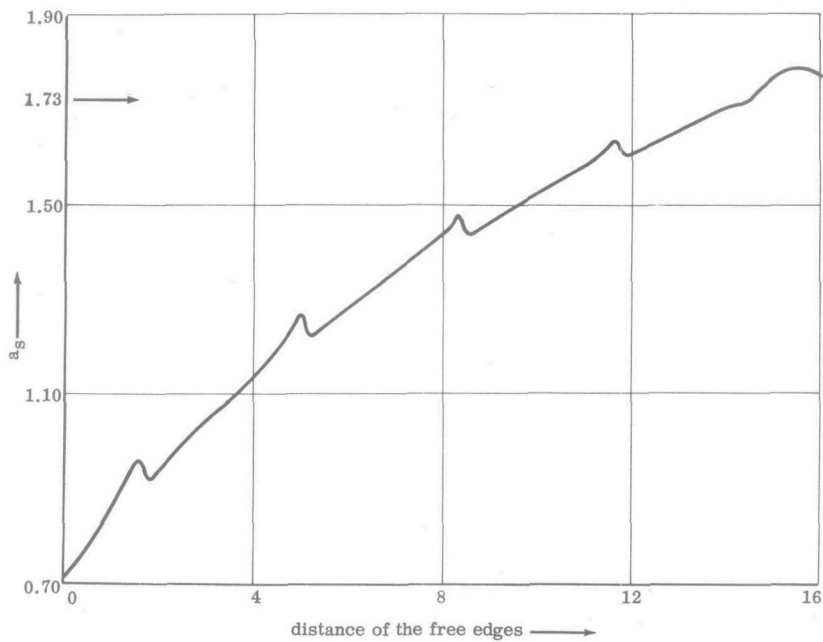


Fig. 4.19. The same configuration as in Fig. 4.18, for oblique incidence ($\theta = 60^\circ$). The absorption coefficient of a single sound absorbing strip, lying in an infinite hard plane, equals the value 1.73, as computed with the method presented in Chapter III.

- EYRING, C.F., Reverberation time in "dead" rooms, *J.Acoust.Soc.Amer.* 1 [1930], 217.
- FANO, U., Zur Theorie der Intensitätsanomalien der Beugung, *Ann.Phys.* 32 [1938], 393.
- FOX, L., An introduction to numerical linear algebra, Clarendon Press, Oxford [1964], p.189.
- HÄGGIUND, J. and SELLEBERG, F., Reflection, absorption and emission of light by opaque optical gratings, *J. Opt.Soc.Amer.* 56 [1966], 1031.
- HEINS, A.E and FESHBACH, H., On the coupling of two half-planes, *Proc. of Symposia in Applied Math.*, V, McGraw-Hill Book Company, Inc., New York [1954], p. 75.
- HOOP, A.T. de, On the plane-wave extinction cross-section of an obstacle, *Appl.Sci.Res.* 7B [1959], 463.
- HOOP, A.T. de, Wiener-Hopf-techniek, Laboratorium voor Theoretische Electrotechniek der Technische Hogeschool te Delft, Delft [1963], p. 10.
- KANTOROVICH, L.V., and KRYLOV, V.I., Approximate methods of higher analysis, P.Noordhoff, Ltd., Groningen [1964], p.42.
- KARP, S.N. and RADLOW, J., On resonance in infinite gratings of cylinders, New York University, Institute of Mathematical Sciences, Division of Electromagnetic Research, Research Report EM-90 [1956].
- KARP, S.N. and RUSSEK, A., Diffraction by a wide slit, *J.Appl.Phys.* 27 [1956], 886.
- KINSIER, L.E. and FREY, A.R., Fundamentals of acoustics, John Wiley & Sons, Inc., New York [1950], p. 397.
- KOSTEN, C.W., International comparison measurements in the reverberation room, *Acustica* 10 [1960], 400.
- KUHL, W., Der Einfluss der Kanten auf die Schallabsorption poröser Materialien, *Acustica* 10 [1960], 264.
- LEVITAS, A and LAX, M., Scattering and absorption by an acoustic strip, *J.Acoust.Soc.Amer.* 23 [1951], 316.
- LIPPMANN, B.A., Note on the theory of gratings, *J.Opt.Soc.Amer.* 43 [1953], 408.
- MANGULIS, V., On the effects of a non-rigid strip in a baffle on the propagation of sound, *J.Sound Vib.*, 2 [1965], 23.
- MILLAR, P.F., Plane wave spectra in grating theory I: Scattering by a finite number of bodies, *Can.J.Phys.* 41 [1963a], 2106.
- MILLAR, R.F., Plane wave spectra in grating theory, II: Scattering by an infinite grating of identical cylinders, *Can.J.Phys.* 41 [1963b], 2135.
- MORSE, P.M. and RUBENSTEIN, P.J., Diffraction of waves by ribbons and slits, *Phys.Rev.* 54 [1938], 895.

REFERENCES

- ARTMANN, K. Zur Theorie des anomalen Reflexion von optischen Strichgittern, Z.Phys. 119 [1942], 119.
- BOOKER, H.G. and CLEMMOW, P.C., The concept of an angular spectrum of plane waves and its relations to that of polar diagram and aperture distribution. Proc.Instn.Elect. Engrs. 97 [1950a], pt III, 11.
- BOOKER, H.G. and CLEMMOW, P.C., A relation between the Sommerfeld theory of radio propagation over a flat earth and the theory of diffraction at a straight edge, Proc. Instn.Elect.Engrs. 97 [1950b] , pt III, 18.
- CLEMMOW, P.C., The plane wave spectrum representation of electromagnetic fields, Pergamon Press, New York,
 [1966a] , p. 3;
 [1966b] , p.25;
 [1966c] , p.75.
- COOK, R.K., Absorption of sound by patches of absorbent materials, J.Acoust. Soc.Amer. 29 [1957] , 324.
- COOK, R.K., Computations on the absorption of sound absorbent patches, Proc. Third International Congress on Acoustics, Elsevier Publishing Company, Amsterdam 1960, Vol. II, p. 883.
- COPSON, E.T., On an integral equation arising in the theory of diffraction, Quart.J.Math. 17 [1946] , 19.
- DANIEL, E.D , On the dependence of absorption coefficients upon the area of the absorbent material, J.Acoust.Soc.Amer 35 [1963] , 571.
- DERYUGIN, I.N., Equations for the coefficients of reflection of waves from a periodically rough surface (in Russian), Dokl.Akad.Nauk SSSR 87 [1952] , 913.
- DERYUGIN, L.N., On the theory of diffraction by a reflecting grid (in Russian), Dokl.Akad.Nauk.SSSR 93 [1953] , 1003.
- DERYUGIN, L.N., The reflection of a laterally polarized plane wave from a surface of rectangular corrugations, Radio Eng. (transl.of Radiotekhn.) 15 [1960] , No.2, 25.
- DERYUGIN, L.N., The reflection of a longitudinally polarized plane wave from a surface of rectangular corrugations, Radio Eng. (transl. of Radiotekhn.) 15 [1960] , No. 5, 9.
- ERDELYI, A., Asymptotic expansions, Dover Publications, Inc., New York [1956], p.47.

- MUSKHELISHVILI, N.I., Singular integral equations, P.Noordhoff, Ltd., Groningen [1953], p. 42.
- NOBLE, B., Methods based on the Wiener-Hopf technique for the solution of partial differential equations, Pergamon Press, New York,
 [1958a], p.48,
 [1958b], p. 15.,
 [1958c], p.6.
- NORTHWOOD, T.D , GRISARU, M.T., and MEDCOF, M.A., Absorption of sound by a strip of absorptive material in a diffuse sound field, J.Acoust. Soc.Amer. 31 [1959], 595.
- NORTHWOOD, T.D., Absorption of diffuse sound by a strip or rectangular patch of absorptive material, J.Acoust.Soc.Amer. 35 [1963], 1173.
- OLINER, A. and HESSEL, A A., A new theory of Wood's anomalies of optical gratings. Appl.Optics 4 [1965], 1275.
- PARKINSON, J.S., Area and pattern effects in the measurements of sound absorption, J.Acoust.Soc.Amer. 2 [1930], 112.
- PELLAM, J.R., Sound diffraction and absorption by an acoustic strip, J.Acoust. Soc. Amer. 11 [1940], 396.
- RAYLEIGH, Lord, On the dynamical theory of gratings, Proc. Roy. Soc. (London) A 79 [1907], 399.
- SABINE, W.C., Collected papers on acoustics, Dover Publications, Inc., New York [1964].
- SENIOR, T.B.A., Diffraction by a semi-infinite metallic sheet, Proc.Roy. Soc. (London) A 213 [1952], 430.
- SOMMERFELD, A., Mathematische Theorie der Diffraction, Math.Ann. 47 [1896], 317.
- TWERSKY, V , On a multiple scattering theory of the finite grating and the Wood anomalies, J.Appl.Phys. 23 [1952], 1099.
- TWERSKY, V., On scattering of waves by an infinite grating, I.R.E.Trans. AP-4 [1956], 330 .
- WHITTAKER, E.T., and WATSON, G N., A course of modern analysis, Cambridge University Press, Cambridge
 [1927a,] p.115,
 [1927b,] p. 117,
 [1927c,] p. 172.
- WOLDE, ten Tj , Measurements on the edge effect in reverberation rooms, Acustica 18 [1967], No. 4.
- WOOD, R.W., On a remarkable case of uneven distribution of light in a diffraction grating spectrum, Phil.Mag. 4 [1902], 396.
- WOOD, R.W., Anomalous diffraction gratings, Phys.Rev. 49 [1935], 928.

ZWIKKER, C and KOSTEN, C.W., Sound absorbing materials, Elseviers
Publishing Company, Inc., Amsterdam [1949], p. 168.

ADDITIONAL REFERENCES

(A) Some experimental investigations of the edge effect.

Publications, mentioned in this section, give a number of experimental results of the observed edge effect.

CHRISLER, V.L., Dependence of sound absorption upon the area and distribution of the absorbent material, *Nat.Bur.Stand., J.Res.* 13 [1934], 169.

FESHBACH, H. and HARRIS, C.M., The effect of non-uniform wall distributions of absorbing material on the acoustics of rooms, *J.Acoust.Soc. Amer.* 28 [1946], 472.

GOMPERTS, M.C., Do the classical reverberation formulae still have a right for existence? *Acustica* 16 [1965-1966], 255.

JUSOFIE, M.J., Schallrichtungs verteilung im Hallraum bei 2000 Hz und Kantenbeugung an absorbierenden Materialien. *Acustica* 13 [1963], 280.

KOJMER, F., and KRNAK, M., Der Einfluss der Fläche des Prüfmaterials auf die Diffusität des Schallfeldes im Hallraum und auf den Schallabsorption grad, *Acustica* 11 [1961], 405.

KUHL, W. and KATH, U., Bemerkung zur messung der Schallabsorption im Hallraum bei vollständiger Diffusität, *Acustica* 10 [1960], 125.

MAA, D.Y., Non-uniform acoustical boundaries in rectangular rooms, *J.Acoust.Soc.Amer.* 12 [1940], 39.

MORRIS, R.M., NIXON, G.M., and PARKINSON, J.S., Variations in sound absorption coefficients as obtained by the reverberation chamber method. *J.Acoust.Soc.Amer.* 9 [1938], 234.

MORSE, P.M., BOLT, R.H. and BROWN, R.L., Acoustic impedance and sound absorption, *J.Acoust.Soc.Amer.* 12 [1940], 217.

MORSE, P.M., and BOLT, R.H., Sound waves in rooms, *Rev.Mod.Phys.* 16 [1944], 69.

OLYNIK, D. and NORTHWOOD, T.D., Comparison of reverberation-room and impedance-tube absorption measurements, *J.Acoust.Soc.Amer.* 36 [1964], 2171.

PEILAM, J.R. and BOLT, R.H., The absorption of sound by small areas of absorbing materials. *J.Acoust.Soc.Amer.* 12 [1940], 24.

RAMER, L.G., The absorption of strips, effects of width and location. *J.Acoust.Soc.Amer.* 12 [1941], 323.

(B) Diffraction by a half-plane.

Publications, mentioned in this section, give a number of investigations of the scattering of a plane wave by a discontinuity in the impedance of the surface.

BARLOW, H.M. and BROWN, J., Radio surface waves, Oxford University Press, London [1962], p.137.

BREITHAUPT, R.W., Diffraction of a cylindrical surface wave by a discontinuity in surface reactance, Proc.I.E.E.E. 51 [1963], 1455.

BRUIJN, A.de, The edge effect of sound absorbing materials, 5e Congrès International d'Acoustique, Liège [1965], H-35.

GRUNBERG, G., Theory of the coastal refraction of electromagnetic waves (in Russian), Akad.Nauk.SSSR, Zh.Eksp.Teo.Fiz. 14 [1944], 84.

KAY, A.F. Scattering of a surface wave by a discontinuity in the reactance, I.R.E.Trans. AP-7 [1959], 22.

(C) Scattering by periodic structures.

Further informations concerning the theory of reflection by periodically uneven surfaces are presented by:

BECKMANN, P. and SPIZZICHINO, A., The scattering of electromagnetic waves from rough surfaces, Pergamon Press, New York [1963].

LYSANOV, Iu.P., Theory of the scattering of waves at periodically uneven surfaces (survey), Soviet Phys.-Acoustics 4 [1958], 1.

Some recent investigations of the scattering by periodic structures, employing DERYUGIN's method, are presented by:

BRUIJN, A.de, The sound absorption of an absorbing periodically uneven surface of rectangular profile, Acustica 18 [1967], No.3.

SHENDEROV, E L., Sound diffraction by slits in a plate of finite thickness, Soviet Phys.-Acoustics 10 [1965], 305.

WIRGIN, A., Diffraction par un réseau de profil rectangulaire illuminé par une onde plane associée à un vecteur champ électrique polarisé parallèlement aux sillons, C.R.Acad.Sc.Paris 262 [1966], No.6, 385.

WIRGIN, A., Diffraction par un réseau de profil rectangulaire illuminé par une onde plane associée à un vecteur champ magnétique polarisé parallèlement aux sillons, C.R.Acad.Sc.Paris 262 [1966], No.9, 579.

Some recent investigations concerning the scattering from a plane surface with periodically varying surface impedance are presented by:

HEAPS, H.S , Reflection of a plane acoustic wave from a surface of non-uniform impedance, J. Acous.Soc.Amer. 28 [1956] , 666.

HEAPS, H.S., Reflection of sound from a periodic scattering layer. 5e Congrès International d'Acoustique, Liège [1965] , K-32.

LYSANOW, Iu.P., Scattering of sound from plane inhomogeneous surfaces with periodically varying acoustic admittance, Soviet-Phys.-Acoustics 1 [1955] , 60.

LYSANOW, Iu.P., On the scattering of sound by a non-uniform surface, Soviet-Phys. - Acoustics 4 [1958] , 45.

SUMMARY

In this thesis we present a contribution to the explanation of the experimentally observed fact that the sound absorption coefficient of sound-absorbing materials as measured in the reverberation chamber, depends upon the dimensions of the test sample. To this aim a calculation is presented for the absorption of sound by three different sound-absorbing structures consisting of materials with known properties.

The cause of this effect can be attributed to the sound diffraction phenomena in the vicinity of the edges of the sample, which result into an additional sound absorption.

In Chapter I we present a general introduction to the intricacies arising in calculating this edge effect.

In Chapter II we treat the diffraction problem where a plane wave is obliquely incident upon the straight edge of an acoustically hard half-plane and an absorbing half-plane. The reflected field consists of two contributions: the specularly reflected plane wave against a rigid wall and a scattered field which can be represented as a superposition of plane waves. The latter spectrum consists partly of undamped travelling waves while the remaining plane waves exhibit an exponential decay in the direction perpendicular to the structure. The total field is forced to satisfy the boundary conditions which hold on each of the two half-planes. This leads to two dual integral equations with the spectral distribution as unknown function. This spectrum function which represent the phase and the amplitude of each specimen of the spectrum, is determined from the integral equations with the aid of the Wiener-Hopf technique. From the obtained results the additional absorption at the edge is computed for a diffusely incident sound field. This absorption is then compared with experimentally observed values. Finally, the influence of the angle of incidence upon the edge effect is considered in detail.

In Chapter III we present the calculation of the edge effect for a sound-absorbing strip, lying in an infinitely large, rigid plane.

The scattered field is again represented as a spectrum of plane waves. Further, the field directly above the strip is expanded into a Fourier series with unknown coefficients. By relating the spatial field to the field directly above the strip with the aid of the boundary conditions on and besides the strip, an infinite system of linear equations is derived, in which the Fourier amplitudes of the field directly above the strip occur as unknowns. The system is solved numerically; from the results the absorption coefficient of the strip is computed.

Special attention has been paid to the approximative solution in which the diffraction of a plane sound wave by a strip is considered as being caused by two separate, non-interacting, absorbing half-planes. This procedure can give very acceptable results for not too small a strip width. This has been verified by comparing the results of the approximate solution with the results obtained from the exact formulation of the problem.

In Chapter IV we present the solution for the problem of the diffraction of a plane sound wave by a sound-absorbing periodically uneven surface of rectangular profile. The field in the grooves is expanded into waveguide modes; the amplitudes of these modes occur as unknowns. The field above the periodic structure is written as an infinite series of plane waves with unknown amplitudes. A finite number of these plane waves is undamped, while the remaining plane waves show an exponential decay in the direction perpendicular to the periodic surface. By relating the field in the grooves to the field above the periodic structure with the aid of the condition of continuity at the interface and employing the boundary conditions, two infinite systems of linear equations are derived in which either the groove field amplitudes or the reflection amplitudes, respectively, occur as unknowns. These systems have been solved numerically. From the results the absorption coefficient of the periodic structure has been computed. The results are presented for the most part in graphical form. Special attention has been paid to the three anomalies occurring in the sound field. These anomalies - which in optics are well-known phenomena - depend upon the geometry of the periodic structure and appear to have large influence upon the values of the absorption coefficient.

SAMENVATTING

In dit proefschrift wordt een bijdrage geleverd tot de verklaring van het experimenteel waargenomen feit dat de geluidsabsorptiecoëfficiënt van geluidsabsorberende materialen, zoals die in de galmkamer wordt gemeten, afhankelijk is van de afmetingen van het monster dat bij de meting gebruikt wordt. Daartoe wordt een berekening gegeven van de geluidsabsorptie van drie geluidsabsorberende configuraties, die zijn opgebouwd uit materialen met bekend veronderstelde eigenschappen.

De oorzaak van dit effect is gelegen in de buigingsverschijnselen van het geluid, die in de nabijheid van de randen van het monster optreden en die een additionele geluidsabsorptie tot gevolg hebben.

In het Eerste Hoofdstuk wordt een algemene inleiding gegeven in de problematiek betreffende de berekeningswijzen van dit randeffect.

In het Tweede Hoofdstuk wordt het buigingsprobleem behandeld, waarbij een vlakke golf scheef invalt op de rechte rand van een akoestisch hard halfvlak en een geluidsabsorberend halfvlak. Het gereflecteerde veld bestaat dan uit twee bijdragen: de geometrisch gereflecteerde vlakke golf tegen een harde wand en een strooiveld, dat voorgesteld wordt als een superpositie van vlakke golven. Dit spectrum bestaat voor een deel uit ongedempte golven, terwijl de overblijvende vlakke golven een exponentiële afname vertonen in de richting loodrecht van de configuratie af. Het totale veld wordt vervolgens aangepast aan de randvoorwaarden, die op elk van de twee halfvlakken gelden. Dit leidt tot twee duale integraalvergelijkingen met de spectrale verdeling als onbekende functie. Deze spectrumfunctie, die de fase en amplitude van elke vlakke golf weergeeft, wordt met behulp van de Wiener-Hopf techniek uit de integraalvergelijkingen bepaald. Met behulp van het verkregen resultaat wordt de additionele absorptie aan de rand voor een diffuus invallend geluidveld numeriek berekend. Deze absorptie wordt vervolgens vergeleken met waarden die uit experimentele gegevens werden gevonden. Tenslotte wordt de invloed van de hoek van inval op het randeffect in detail beschouwd.

In het Derde Hoofdstuk wordt de berekening van het randeffect gegeven van een geluidabsorberende strook, die op een oneindig groot hard vlak ligt. Het strooiveld wordt wederom voorgesteld door een spectrum van vlakke golven; voorts wordt het veld direct boven de strook ontwikkeld in een fourierreeks met onbekende coëfficiënten. Door het ruimtelijke veld en het veld direct boven de strook aan elkaar aan te passen door middel van de randvoorwaarden op en naast de strook, wordt een oneindig stelsel vergelijkingen afgeleid, waarin de fourier-

amplituden van het veld juist boven de strook als onbekenden optreden. Dit stelsel wordt numeriek opgelost, waarna de absorptiecoëfficiënt van de strook wordt berekend.

Speciale aandacht wordt besteed aan de benaderende oplossingswijze, waarbij de geluidverstrooiing van een vlakke golf aan een strook wordt opgevat als te zijn veroorzaakt door twee van elkaar gescheiden, dus elkaar niet beïnvloedende, absorberende halfvlakken. Deze oplossing kan voor niet al te kleine strookbreedten tot zeer acceptabele resultaten leiden. Dit is bewezen door de resultaten van de benaderende zienswijze te vergelijken met de resultaten die uit de exacte formulering van het probleem zijn verkregen.

In het Vierde Hoofdstuk wordt een oplossing gegeven voor het vraagstuk van de verstrooiing van een vlakke geluidgolf door een geluidabsorberend, periodiek oneffen, oppervlak voorzien van groeven met een rechthoekige doorsnede. Het veld in de groeven wordt ontwikkeld in trillingswijzen, die in een golfpijp kunnen optreden; de amplituden van deze trillingswijzen treden als onbekenden op. Het veld boven de periodieke structuur wordt geschreven als een oneindige reeks van vlakke golven met voorlopig, onbekende amplituden. Een deel van deze vlakke golven is ongedempt, terwijl de overblijvende vlakke golven een exponentiële afname vertonen in de richting loodrecht op het periodieke oppervlak. Door het veld in de groeven en het veld boven de periodieke structuur aan elkaar aan te passen met behulp van de continuïteitsvoorwaarden van het geluidveld in de opening van de groeven, worden twee oneindige stelsels vergelijkingen afgeleid, waarin de groefamplituden en de reflectieamplituden respectievelijk optreden als onbekenden. Deze stelsels werden numeriek opgelost, waarna de absorptiecoëfficiënt van deze periodieke structuur kon worden berekend. De resultaten van deze numerieke oplossingsmethode worden merendeels in grafische vorm weergegeven. Speciale aandacht wordt besteed aan de drie anomalieën, die het geluidveld kan vertonen. Deze anomalieën - die in de optica een bekend verschijnsel zijn - hangen samen met de verschillende afmetingen in de periodieke structuur en blijken in bepaalde gevallen een bijzonder sterke invloed op de waarde van de absorptiecoëfficiënt te hebben.

1. De additionele geluidabsorptie, die wordt veroorzaakt door de buiging van geluidgolven aan de rand van een geluidabsorberend monster, kan worden beschouwd als een plaatselijk randeffect. Dit resultaat biedt de mogelijkheid om op de met de nagalmmethode verkregen waarden van de absorptiecoëfficiënt op een eenvoudige wijze een correctie aan te brengen voor de omstandigheid dat het monster niet oneindig uitgebreid is bij de meting.

Dit proefschrift, Hoofdstuk III,
C.W. KOSTEN, *Acustica* 10 [1960], 400.

2. De mate van diffusiteit van het geluidveld in de nagalmmkamer heeft een zo grote invloed op de gemeten waarde van de randeffectcoëfficiënt b_{stat} , dat het vergelijken van meetresultaten, die voor deze coëfficiënt in verschillende nagalmmkamers zijn verkregen, zeer twijfelachtig wordt.

Dit proefschrift, Hoofdstuk II.

3. De wijze waarop OLINER en HESSEL tot het optreden van een zogenaamde oppervlakteresonantie besluiten bij reflectie door een oppervlak met periodiek veranderde eigenschappen, is onnauwkeurig. Zij brengen hier slechts de invloed in rekening van de diagonaalelementen in de coëfficiëntenmatrix van het stelsel lineaire vergelijkingen dat deze reflectie beschrijft; dit is alleen geoorloofd, indien deze diagonaalelementen dominant zijn ten opzichte van de andere matrixelementen, hetgeen in hun stelsel niet het geval is. Het stelsel vergelijkingen (4.25) in dit proefschrift bezit deze eigenschap wel en is derhalve beter geschikt om de oppervlakteresonanties te localiseren.

A.A. OLINER en A. HESSEL, *Appl. Optics*
4 [1965], 1275,
Dit proefschrift, Hoofdstuk IV.

4. De methode die BREITHAUPT toepast om de integralen, die bij het "factoriseren" in de Wiener-Hopftechniek optreden, numeriek te bepalen (methode van Gauss, onder toepassing van Laguerre-polynomen) is onjuist, daar de optredende integranden op het oneindige geen exponentieel gedrag vertonen.

R.W. BREITHAUPT, *Proc. I.E.E.E.* 51
[1963], 1455.

5. De bewering van SHENDEROV, dat bij doorlating van geluidgolven door een vlakke plaat van eindige dikte die van periodiek gelegen spleten is voorzien, de doorlatingsfactor nul wordt bij het optreden van een anomalie van Wood is onjuist. Het door hem gebruikte stelsel vergelijkingen geeft namelijk te weinig informatie over het verstrooide veld bij het optreden van een anomalie van Wood.

E.L. SHENDEROV, *Soviet Phys.-Acoustics*
10 [1965], 305.

6. De wijze waarop MECHEL en WILLE de absorptie- en de verstrooiingsdoorsnede van een geluidabsorberende bol numeriek bepalen (namelijk door de theorie van Mie te gebruiken), levert grote moeilijkheden op bij waarden van de straal die groot zijn ten opzichte van de golf lengte. Het zou juister geweest zijn voor die waarden een asymptotische methode - die bij voorbeeld met behulp van de transformatie van Watson kan worden verkregen - te gebruiken.

Fr. MECHEL en P. WILLE, 5e Congrès Int. d'Acoustique,
Liège [1965], K-17

Fr. MECHEL en P. WILLE, *Acustica* 16 [1965], 101.

7. Het is op akoestische gronden niet duidelijk waarom de boring van een hobo niet zuiver kegelvormig zou zijn, temeer daar afwijkingen van de kegelvorm vaak tot onzuiverheden in het lage register leiden.

C.J. NEDERVEEN en A. de BRUIJN,
Acustica 18 [1967], 47.

P. BATE, The Oboe,
Ernest Benn, Ltd, London [1962], p. 83.

8. Het begrip "akoestisch zacht" (Eng. "sound-soft") dat wiskundigen vaak gebruiken ter aanduiding van de eigenschappen van een geluidverstrooiend obstakel dat geen van nul verschillende waarde van de geluiddruk op zijn oppervlak toelaat, suggereert dat er door het obstakel akoestisch vermogen zou worden geabsorbeerd in tegenstelling tot het geval van akoestisch harde (Eng. "sound-hard") obstakels. Dit is niet geval, zodat het aanbeveling verdient de -misleidende- benaming "sound-soft" te vervangen door "perfectly compliant".

B.NOBLE, Methods based on the
Wiener-Hopf technique,
Pergamon Press, New York [1958], p. 51
D.S.JONES, Theory of Electromagne-
tism, Pergamon Press, Oxford [1964], p. 451.

9. Onder natuurkundigen kunnen soms merkwaardigen misverstanden heersen omtrent het vakgebied der akoestiek. Als een van de oorzaken kan worden beschouwd de omstandigheid dat veel overzichtsartikelen over de akoestiek in algemeen georiënteerde natuurkundige tijdschriften en leerboeken te vaag zijn en te weinig informatie bieden over de werkelijke problemen waarmee akoestici zich bezighouden.

R. B. LINDSAY, Education in Acoustics,
J. Acoust. Soc. Amer. 37 [1965], 217.

10. Terecht wijst SIMON VESTDIJK erop, dat de "differentiële waardekritiek", d.w.z. het bepalen van de waarde van muziek door het vergelijken van onderdelen (binnen één compositie of binnen de grenzen van een oeuvre), te weinig de aandacht geniet van de zijde der musicologen.

S.VESTDIJK,
Het eerste en het laatste,
Uitg. Bert Bakker/Daamen N.V.,
Den Haag [1956].

"De kamermuziek van Brahms,
een onderzoek"
uit - Hoe schrijft men over muziek? -,
Uitg. De Bezige Bij, Amsterdam,
Uitg. Nijgh & van Ditmar, 's-Gravenhage
[1963], p. 233.

N.LOESER,
Simon Vestdijk en de muziekethiek,
Mens en Melodie 12 [1957], 140.